Electronic Supplementary Material (ESI) for Organic Chemistry Frontiers.

Supporting information

Table of contents

1. Materials and General methods

All chemicals and solvents were purified according to the standard procedure.[S1] The compounds(**1**, **2**, **7, 8, 22, 23, 24,** and **25**) were synthesized according to our previous reports.[S2]

The melting points were determined on a WRS-2 melting point apparatus. Thermogravimetric analyses (TGA) were conducted on 1090B type thermal analyzer (Dupont Engineering Polymers). The high resolution mass spectral analysis (HRMS) was carried out on Bruker APEX II type mass spectrometer. The infrared (IR) spectra were recorded on the PerkinElmer Spectrum 400 spectrometer with the resolution of 2 cm^{-1}.

The ^{1}H NMR, ^{13}C NMR spectra were recorded on a Bruker Advance III 400 MHz(100 MHz for ^{13}C NMR) or a VARIAN INOVA 600MHz (150 MHz for ^{13}C NMR) spectrometer. Chemical shifts for ^{1}H NMR spectra are reported in parts per million (ppm, δ scale) downfield from tetramethylsilane, and referenced internally to the residual proton in the solvent ($CDCl_3$: δ 7.27, D_8-THF:3.58). Chemical shifts for ^{13}C NMR spectra are reported in parts per million (ppm, δ scale) downfield from tetramethylsilane, and are referenced to the ^{13}C resonance of the NMR solvent ($CDCl_3$: δ 77.00, D_8-THF: δ67.00). Data are reported as follows: Chemical shift, multiplicity (s = singlet, d = doublet, t = triplet, q = quartet, m = multiplet), coupling constants. *J*, are reported in hertz.

Cyclic voltammetry redox potential were obtained by cyclic voltammetry method on a RST 5000 electrochemical analyzer, with glassy carbon discs as working electrode, Pt wire as the counter electrode, and SCE electrode as the reference electrode. Measurement conditions: solvent, CH_2Cl_2; concentration, 1×10^{-4}mol L^{-1}; supporting electrolyte, (n-Bu)$_4NPF_6$ (0.1 M); scan speed, 0.05 V s^{-1}; temperature, 20 ºC.

The UV-Vis absorption spectra were measured on a UV-2006 UV-Specterophotometer. Fluorescence excitation and emission were recorded on a RF-5301(pc)s Spectrofluorophotometer. Fluorescence lifetime and steady state were measured on a FLS920 Spectrofluorophotometer.

The single-crystal X-ray diffraction was carried out on a SuperNova (Agilent) diffractometer. The crystal structure was solved by a direct method *SIR*2004[S3] and refined by full-matrix least-square method on F^2 by means of *SHELX*L-97.[S4] The calculated positions of the hydrogen atoms were included in the final refinement.

All the calculations were performed with Gaussian 16 software package.[S5] Geometry optimizations were carried out using B3LYP[S6]/IEFPCM(CH_2Cl_2)[S7] method. The UV-Vis absorption spectra were calculated at TD-ωB97XD /IEFPCM(CH_2Cl_2) (nstates = 40, root = 1) level of theory using optimized structures. The optimized structures and molecular orbitals were displayed using Chemcraft.[S8] The calculated UV-Vis absorption spectra were displayed using Multiwfn software[S9].

2. Synthesis

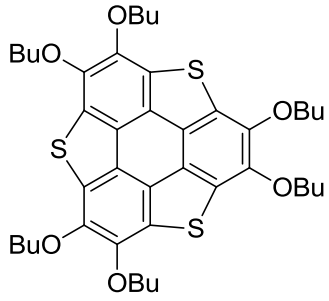

1

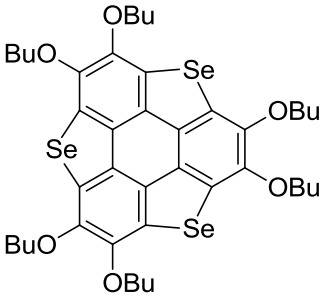

2

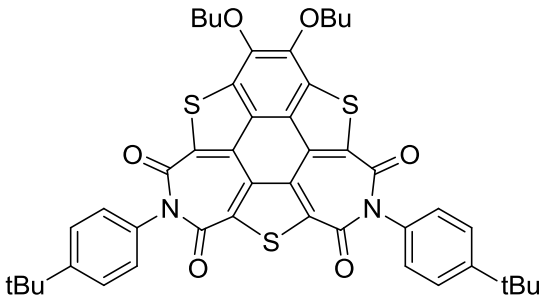

7

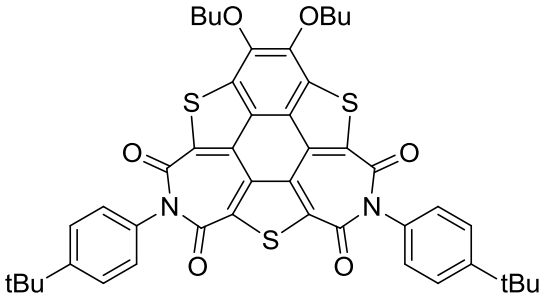

8

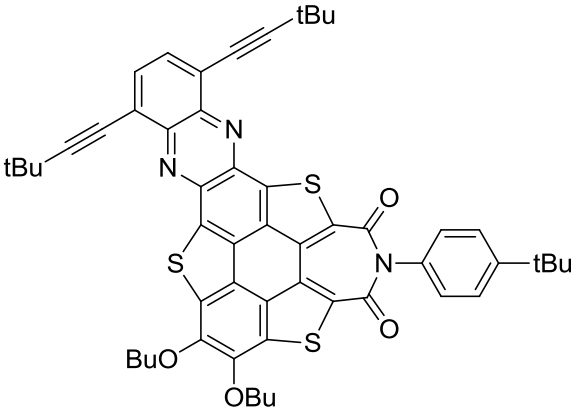

16

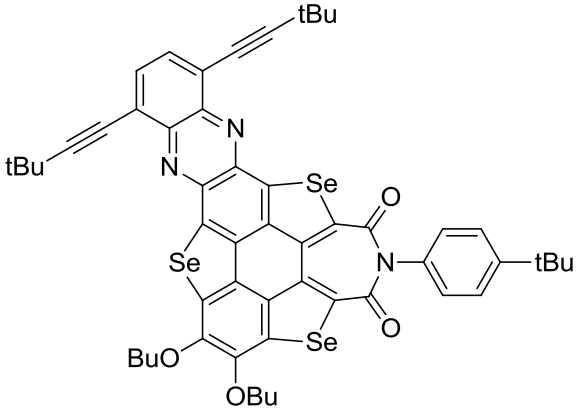

17

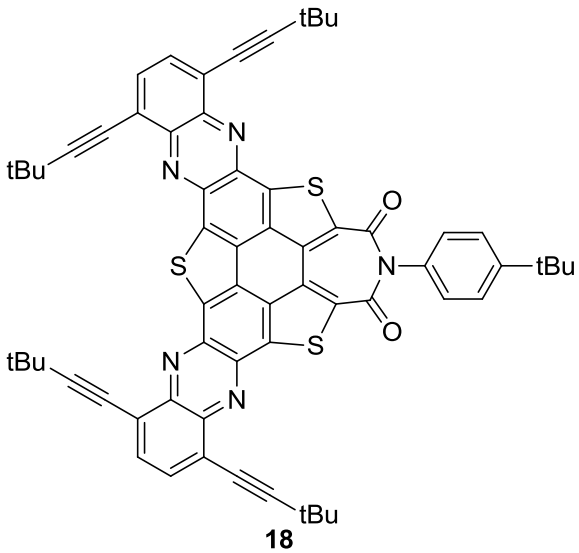

18

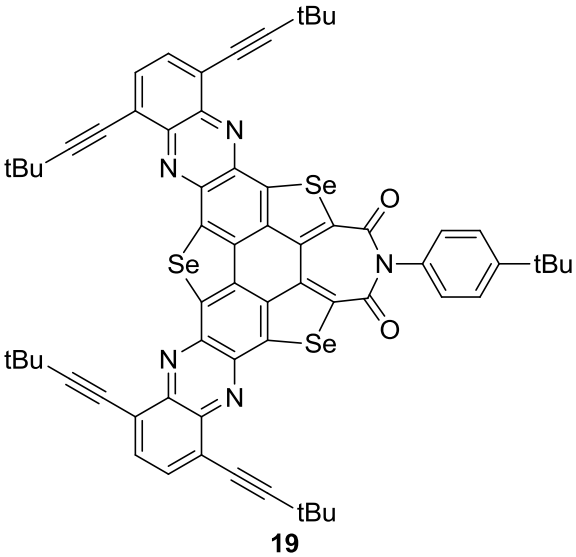

19

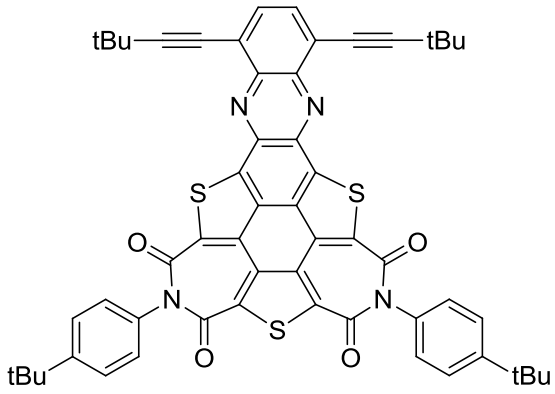

20

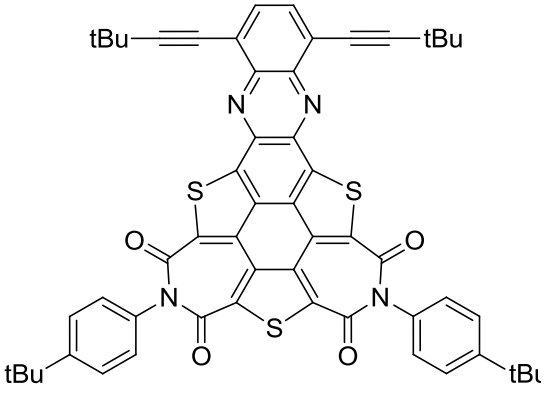

21

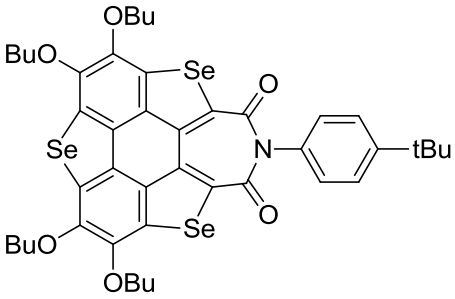

22

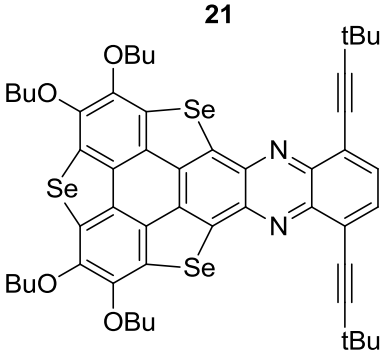

23

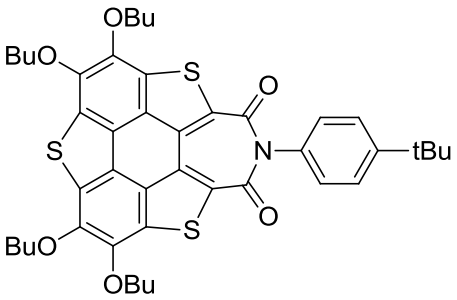

24

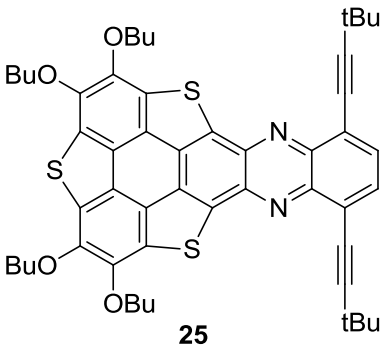

25

Experimental details:

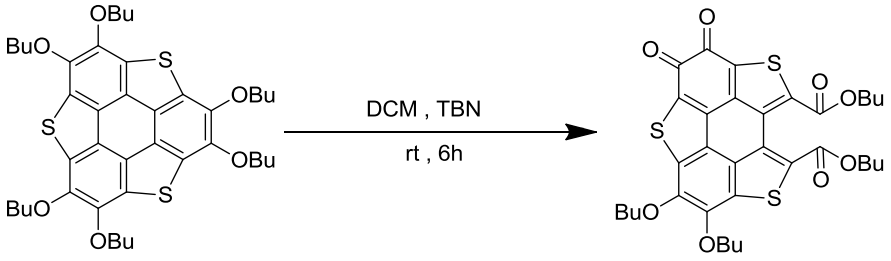

1 **3**

3: Compound **1** (75 mg, 0.1 mmol) was dissolved in CH_2Cl_2 (10 mL), then *tert*-butyl nitrite (TBN, 128 μL, 1.0 mmol) was added. The resulting mixture was stirred at room temperature (RT) for 6 h. The solvent was removed by evaporation under reduced pressure. The crude product was further purified by column chromatography on silica-gel (CH_2Cl_2) to afford **4** as black powder (37 mg, yield,

55%). mp: 192.4-193.1 °C; ^{1}H NMR (400 MHz, $CDCl_3$) δ 4.46-4.36 (m, *J* = 6.4 Hz, 8H), 1.90-1.75(m, 8H), 1.65-1.54(m, 4H), 1.54-1.46(m, 4H), 1.05-0.98(m, 8H); ^{13}C NMR (100 MHz, $CDCl_3$) *δ* 175.0, 171.7, 162.5, 161.9, 148.8, 146.5, 142.8, 141.5, 136.0, 134.5, 134.5, 132.4, 130.8, 129.7, 128.3, 127.3, 125.3, 124.7, 73.9, 73.0, 66.5, 66.2, 12.4, 32.2, 30.6, 30.5, 19.2, 19.2, 13.9, 13.9, 13.8, 13.8; HRMS($C_{34}H_{36}O_8S_3$+H): calculated for: 669.1645, found: 669.1663.

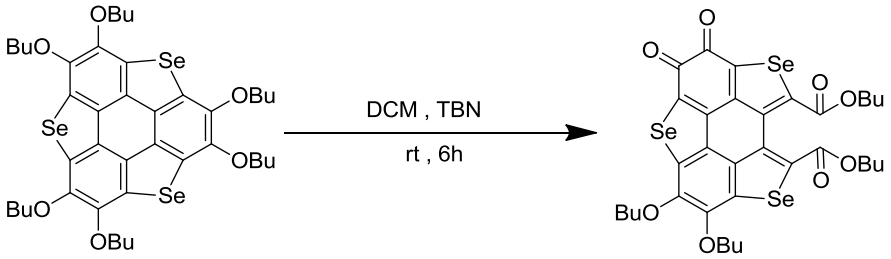

2 **4**

4: Compound **2** (89 mg, 0.1 mmol) was dissolved in CH_2Cl_2 (10 mL), then TBN (128 μL, 1.0mmol) was added. The resulting mixture was stirred at RT for 6 h. The solvent was removed by evaporation under reduced pressure. The crude product was further purified by column chromatography on silica-gel (CH_2Cl_2) to afford **5** as black powder (53 mg, yield, 65%). mp: 148.5-149.3 °C; ^{1}H NMR (400 MHz, $CDCl_3$) δ 4.41 (t, *J* = 6.5 Hz, 2H), 4.35-4.31 (m, 6H), 1.89-1.75(m , 8H), 1.64-1.44 (m, 8H), 1.05-0.98 (m, 12H); ^{13}C NMR (100MHz, $CDCl_3$) δ 176.2, 173.9, 164.3, 163.6, 150.7, 150.5, 148.1, 145.2, 140.4, 139.6, 138.9, 138.0, 135.2, 133.2, 132.3, 130.9, 129.6, 129.3, 73.9, 73.3, 66.3, 66.0, 32.5, 32.3, 30.6, 30.5, 19.3, 19.2, 19.2, 13.9, 13.8, 13.7; HRMS($C_{34}H_{36}O_8Se_3$+H): calculated for: 810.9986, found: 811.0021.

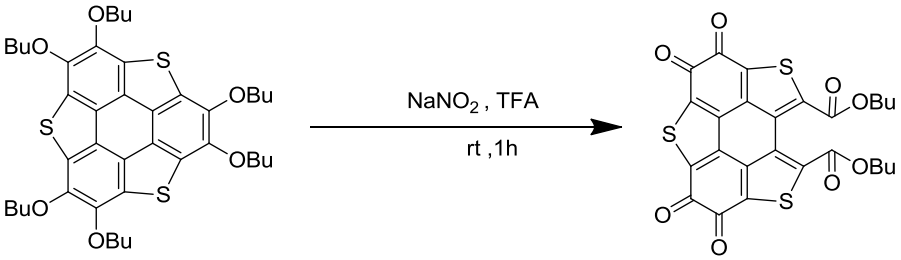

1 **5**

5: Compound **1** (75 mg, 0.1 mmol) and $NaNO_2$ (69 mg, 1.0mmol) were dissolved in TFA (10 mL) in a 20 mL bottle with the lid screwed immediately. The reaction mixture was stirred for 10 minute at room temperature, then the lid was unscrewed to introduce air for 5 seconds. Repeating the same operation for 6 times. Finally, the reaction was quenched by adding distilled water and the mixture was extracted with CH_2Cl_2 (3 × 20 mL). The organic layers were combined and dried over anhydrous Na_2SO_4, then concentrated in vacuo. The crude product was further purified by column chromatography on silica-gel (CH_2Cl_2: EA, 50 : 1, *v/v*) to afford **6** as brownish red solid (17 mg, yield, 42%). mp: 223.1-223.8 °C; ^{1}H NMR (600MHz, $CDCl_3$) δ 4.39(t, *J* =6.6 Hz, 4H), 1.81(p, *J* =6.8 Hz, 4H), 1.55-1.47(m, 4H), 1.02(t, *J* =7.3 Hz, 4H); ^{13}C NMR (150 MHz, $CDCl_3$) δ 172.7, 172.2, 161.5,

143.4, 139.9, 138.5, 136.1, 132.4, 127.3, 67.0, 30.4, 19.1, 13.7; HRMS ($C_{26}H_{18}O_8S_3$+H): calculated for: 555.0237, found: 555.0230.

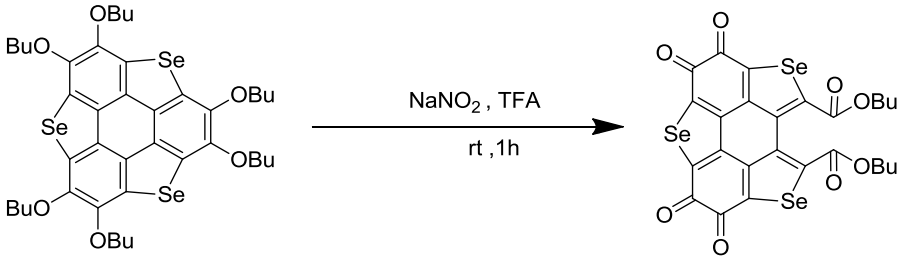

2 **6**

6: Compound **2** (89 mg, 0.1 mmol) and $NaNO_2$ (69 mg, 1.0 mmol) were dissolved in TFA (10 mL) in a 20 mL bottle with the lid screwed immediately. The reaction mixture was stirred for 10 minute at room temperature, then the lid was unscrewed to introduce air for 5 seconds. Repeating the same operation for 6 times. Finally, the reaction was quenched by adding distilled water and the mixture was extracted with CH_2Cl_2 (3 × 20 mL). The organic layers were combined and dried over anhydrous Na_2SO_4, then concentrated in vacuo. The crude product was further purified by column chromatography on silica-gel (CH_2Cl_2: EA, 50 : 1, *v/v*) to afford **7** as brownish red solid (25 mg, yield, 46%). mp: 239.1-239.7 ºC; ^{1}H NMR (400 MHz, $CDCl_3$) δ 4.35(t, *J* = 6.7 Hz, 4H), 1.82-1.75(m, 4H), 1.53-1.44(m, 4H), 1.01(t, *J* = 7.4 Hz, 4H); ^{13}C NMR (100 MHz, $CDCl_3$) δ 173.8, 173.6, 163.2, 150.8, 145.4, 143.0, 139.6, 138.7, 130.6, 66.8, 30.4, 19.2, 13.7; HRMS($C_{26}H_{18}O_8Se_3$+H): calculated for: 696.8578, found: 696.8571.

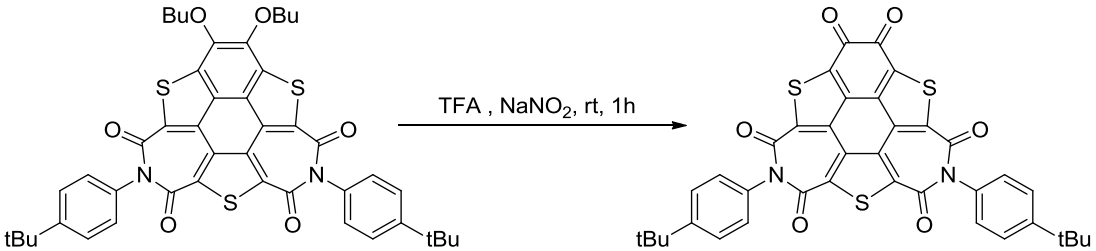

7 **9**

9: Compound **2** (82 mg, 0.1 mmol) and $NaNO_2$ (69 mg, 1.0 mmol) were dissolved in TFA (10 mL) in a 20 mL bottle with the lid screwed immediately. The reaction mixture was stirred for 10 minute at room temperature, then the lid was unscrewed to introduce air for 5 seconds. Repeating the same operation for 6 times. Finally, the reaction was quenched by adding distilled water and the mixture was extracted with CH_2Cl_2 (3 × 20 mL). The organic layers were combined and dried over anhydrous Na_2SO_4, then concentrated in vacuo. The crude product was further purified by column chromatography on silica-gel (CH_2Cl_2) to afford **9** as red solid (63 mg, yield, 90%). mp: >300ºC; ^{1}H NMR (400 MHz, Chloroform-*d*) δ 7.60 (d, *J* = 8.1 Hz, 4H), 7.21 (d, *J* = 8.0 Hz, 4H), 1.39 (s, 18H). Due to poor solubility, the crude product has not ^{13}C NMR.

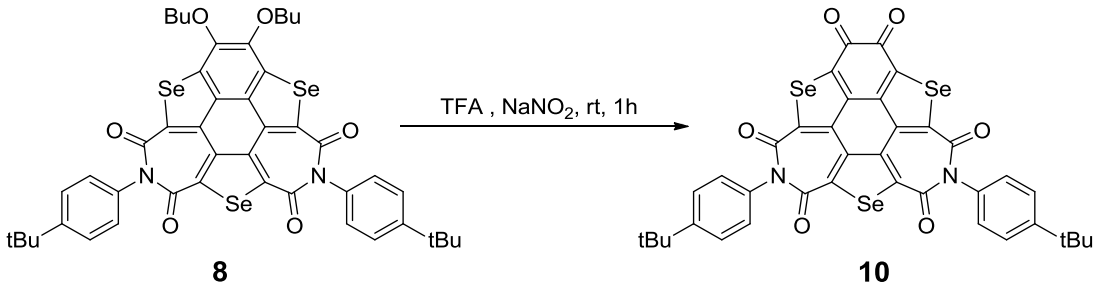

8 **10**

10: Compound **2** (96 mg, 0.1 mmol) and $NaNO_2$ (69 mg, 1.0 mmol) were dissolved in TFA (10 mL) in a 20 mL bottle with the lid screwed immediately. The reaction mixture was stirred for 10 minute at room temperature, then the lid was unscrewed to introduce air for 5 seconds. Repeating the same operation for 6 times. Finally, the reaction was quenched by adding distilled water and the mixture was extracted with CH_2Cl_2 (3 × 20 mL). The organic layers were combined and dried over anhydrous Na_2SO_4, then concentrated in vacuo. The crude product was further purified by column chromatography on silica-gel (CH_2Cl_2) to afford **9** as red solid (77 mg, yield, 91%). mp: >300ºC; ^{1}H NMR (400 MHz, Chloroform-*d*) δ 7.60 (d, *J* = 7.9 Hz, 4H), 7.21 (d, *J* = 7.8 Hz, 4H), 1.39 (s, 18H). Due to poor solubility, the crude product has not ^{13}C NMR.

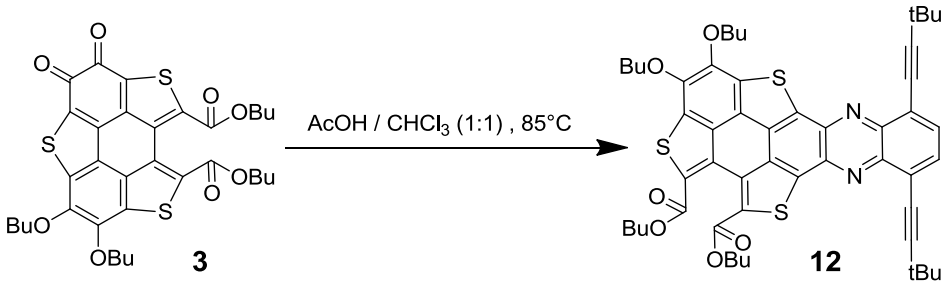

3 **12**

12: Compound **3** (334 mg, 0.5 mmol) and 3,6-bis(3,3-dimethylbut-1-yn-1-yl)benzene-1,2-diamine (**11**, 201 mg, 0.75 mmol) were dissolved in AcOH (20 mL) and $CHCl_3$ (20 mL). The resulting mixture was stirred at 85℃ for 4 h under the inert atmosphere. After cooling down to RT, the solvent was removed by evaporation under reduced pressure. The crude product was further purified by column chromatography on silica-gel (CH_2Cl_2: petro ether, 1 : 1, *v/v*) to afford **12** as red powder (361 mg, yield, 81%). mp: 215.4-216.1 ºC; ^{1}H NMR (600 MHz, $CDCl_3$): δ7.88(q, *J* =7.5 Hz, 2H), 4.57(t, *J* =6.5 Hz, 2H), 4.47-4.38(m, 6H), 1.98-1.78(m, 8H), 1.72-1.61(m, 4H), 1.56-1.46(m, 22H), 1.09-1.00(m, 12H); ^{13}C NMR (150 MHz, $CDCl_3$) :δ 163.3, 163.2, 148.1, 146.1, 142.2, 142.1, 141.6, 140.6, 137.9, 137.6, 134.5, 133.0, 133.0, 132.4, 131.8, 131.1, 130.8, 130.4, 129.5, 128.4, 127.9, 126.2, 123.7, 123.5, 107.8, 107.7, 76.1, 76.0, 73.8, 72.9, 65.8, 65.7, 32.4, 32.2, 31.1, 31.0, 30.7, 30.6, 28.7, 19.3, 19.2, 19.2, 13.9, 13.8; HRMS ($C_{52}H_{56}N_2O_6S_3$+H): calculated for: 901.3373, found: 901.3395.

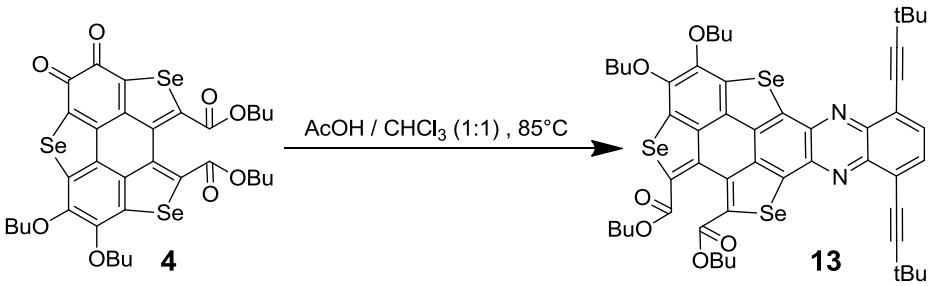

13: Compound **4** (405 mg, 0.5 mmol) and **11** (201 mg, 0.75 mmol) were dissolved in AcOH (20 mL) and $CHCl_3$ (20 mL). The resulting mixture was stirred at 85℃ for 4 h under the inert atmosphere. After cooling down to RT, the solvent was removed by evaporation under reduced pressure. The crude product was further purified by column chromatography on silica-gel (CH_2Cl_2: petro ether, 1 : 1, *v/v*) to afford **13** as red powder (442 mg, yield, 85%). mp: 198.3-199.5℃; ^{1}H NMR (400 MHz, $CDCl_3$) δ 7.91-7.85 (m, 2H), 4.47(t, *J* =6.5 Hz, 2H), 4.41-4.34(m, 6H), 1.95-1.77(m, 4H), 1.70-1.60(m, 2H), 1.57(d,*J* =1.3 Hz 18H), 1.54-1.45(m, 4H), 1.08-0.98(m, 12H); ^{13}C NMR (150 MHz, $CDCl_3$) δ 164.9, 164.8, 149.1, 148.0, 143.3, 142.7, 142., 6142.5, 141.5, 140.8, 139.6, 137.1, 135.7, 135.3, 133.4, 132.9, 132.6, 132.4, 132.3, 132.0, 131.3, 130.7, 123.6, 123.5, 107.6, 107.6, 76.0, 73.7, 73.1, 65.8, 65.6, 32.5, 32.3, 31.1, 30.6, 30.6, 28.7, 19.4, 19.3, 19.3, 13.9, 13.9, 13.8; HRMS($C_{52}H_{56}N_2O_6Se_3$+H): calculated for: 1043.1715; found: 1043.1738.

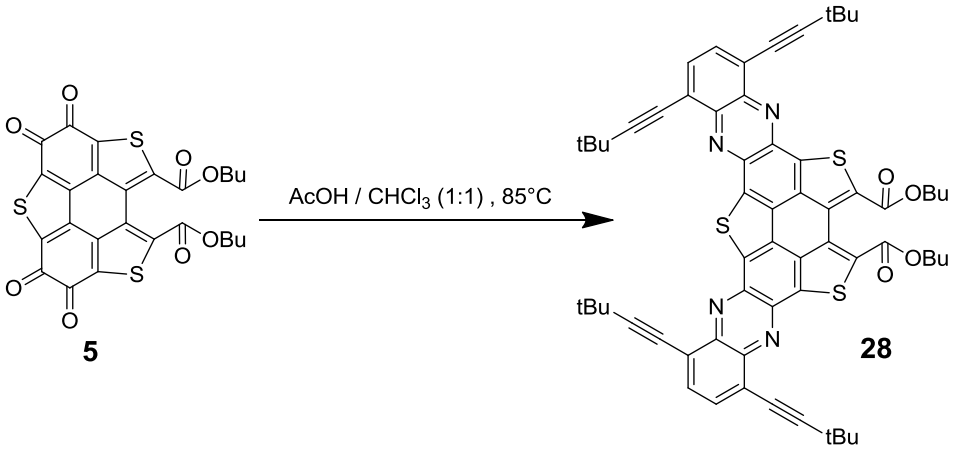

28: Compound **5** (277 mg, 0.5 mmol) and **11** (295 mg, 1.1 mmol) were dissolved in AcOH (20 mL) and $CHCl_3$ (20 mL). The resulting mixture was stirred at 85℃ for 4 h under the inert atmosphere. After cooling down to RT, the solvent was removed by evaporation under reduced pressure. The crude product was further purified by column chromatography on silica-gel (CH_2Cl_2: petro ether, 1 : 1, *v/v*) to afford **28** as yellow powder (382 mg, yield, 75%). mp: >300℃; ^{1}H NMR (400 MHz, $CDCl_3$) δ 7.94(s, 4H), 4.49(t, *J* =6.6 Hz,4H), 1.85(dq,*J* =8.4, 6.6 Hz 4H),1.60(d, *J* =1.9 Hz, 36H),1.60-1.54(m, 4H), 1.04(t, *J* =7.4 Hz, 6H); ^{13}C NMR (150 MHz, $CDCl_3$) δ 163.1, 142.5, 142.2, 141.7, 141.1, 137.9, 137.3, 135.4, 134.7, 133.1, 133.0, 131.1, 128.1, 123.8, 123.7, 108.1, 108.0, 75.9, 75.9, 66.0, 31.2, 31.1, 31.1, 30.6, 28.8, 19.3, 13.8; HRMS ($C_{64}H_{58}N_4O_4Se$+H): calculated for: 1091.3697; found: 1091.9710.

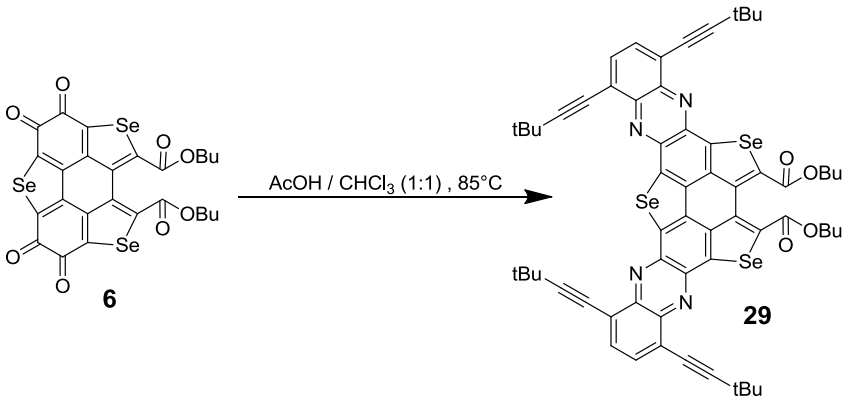

29: Compound **6** (348 mg, 0.5 mmol) and **11** (295 mg, 1.1 mmol) were dissolved in glacial acetic acid (20 mL) and TCM (20 mL). The resulting mixture was stirred at 85℃ for 4 h under the inert atmosphere. After cooling down to RT, the solvent was removed by evaporation under reduced pressure. The crude product was further purified by column chromatography on silica-gel (CH_2Cl_2: petro ether, 1 : 1, *v/v*) to afford **29** as yellow powder (458 mg, yield, 79%). mp: >300℃;^{1}H NMR (600 MHz, $CDCl_3$) δ 7.89 (s, 4H), 4.44 (t, *J* = 6.7 Hz, 4H), 1.85 (p, *J* = 6.7 Hz, 4H), 1.60 (d, *J* = 1.7 Hz, 40H), 1.04 (t, *J* = 7.4 Hz, 6H);^{13}C NMR (150 MHz, $CDCl_3$) δ 164.7, 143.2, 142.7, 142.5, 142.5, 141.9, 140.6, 139.6, 138.9, 135.1, 132.9, 132.9, 131.9, 123.7, 123.7, 107.8, 76.0, 65.9, 31.1, 31.1, 30.6, 28.7, 19.3, 13.8; HRMS ($C_{64}H_{58}N_4O_4Se_3$+H): calculated for: 1161.2075; found: 1161.2089.

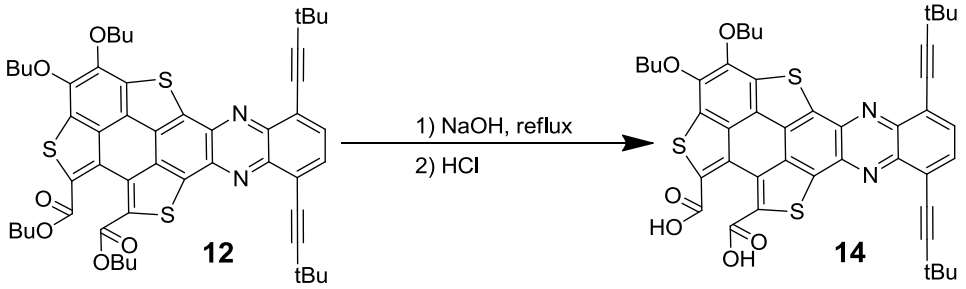

14: Compound **12** (450 mg, 0.5 mmol) and NaOH (400 mg, 10 mmol) were dissolved in the mixed solvent of THF (20 mL)-EtOH (20mL)-H_2O (2 mL), then stirred at 85℃ for 12 h. After cooling down to RT, the reaction was quenched by adding HCl aqueous (3 N) and extracted with CH_2Cl_2 (3 × 50 mL). The organic layers were combined and dried over anhydrous Na_2SO_4, and then concentrated under reduced pressure. The crude product was purified by column chromatography on silica-gel (CH_2Cl_2: MeOH, 3 : 1, *v/v*) to afford **14** as red powder (245 mg, yield, 62%). mp: >300℃; ^{1}H NMR (400 MHz, THF-d_8) δ 7.85 (q, *J* = 7.5 Hz, 2H), 4.56 (t, *J* = 6.4 Hz, 2H), 4.41 (t, *J* = 6.3 Hz, 2H), 1.97 – 1.85 (m, 5H), 1.68 (dt, *J* = 12.4, 4.8 Hz, 4H), 1.56 (d, *J* = 2.5 Hz, 19H), 1.07 (q, *J* = 7.6 Hz, 6H). ^{13}C NMR (150 MHz, THF-d_8) δ 164.0, 148.3, 146.7, 142.4, 142.3, 142.0, 140.9, 140.4, 138.1, 135.5, 134.3, 133.1, 132.7, 132.4, 131.5, 130.9, 130.5, 129.8, 128.5, 127.8, 126.5, 124.4, 124.3, 107.3, 107.2, 77.0, 76.9, 74.0, 73.2, 33.1, 32.8, 31.1, 31.1, 29.1, 29.0, 19.8, 19.7, 13.9, 13.9; HRMS($C_{44}H_{40}N_2O_4S_3$+H): calculated for: 789.2121, found: 789.2147.

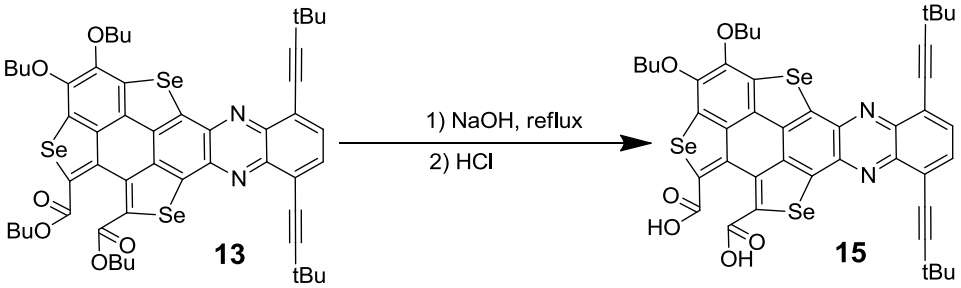

15: Compound **13** (520 mg 0.5 mmol) and NaOH (400 mg, 10 mmol) were dissolved in the mixed solvent of THF (20 mL)-EtOH (20mL)-H_2O (2 mL), then stirred at 85℃ for 12 h. After cooling down to RT, the reaction was quenched by adding HCl aqueous (3 N) and extracted with CH_2Cl_2 (3 × 50 mL). The organic layers were combined and dried over anhydrous Na_2SO_4, and then concentrated under reduced pressure. The crude product was further purified by column chromatography on silica-gel (CH_2Cl_2: MeOH, 3 : 1, *v/v*) to afford **15** as red powder (279 mg , yield, 60%). mp: >300℃; ^{1}H NMR (600 MHz, THF-d_8) δ 7.76 (q, *J* = 7.3 Hz, 2H), 4.37 (t, *J* = 6.3 Hz, 4H), 1.91 – 1.85 (m, 4H), 1.71 – 1.65 (m, 4H), 1.58 (d, *J* = 2.3 Hz, 18H), 1.08 (td, *J* = 7.4, 4.0 Hz, 6H); ^{13}C NMR (150 MHz, THF-d_8) δ 164.8, 149.5, 147.8, 143.1, 142.9, 142.5, 141.6, 141.3, 140.7, 137.8, 137.2, 136.2, 135.9, 135.3, 132.9, 132.5, 132.32, 131.3, 130.8, 130.8, 129.6, 124.4, 124.1, 107.0, 106.9, 77.1, 77.1, 73.6, 73.1, 33.2, 33.0, 31.3, 31.2, 29.1, 19.9, 19.9, 14.0, 13.9; HRMS($C_{44}H_{40}N_2O_4Se_3$+H): calculated for: 931.0440, found: 931.0463.

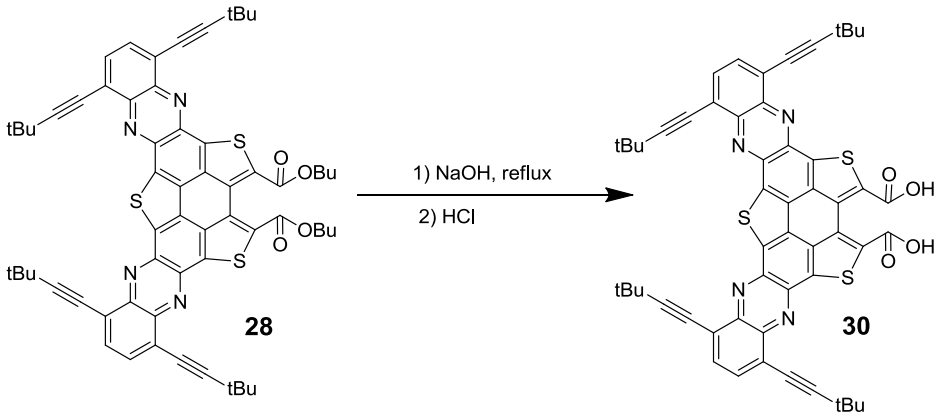

30: Compound **28** (501 mg 0.5 mmol) and NaOH (400 mg, 10 mmol) were dissolved in the mixed solvent of THF (20 mL)-EtOH (20mL)-H_2O (2 mL), then stirred at 85℃ for 12 h. After cooling down to RT, the reaction was quenched by adding HCl aqueous (3 N) and extracted with CH_2Cl_2 (3 × 50 mL). The organic layers were combined and dried over anhydrous Na_2SO_4, and then concentrated under reduced pressure. Due to poor solubility, the crude product was not further purified.

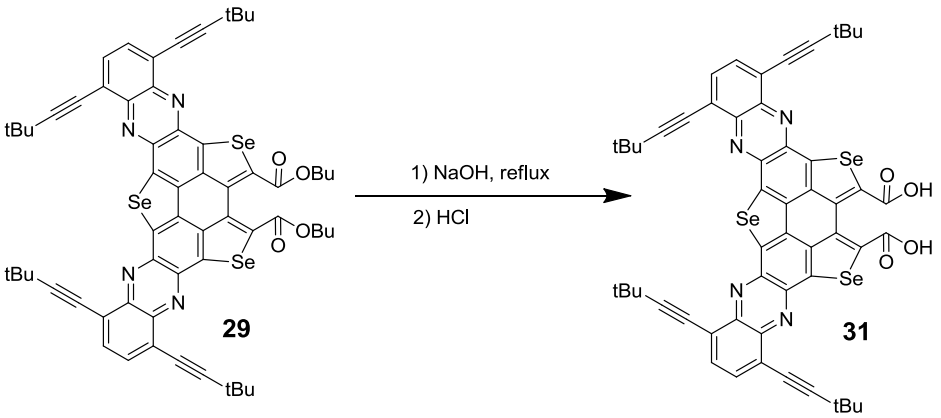

31: Compound **29** (558 mg 0.5 mmol) and NaOH (400 mg, 10 mmol) were dissolved in the mixed solvent of THF (20 mL)-EtOH (20mL)-H_2O (2 mL), then stirred at 85℃ for 12 h. After cooling down to RT, the reaction was quenched by adding HCl aqueous (3 N) and extracted with CH_2Cl_2 (3 × 50 mL). The organic layers were combined and dried over anhydrous Na_2SO_4, and then concentrated under reduced pressure. Due to poor solubility, the crude product was not further purified.

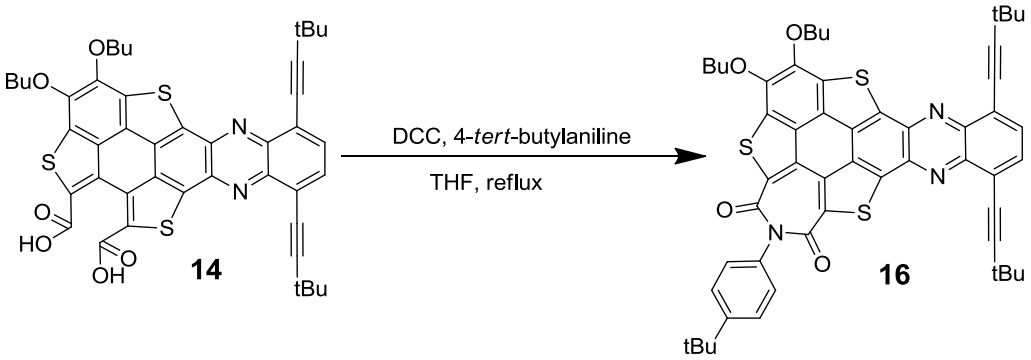

16: Compound **14** (160 mg, 0.2 mmol), 4-*tert*-butylaniline (40 μL, 0.25 mmol) and 1,3-dicyclohexylcarbodiimide (DCC, 412 mg, 2 mmol) were dissolved in anhydrous THF (50 mL). The resulting mixture was stirred at 80 ^oC for 8 h under nitrogen. After cooling down to RT, the reaction was quenched by adding distilled water and extracted with CH_2Cl_2 (3 × 15 mL). The organic layers were combined and dried over anhydrous Na_2SO_4, then concentrated under reduced pressure. The crude product was purified by column chromatography on silica-gel (eluent, CH_2Cl_2: petro ether, 1 : 1, v/v) to afford **16** as red powder (36 mg, yield, 20 %). mp: >300 ^oC; ^1H NMR (400 MHz, $CDCl_3$) δ 7.90 (d, *J* = 7.4 Hz, 1H), 7.80 (d, *J* = 7.4 Hz, 1H), 7.60 (d, *J* = 8.1 Hz, 2H), 7.32 (d, *J* = 8.1 Hz, 2H), 4.59 (t, *J* = 6.5 Hz, 2H), 4.35 (t, *J* = 6.4 Hz, 2H), 1.89 (dt, *J* = 29.1, 7.4 Hz, 4H), 1.57 (d, *J* = 18.1 Hz, 22H), 1.43 (s, 9H), 1.05 (dt, *J* = 14.9, 7.3 Hz, 6H).^{13}C NMR (150 MHz, $CDCl_3$) δ 161.8, 161.7, 150.8, 150.1, 146.28, 142.6, 141.6, 141.3, 140.3, 139.9, 138.5, 137.6, 135.3, 133.7, 133.6, 133.3, 132.5, 131.6, 130.2, 129.5, 127.6, 127.4, 127.3, 126.5, 125.9, 123.9, 123.6, 108.6, 1078.0, 34.7, 32.3, 32.1, 31.5, 31.1, 31.0, 29.7, 28.7, 19.2, 19.2, 13.9, 13.9; HRMS($C_{54}H_{51}N_3O_4S_3$+H): calculated for: 902.3114, found: 902.3101.

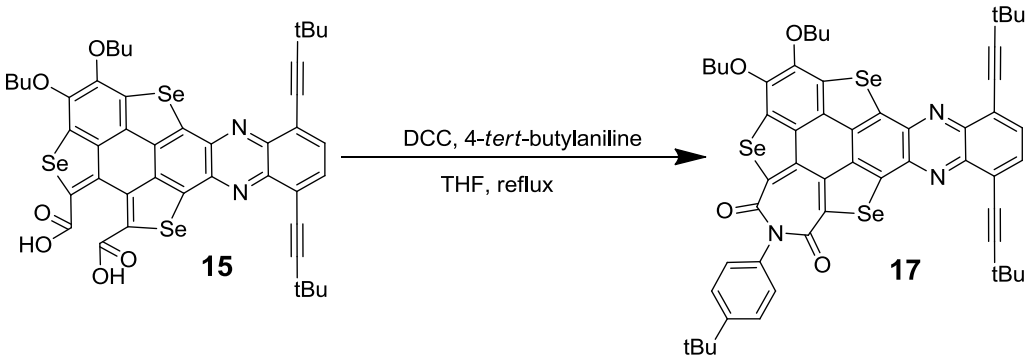

17: Compound **15** (190 mg, 0.2 mmol), 4-*tert*-butylaniline(40 μL, 0.25 mmol) and DCC (412 mg, 2 mmol) were dissolved in anhydrous THF (50 mL). The resulting mixture was stirred at 80 °C for 8 h under nitrogen. After cooling down to RT, the reaction was quenched by adding distilled water and extracted with CH_2Cl_2 (3 × 50 mL). The organic layers were combined and dried over anhydrous Na_2SO_4, then concentrated under reduced pressure. The crude product was further purified by column chromatography on silica-gel (CH_2Cl_2: petro ether, 1 : 1, v/v) to afford **17** as red powder (53 mg, yield, 25%). mp: >300 °C;^{1}H NMR (400 MHz, $CDCl_3$) δ 7.79 (d, *J* = 7.3 Hz, 1H), 7.63 (d, *J* = 7.4 Hz, 1H), 7.57 (d, *J* = 8.2 Hz, 2H), 7.35 (d, *J* = 8.1 Hz, 2H), 4.37 (t, *J* = 6.4 Hz, 2H), 4.15 (t, *J* = 6.3 Hz, 2H), 1.88 – 1.75 (m, 4H), 1.58 (d, *J* = 15.8 Hz, 22H), 1.45 (s, 9H), 1.03 (dt, *J* = 10.4, 7.3 Hz, 6H).^{13}C NMR (150 MHz, $CDCl_3$) δ 162.5, 162.5, 150.9, 150.7, 147.8, 145.7, 142.8, 142.4, 142.1, 141.5, 141.0, 140.1, 137.4, 136.5, 135.0, 133.6, 133.2, 132.9, 132.2, 131.1, 130.8, 130.7, 130.1, 129.3, 127.5, 126.3, 123.6, 123.5, 108.2, 107.7, 76.3, 75.7, 73.0, 72.1, 34.7, 32.4, 31.5, 31.1, 28.7, 19.3, 13.9. HRMS($C_{54}H_{51}N_3O_4Se_3$+H): calculated for: 1044.1456, found: 1044.1461.

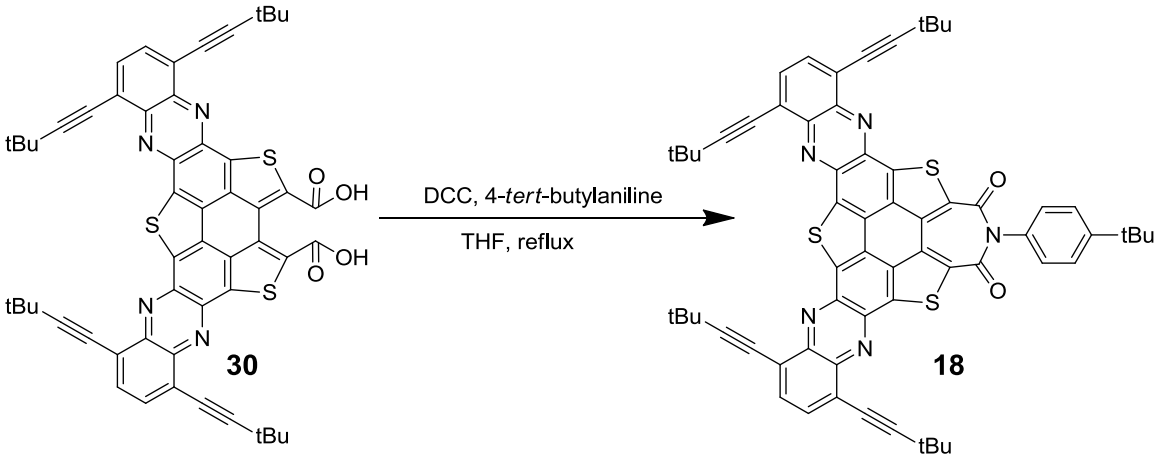

18: Compound **30** (182 mg, 0.2 mmol), 4-*tert*-butylaniline(40 μL, 0.25 mmol) and DCC (412 mg, 2 mmol) were dissolved in anhydrous THF (50 mL). The resulting mixture was stirred at 80 °C for 8 h under nitrogen. After cooling down to RT, the reaction was quenched by adding distilled water and extracted with CH_2Cl_2 (3 × 50 mL). The organic layers were combined and dried over anhydrous Na_2SO_4, then concentrated under reduced pressure. The crude product was further purified by column chromatography on silica-gel (CH_2Cl_2: petro ether, 2 : 1, v/v) to afford **18** as red powder (37 mg, yield, 18%). mp: >300 °C;^{1}H NMR (400 MHz, $CDCl_3$) δ 7.87 (s, 4H), 7.62 (d, *J* = 8.5 Hz, 2H), 7.36 (d, *J* = 8.3 Hz, 2H), 1.55 (s, 18H), 1.43 (s, 9H).^{13}C NMR (150 MHz, $CDCl_3$) δ 161.9, 151.1, 143.1,

142.4, 141.4, 140.8, 139.9, 139.0, 137.7, 134.1, 133.50, 133.1, 130.6, 127.7, 127.5, 126.6, 124.0, 123.7, 108.9, 108.3, 75.7, 75.6, 34.8, 31.5, 31.1, 31.1, 31.0, 29.7, 28.8, 28.7. HRMS($C_{64}H_{53}N_5O_5Se_3$+H): calculated for: 1020.3434, found: 1020.3434.

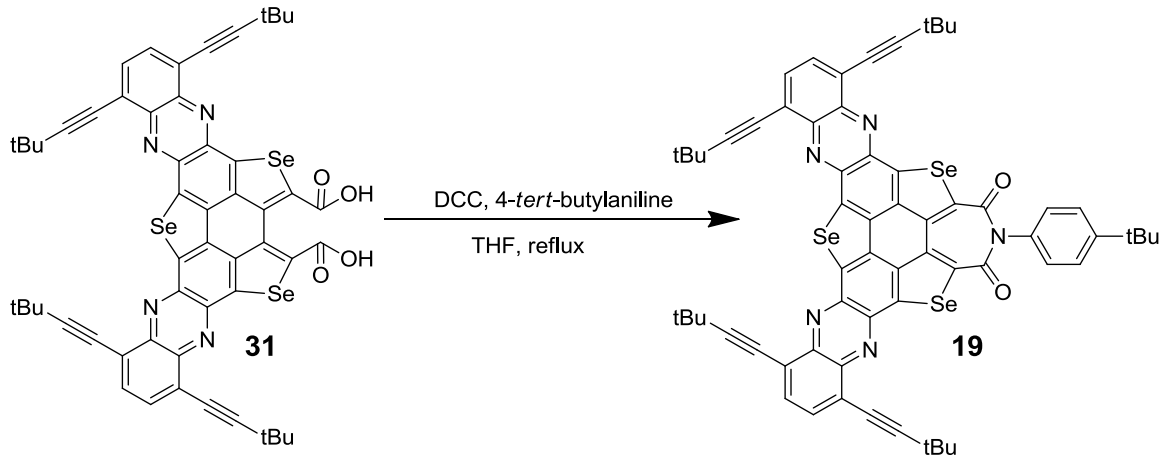

19: Compound **31** (210 mg, 0.2 mmol), 4-*tert*-butylaniline(40 μL, 0.25 mmol) and DCC (412 mg, 2 mmol) were dissolved in anhydrous THF (50 mL). The resulting mixture was stirred at 80 °C for 8 h under nitrogen. After cooling down to RT, the reaction was quenched by adding distilled water and extracted with CH_2Cl_2 (3 × 50 mL). The organic layers were combined and dried over anhydrous Na_2SO_4, then concentrated under reduced pressure. The crude product was further purified by column chromatography on silica-gel (CH_2Cl_2: petro ether, 2 : 1, v/v) to afford **17** as red powder (35 mg, yield, 15%). mp: >300 °C; ^{1}H NMR (400 MHz, $CDCl_3$ with 2 drops D-TFA) δ 7.97 – 7.86 (m, 4H), 7.64 (d, *J* = 8.2 Hz, 2H), 7.38 (d, *J* = 8.1 Hz, 2H), 1.58 (d, *J* = 3.0 Hz, 36H), 1.42 (s, 9H).; Due to poor solubility, we failed to obtain ^{13}C NMR. HRMS($C_{64}H_{53}N_5O_5Se_3$+H): calculated for: 1162.1776, found: 1162.1801.

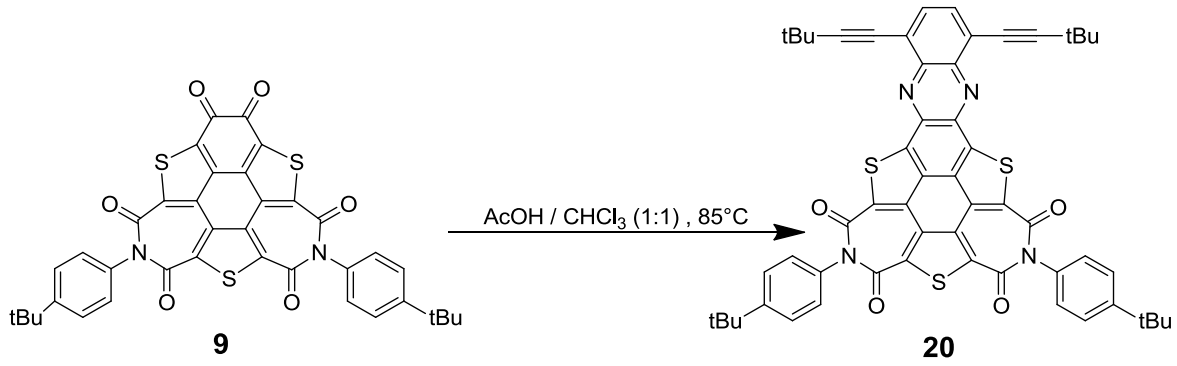

20: Compound **9** (70 mg, 0.1 mmol) and **11** (32mg, 0.12 mmol) were dissolved in glacial acetic acid (20 mL) and TCM (20 mL). The resulting mixture was stirred at 85℃ for 4 h under the inert atmosphere. After cooling down to RT, the solvent was removed by evaporation under reduced pressure. The crude product was further purified by column chromatography on silica-gel (CH_2Cl_2: petro ether, 2 : 1, *v/v*) to afford **20** as yellow powder (80 mg, yield, 85%). mp: >300℃; ^{1}H NMR (600 MHz, Chloroform-*d*) δ 7.86 (s, 1H), 7.60 (d, *J* = 8.3 Hz, 2H), 7.26 (d, *J* = 7.3 Hz, 4H), 1.54 (s, 9H), 1.43 (s, 9H). ^{13}C NMR (151 MHz, $CDCl_3$) δ 161.0, 160.7, 151.5, 141.7, 141.6, 140.9, 138.5, 138.2,

136.3, 133.8, 132.2, 129.8, 127.3, 126.7, 125.8, 124.0, 109.3, 75.3, 34.8, 31.4, 31.0, 28.8.HRMS ($C_{56}H_{46}N_4O_4S_3$+H): calculated for: 935.2754; found: 935.2751.

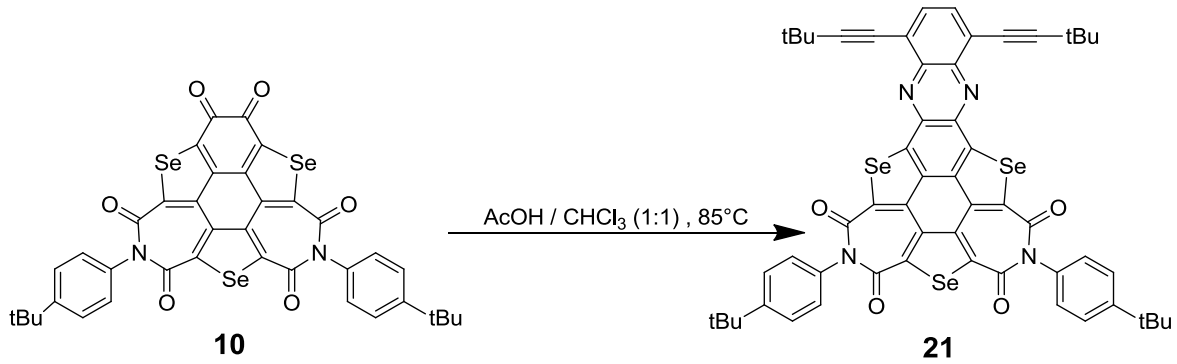

20: Compound **9** (85mg, 0.1 mmol) and **11** (32mg, 0.12 mmol) were dissolved in glacial acetic acid (20 mL) and TCM (20 mL). The resulting mixture was stirred at 85℃ for 4 h under the inert atmosphere. After cooling down to RT, the solvent was removed by evaporation under reduced pressure. The crude product was further purified by column chromatography on silica-gel (CH_2Cl_2: petro ether, 2 : 1, *v/v*) to afford **20** as yellow powder (90 mg, yield, 86%). mp: >300℃; ^{1}H NMR (600 MHz, Chloroform-*d*) δ 7.75 (s, 1H), 7.57 (d, *J* = 8.5 Hz, 2H), 7.25 (s, 1H), 1.55 (s, 9H), 1.43 (s, 10H). ^{13}C NMR (151 MHz, $CDCl_3$) δ 161.9, 161.8, 151.5, 149.5, 145.0, 143.1, 142.4, 140.8, 136.2, 136.0, 133.5, 133.3, 129.9, 127.2, 126.6, 123.8, 109.1, 75.5, 34.8, 31.4, 31.1, 31.1, 28.8.HRMS ($C_{56}H_{46}N_4O_4Se_3$+H): calculated for:1077.1095; found: 1077.1096.

3. Crystal Structure Analysis

3.1 Experimental details on crystal growth

The single crystals of **4** (black needle), and **6** (black needle) were obtained by slowly evaporating their CH_2Cl_2-MeOH (1 : 1, *v*/*v*), CH_2Cl_2 solutions at room temperature, respectively.

Selected crystallographic data of **4** and **6**.

	4	**6**
CCDC number	2057108	2057109
Empirical formula	$C_{68}H_{72}O_{16}Se_6$	$C_{26}H_{18}O_8Se_3$
Formula weight	1619.01	695.31
Temperature [K]	150.00(10)	173.00
λ [Å]	1.54184(Cu- Kα)	0.71073(Mo-Kα)
Crystal size [mm^3]	0.07×0.04×0.02	0.4×0.2×0.1
Crystal system	monoclinic	triclinic
space group	$P2_1/c$	P-1
a [Å]	16.2433(4)	8.7375(5)
b [Å]	19.4044(5)	9.6492(7)
c [Å]	21.7744(6)	15.5120(12)
α [°]	90	107.499(7)
β [°]	108.927(3)	98.427(6)
γ [°]	90	99.971(5)
V [$Å^3$]	6492.0(3)	1200.68(16)
Z	4	2
d_{calc} [g cm^{-3}]	1.656	1.9231
μ [mm^{-1}]	4.561	4.647
2θmax [°]	152.402	57.26
Data/restraints/parameters	12821/65/893	5440/0/336
GooF	1.043	1.021
R [$I > 2\sigma(I)$]	0.071	0.0540
wR_2	0.1801	0.0888

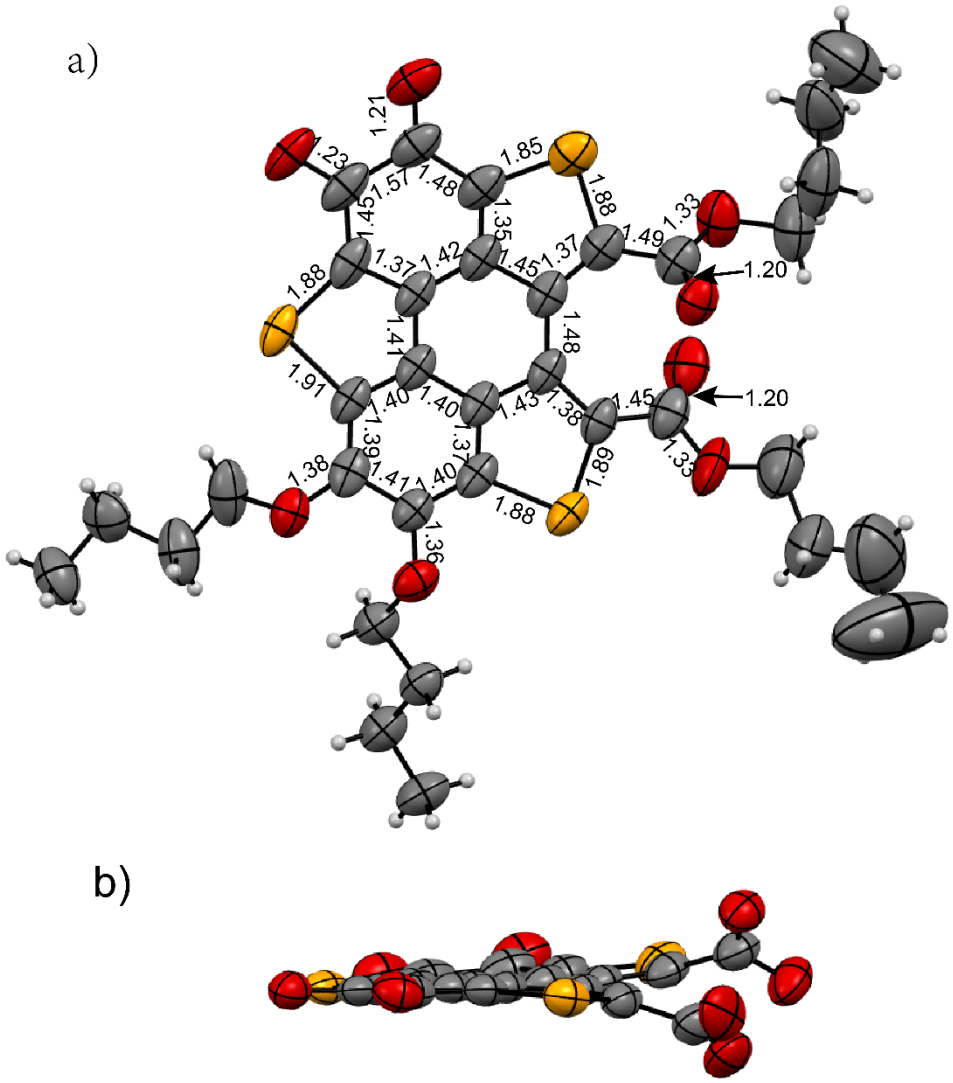

Figure S1. a) Top view and b) side view of compound **4**. The selected bond lengths are in unit of Å. The *n*-Bu groups and H atoms are omitted for clarity in b).The cyan, grey, red, yellow balls represent hydrogen, carbon, oxygen, and selenium atoms, respectively.

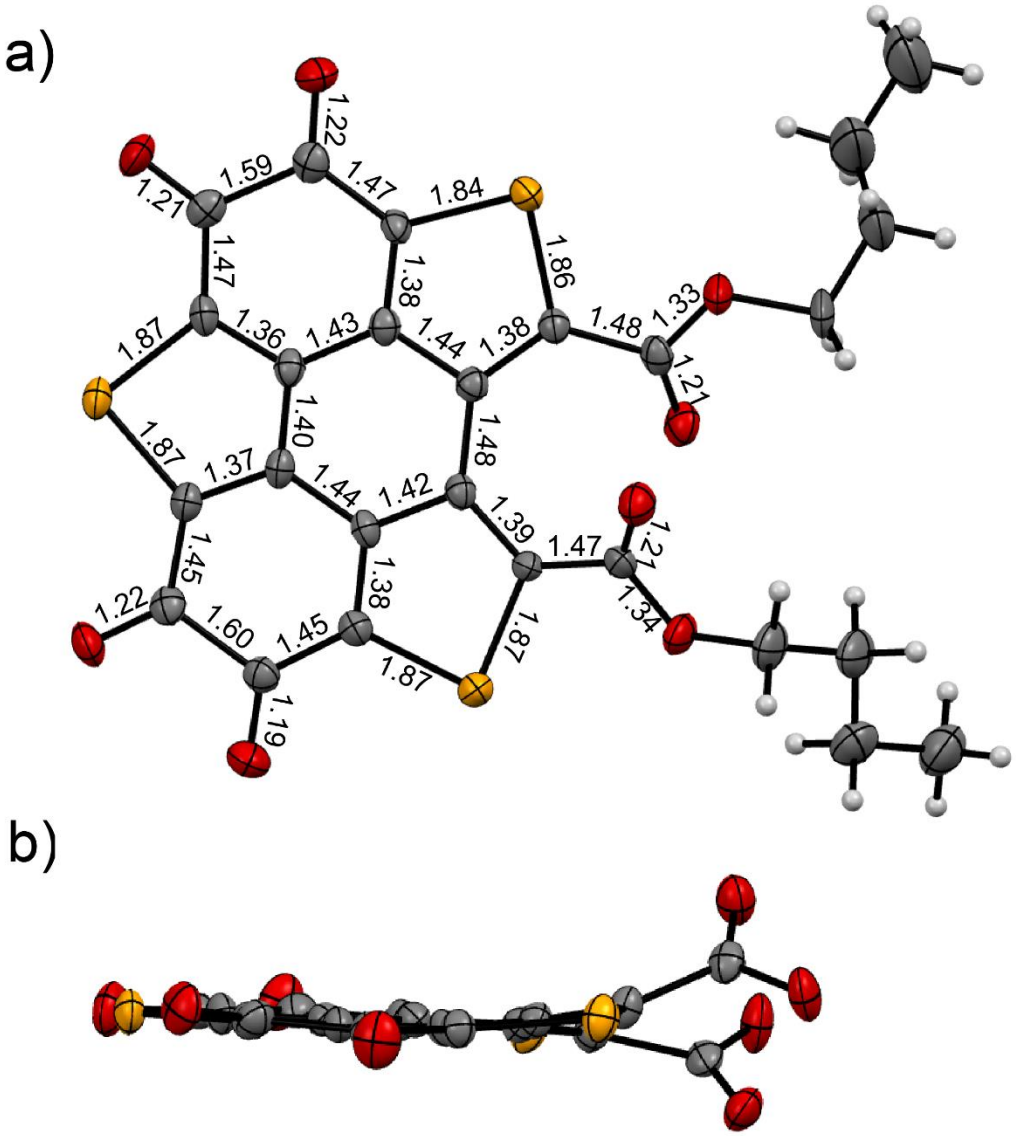

Figure S2. a) Top view and b) side view of compound **6**. The selected bond lengths are in unit of Å. The *n*-Bu groups and H atoms are omitted for clarity in b). The cyan, grey, red, yellow balls represent hydrogen, carbon, oxygen, and selenium atoms, respectively.

4. Photophysical Study

4.1 Spectroelectrochemistry of 3, 4, 5, 6, 9, and 10

The in-situ investigation of the absorption spectra of **3, 4, 5, 6, 9,** and **10** under constant electrochemical reduction potential was performed on a Zahner CIMPS type photo-electrochemical workstation using a standard three-electrode electrochemical cell with an transparent indium tin oxide (ITO) as the working electrode, Pt rod as the counter electrode, a SCE as the reference electrode and a tungsten halogen lamp (500 W) as light source. Measurement conditions: solvent, CH_2Cl_2; concentration, 1×10^{-4} mol L^{-1}; supporting electrolyte, $(n\text{-Bu})_4NPF_6$ (0.1 M); temperature, 20 ºC.

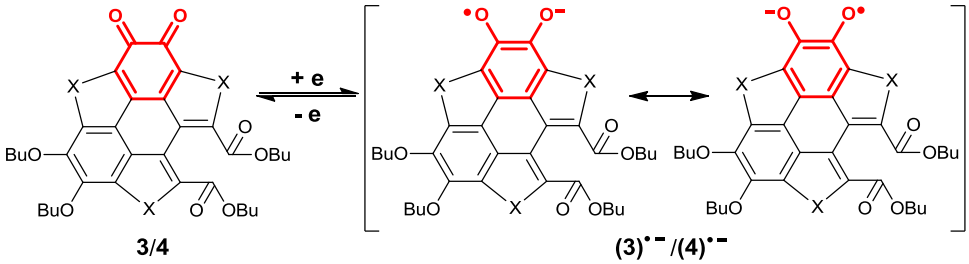

Scheme S1. The reaction of **3/4** under the electrochemical condition.

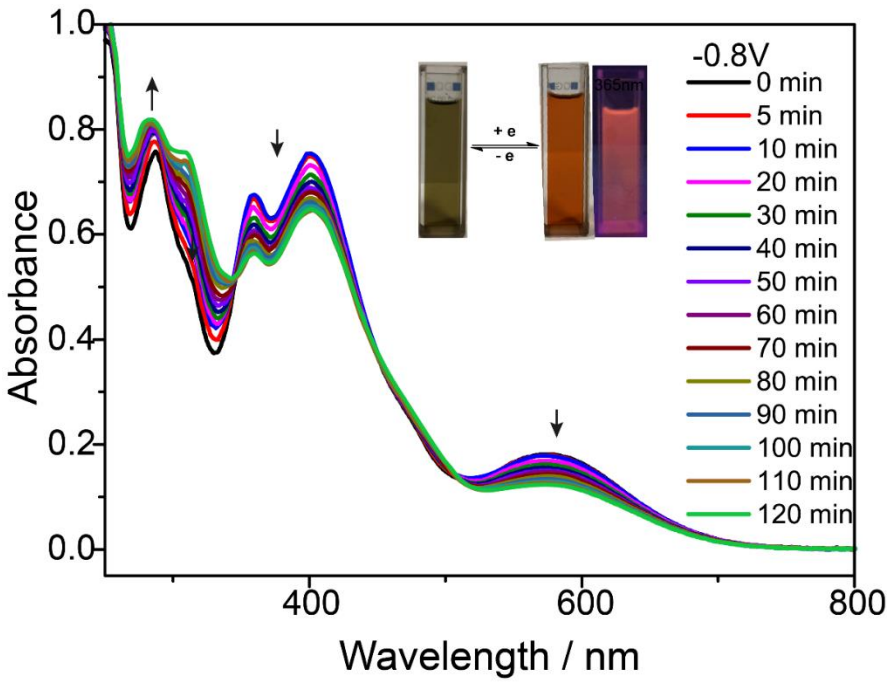

Figure S3. Time-dependent UV-Vis spectra of **3** in CH_2Cl_2 (10^{-4} mol L^{-1}) under reduction potential of -0.8 V, along with the photographs of **3** in CH_2Cl_2 (10^{-4} mol L^{-1}) before and after reduction.

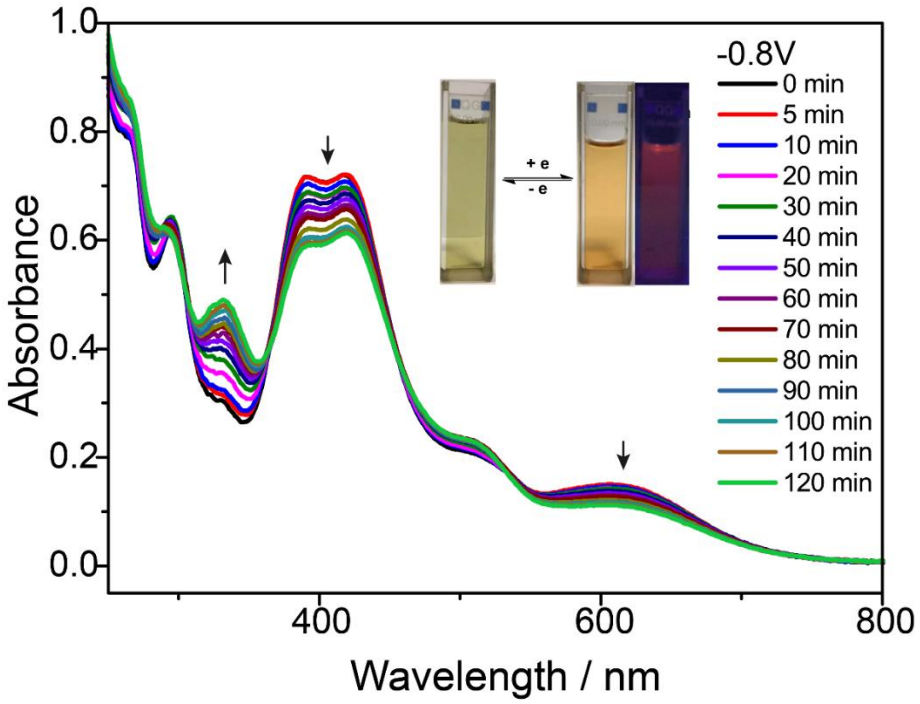

Figure S4. Time-dependent UV-Vis spectra of **4** in CH_2Cl_2 (10^{-4} mol L^{-1}) under reduction potential of -0.8 V, along with the photographs of **4** in CH_2Cl_2 (10^{-4} mol L^{-1}) before and after reduction.

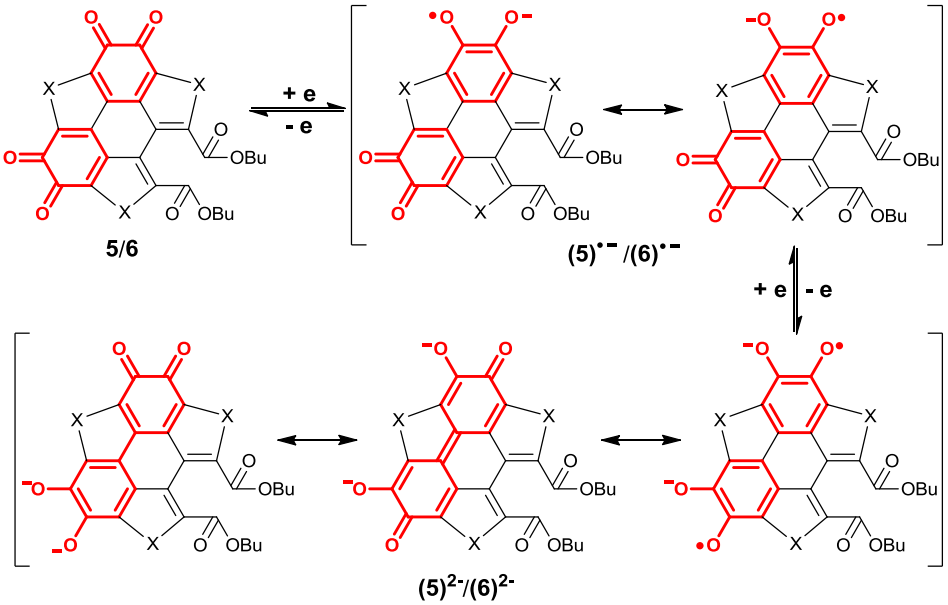

Scheme S2. The reaction of **5/6** under the electrochemical condition.

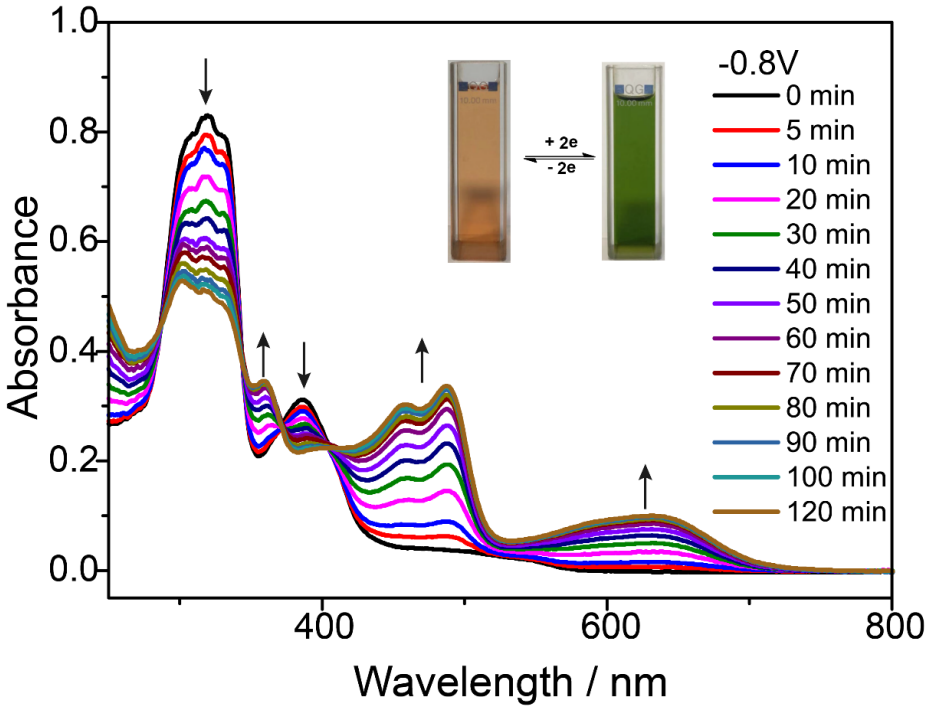

Figure S5. Time-dependent UV-Vis spectra of **5** in CH_2Cl_2 (10^{-4} mol L^{-1}) under reduction potential of -0.8 V, along with the photographs of **5** in CH_2Cl_2 (10^{-4} mol L^{-1}) before and after reduction.

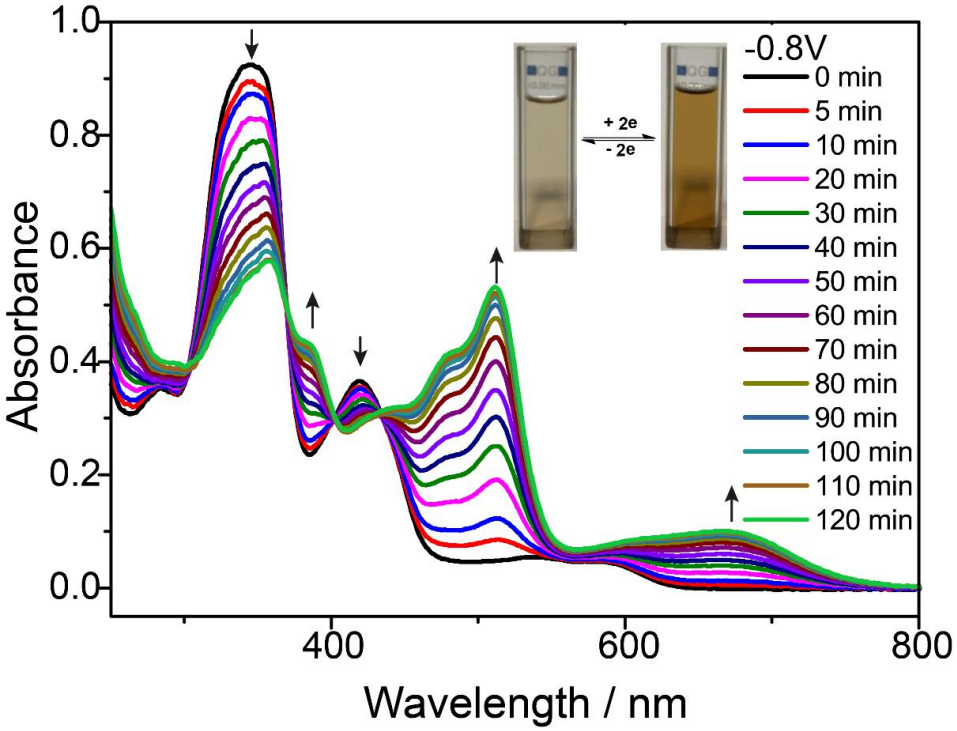

Figure S6. Time-dependent UV-Vis spectra of **6** in CH_2Cl_2 (10^{-4} mol L^{-1}) under reduction potential of -0.8 V, along with the photographs of **6** in CH_2Cl_2 (10^{-4} mol L^{-1}) before and after reduction.

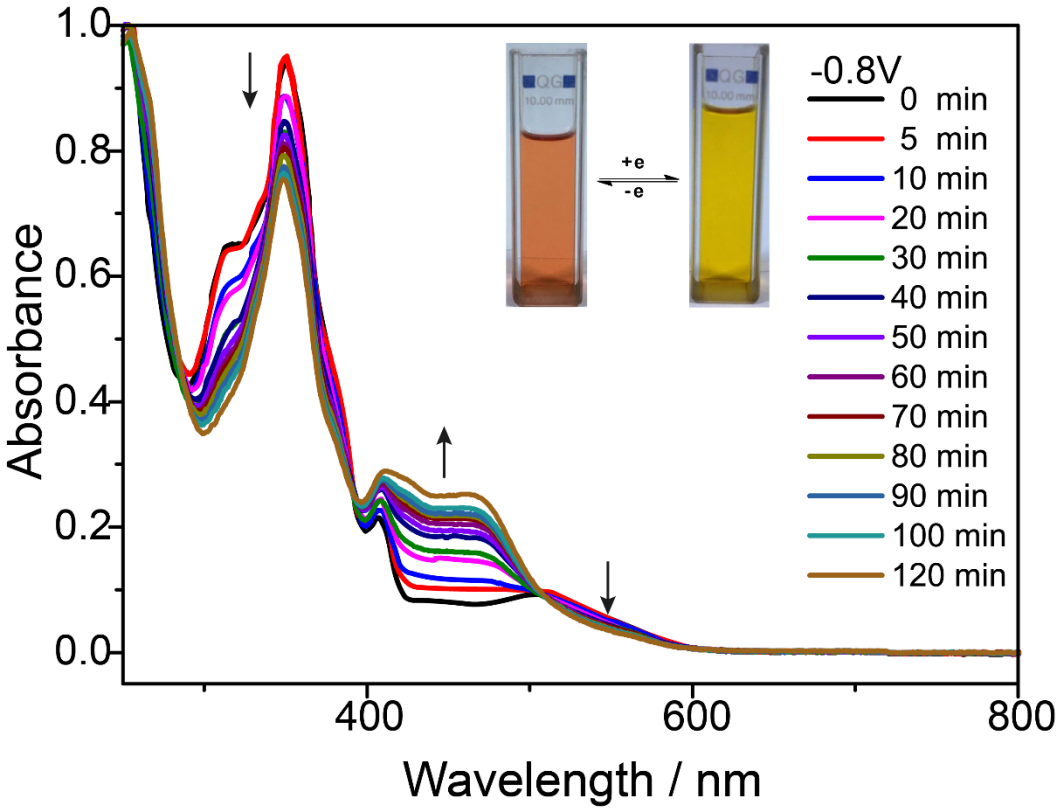

Figure S7. Time-dependent UV-Vis spectra of **9** in CH_2Cl_2 (10^{-4} mol L^{-1}) under reduction potential of -0.8 V, along with the photographs of **9** in CH_2Cl_2 (10^{-4} mol L^{-1}) before and after reduction.

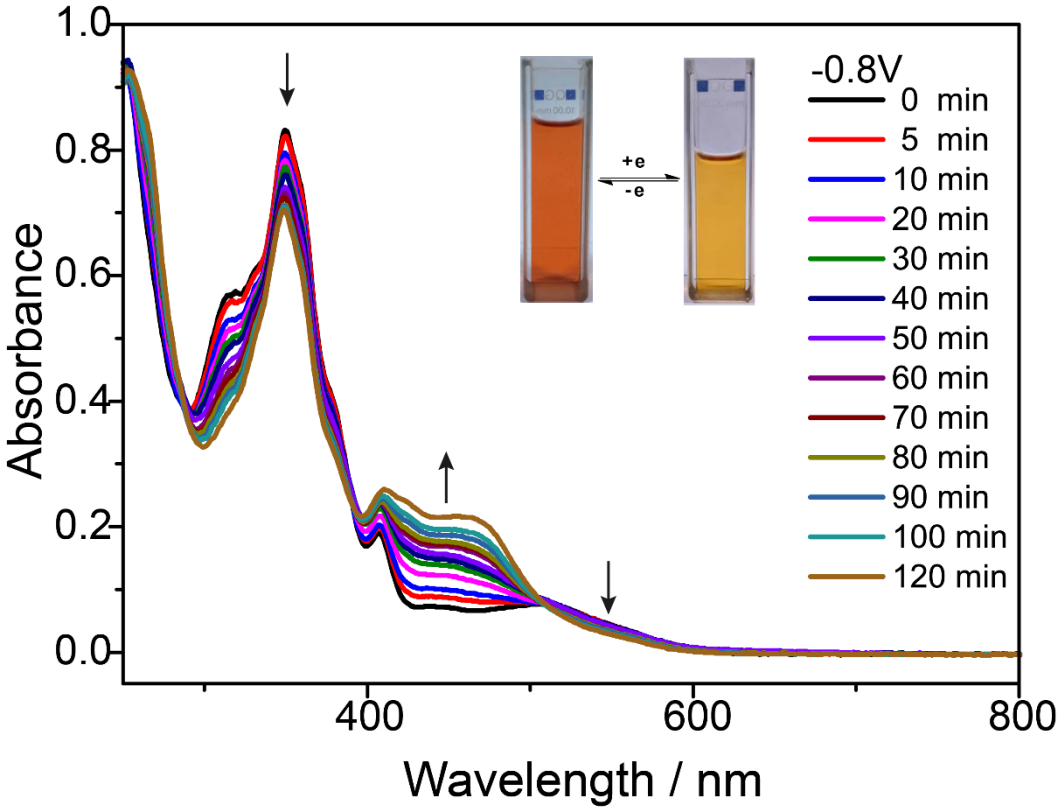

Figure S8. Time-dependent UV-Vis spectra of **10** in CH_2Cl_2 (10^{-4} mol L^{-1}) under reduction potential of -0.8 V, along with the photographs of **10** in CH_2Cl_2 (10^{-4} mol L^{-1}) before and after reduction.

4.2 UV-Vis spectra

The UV-Vis spectra of the compounds so far obtained were measured in their dichloromethane (CH_2Cl_2) solution (c=1.0 ×10^{-5} mol L^{-1}) at 20℃ on a UV-2600 UV-Vis spectrometer (Shimadzu).

Table S1. UV-Vis spectra of compounds **1-10, 16-25** in CH_2Cl_2 solution.

Comp.	λ_{max}/nm	log ε	λ_{max}/nm	log ε	λ_{max}/nm	log ε	λ_{max}/nm	log ε
1	314	4.91	345	4.35				
2	312	4.82	341	4.36				
3	287	4.26	360	4.22	402	4.27	578	3.65
4	295	4.23	393	4.30	419	4.30	610	3.60
5	319	4.70	387	4.27				
6	350	4.45	423	4.05				
7	321	4.50	393	4.36	424	4.34		
8	262	4.61	335	4.27	413	4.43	437	4.39
9	350	4.53	408	3.89	506	3.52		
10	350	4.51	406	3.93	510	3.49		
16	298	4.67	336	4.46	404	4.36	429	4.40
17	306	4.72	343	4.53	440	4.60		
18	284	4.93	379	4.86	399	4.86		
19	286	4.92	350	4.62	396	4.83	412	4.86
20	274	4.69	350	4.73	380	4.70		
21	278	4.80	378	4.80	396	4.79		
22	268	4.79	313	5.01	378	4.71	496	4.37
23	278	4.72	311	4.86	379	4.68	487	4.27
24	304	4.33	364	4.67	449	4.06	514	4.09
25	302	4.35	358	4.69	434	3.93	502	3.94

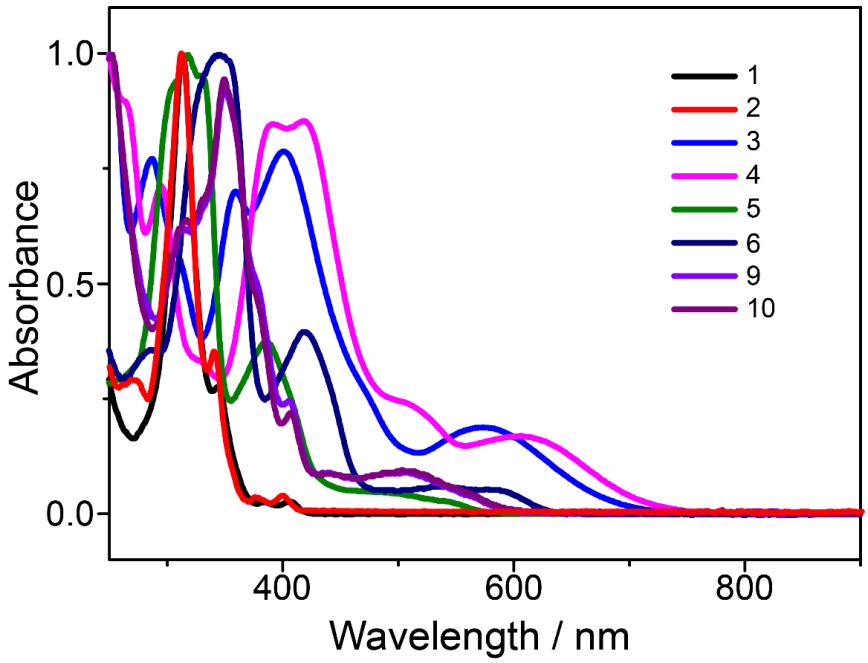

Figure S9. UV-Vis absorption spectra of **1-6, 9-10** in CH_2Cl_2 (10^{-5} mol L^{-1}) at 20℃.

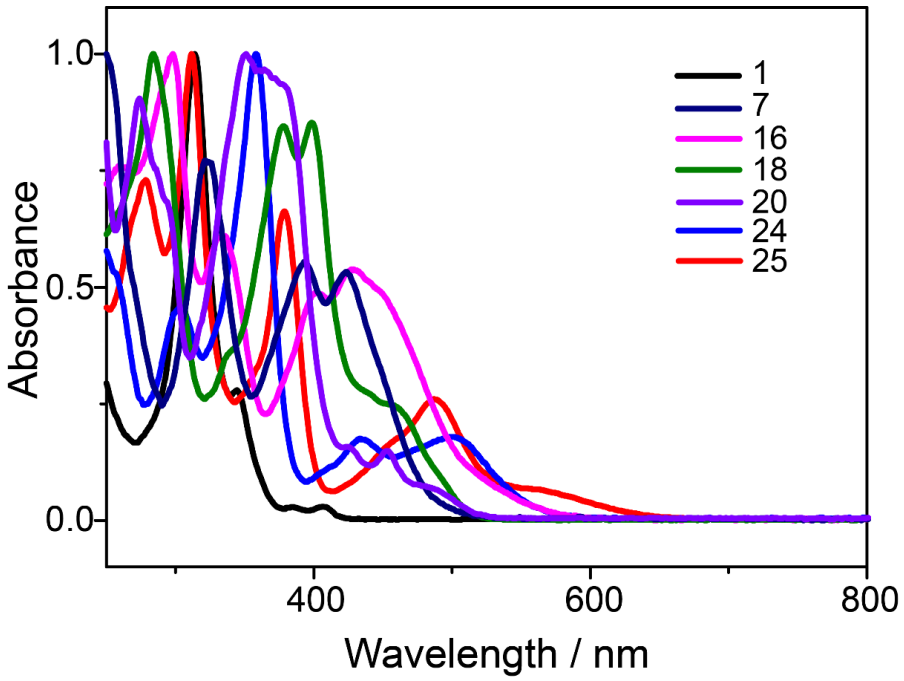

Figure S10. UV-Vis absorption spectra of **1, 7, 16, 18, 20, 24, 25** in CH_2Cl_2 (10^{-5} mol L^{-1}) at 20℃.

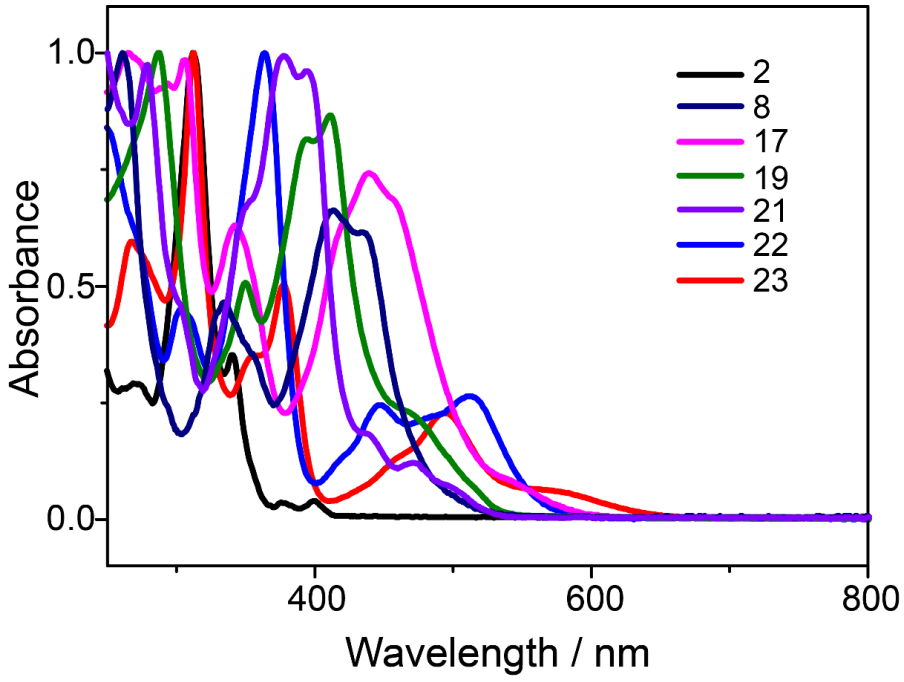

Figure S11. UV-Vis absorption spectra of **2, 8, 17, 19, 21-23**in CH_2Cl_2 (10^{-5} mol L^{-1}) at 20℃.

4.3 Fluorescence

Fluorescence excitation and emission spectra were recorded with an RF-5301(pc)s Spectrofluorophotometer, fluorescence lifetime and steady state were measured on FLS920 Spectrofluorophotometer. Measurement conditions: solvent, CH_2Cl_2; concentration, 10^{-4} mol L^{-1}, temperature, 20℃.

Table S2. The emission and excitation properties of compounds **16-19, 22-23** in CH_2Cl_2 solution.

Comp.	λ_{ex} / nm	λ_{em} / nm	Stocks shift /cm^{-1}	Φ_F / %	τ_1 /ns	τ_2 /ns	τ_3 /ns
16	533	691	4289	1.69	1.11(96.5%)	5.81(3.5%)	
17	535	637	2993	0.15	0.35(30.5%)	4.17(43%)	9.74(26.5%)
18	493	556	2298	5.71	3.99(100%)		
19	500	571	2486	0.13	0.19(73.7%)	4.08(26.3%)	
22	536	638	2982	17.22	6.42(100%)		
24	525	638	3373	43.2	19.20(100%)		

λ_{ex}: excitation wavelength; λ_{em}: maximum emission wavelength; Φ_F: fluorescence quantum yield; τ_1: fluorescence lifetime

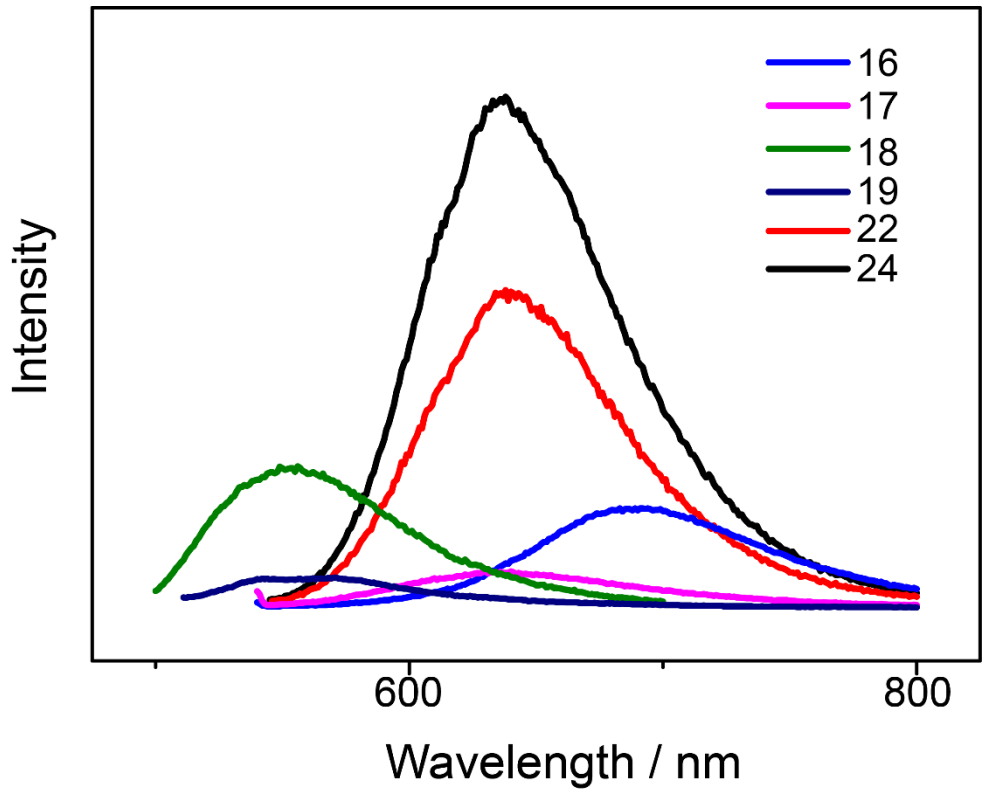

Figure S12. Emission spectra of **16-19, 22, 24** in CH_2Cl_2 (10^{-4} mol L^{-1}) at 20℃.

5. Thermogravimetric Analyses (TGA)

Thermogravimetric analyses (TGA) were conducted on 1090B type thermal analyzer (Dupont Engineering polymers).

Table S3. Thermal stability of compounds **16, 18, 20, 22 and 24**.

Comp.	**16**	**18**	**20**	**24**	**25**
T_d / ℃	340	356	394	332	318

T_d: degradation temperature

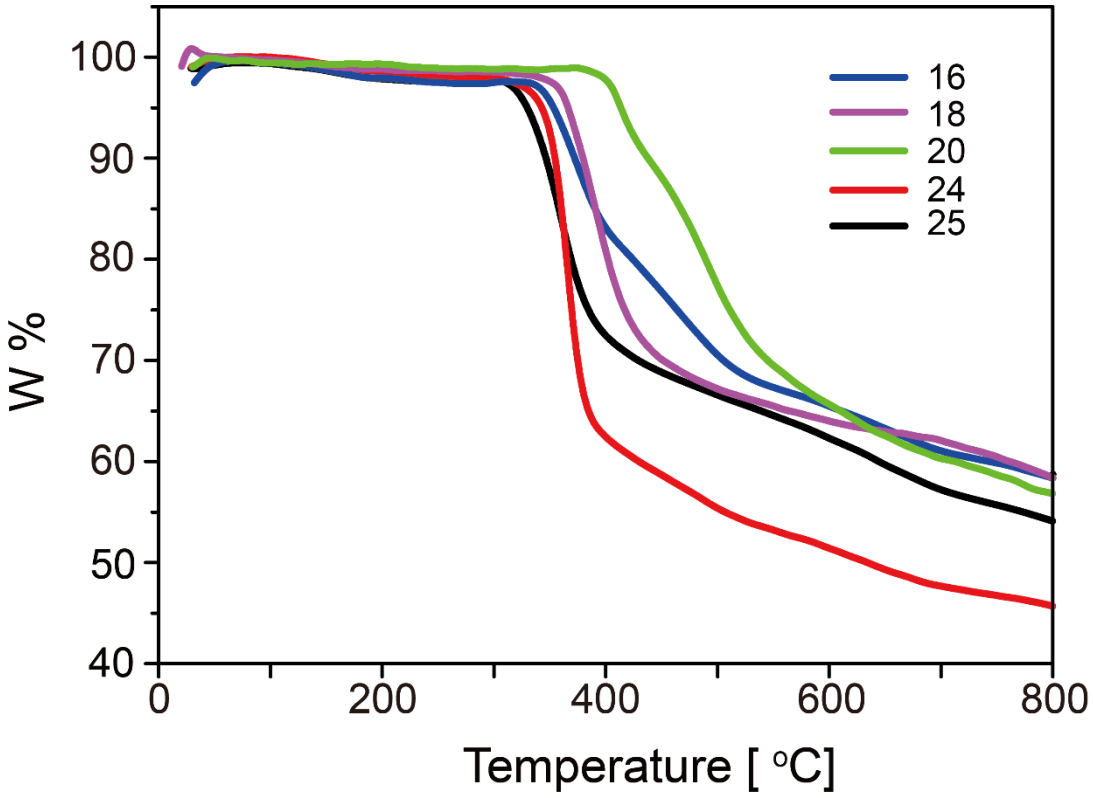

Figure S13. Thermogravimetric analyses of compounds **16, 18, 20, 22, 24, 25.**

Table S4. Thermal stability of compounds **17, 19, 21, 23 and 25**.

Comp.	**17**	**19**	**21**	**22**	**23**
T_d / ℃	355	392	403	337	327

T_d: degradation temperature

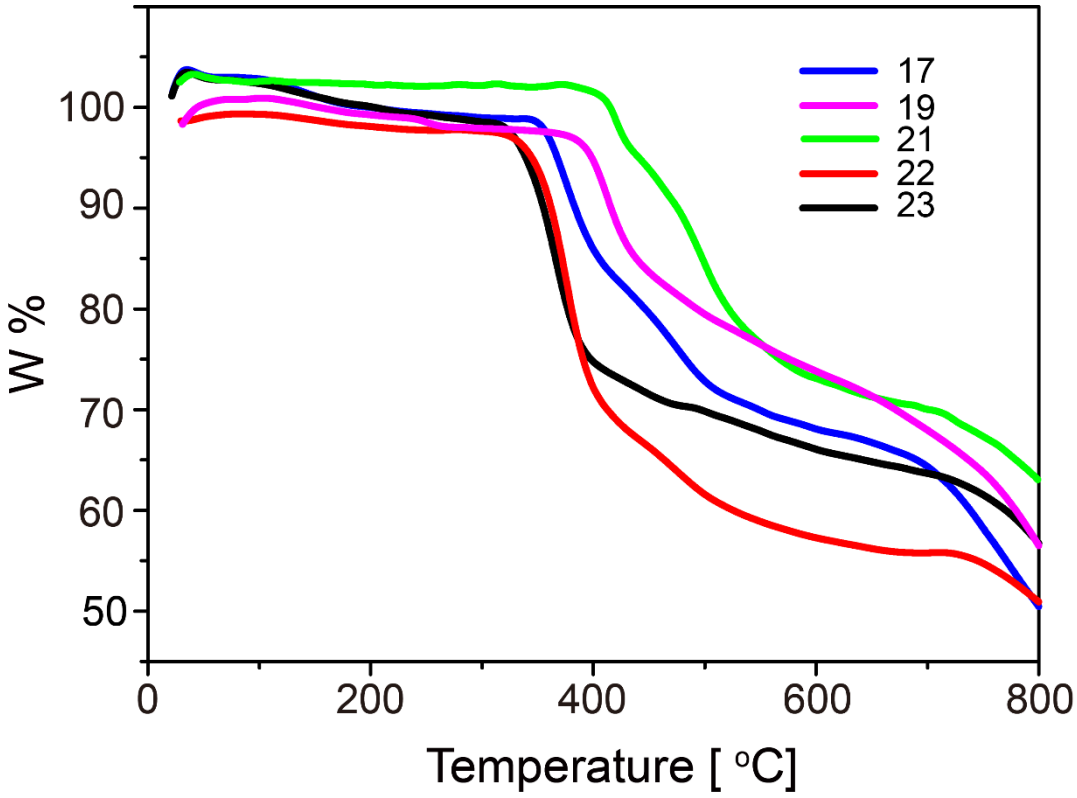

Figure S14. Thermogravimetric analyses of compounds **17, 19, 21, 22, 23.**

6. Electrochemical spectra

The redox potentials were obtained by CV and DPV methods on RST 5000 electrochemical analyzer with glassy carbon discs as the working electrode, Pt wire as the counter electrode, and SCE electrode as the reference electrode. Measurement conditions: solvent, CH_2Cl_2; concentration, 1×10^{-4} mol L^{-1}; supporting electrolyte, $(n\text{-Bu})_4NPF_6$ (0.1 M); scan speed, 50 mV S^{-1}; temperature, 20℃.

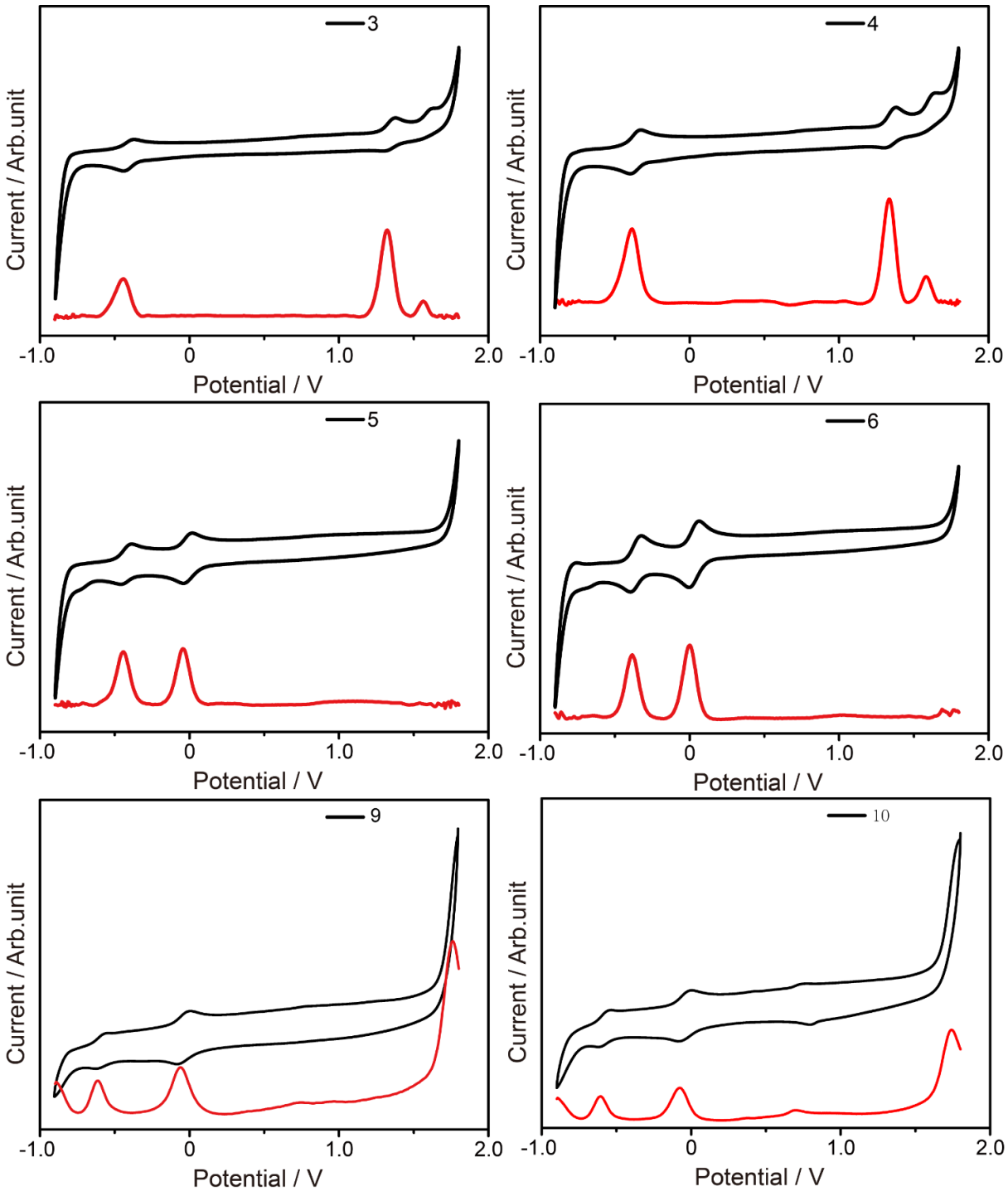

Figure S15. CV and DPV of **3, 4, 5, 6, 7, 9**, and **10** in CH_2Cl_2 ($c = 10^{-4}$ mol L^{-1}) at RT. Reference electrode: SCE.

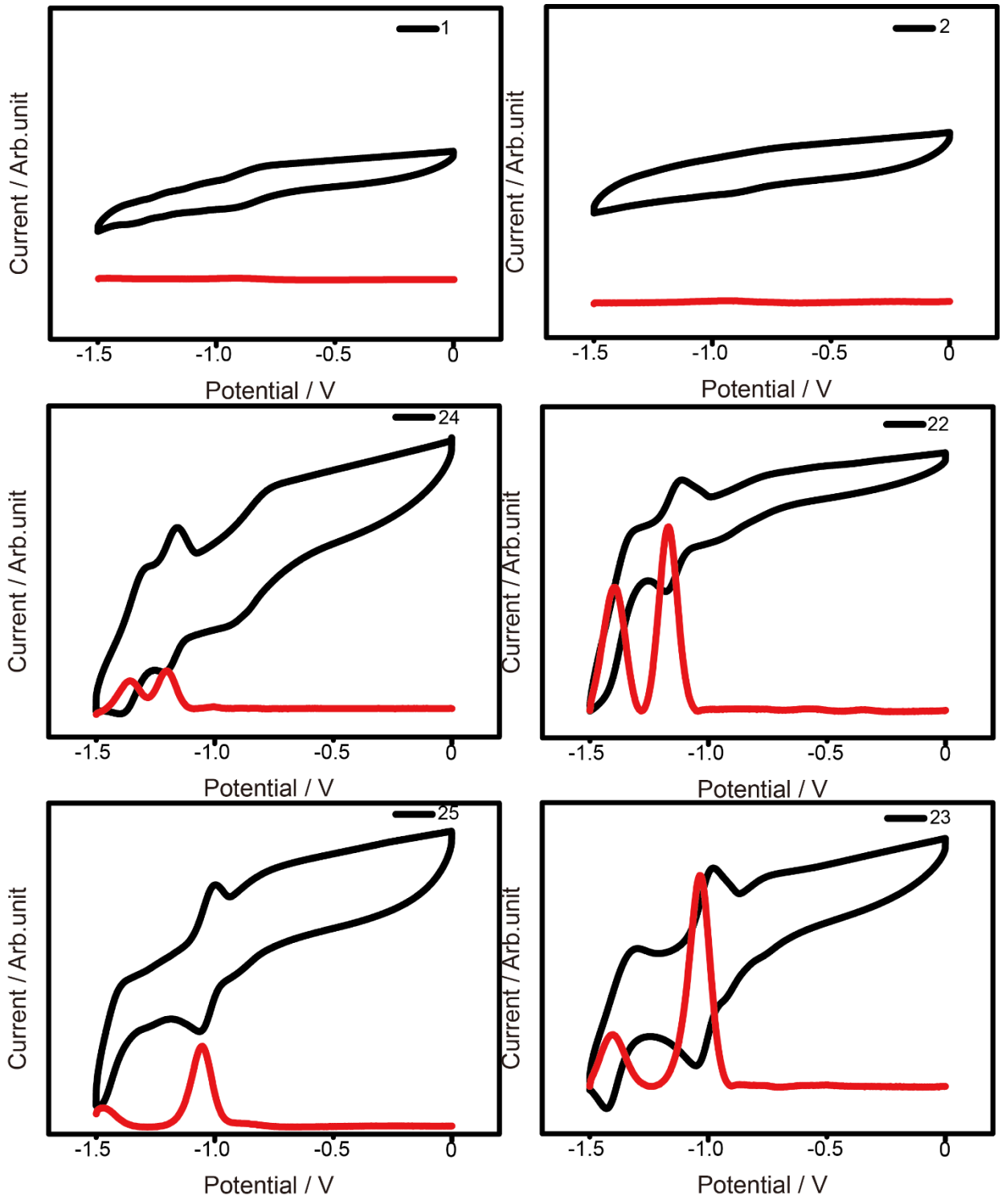

Figure S16. CV and DPV of **1-2** and **22-25** in CH_2Cl_2 (c = 10^{-4} mol L^{-1}) at RT. Reference electrode: SCE.

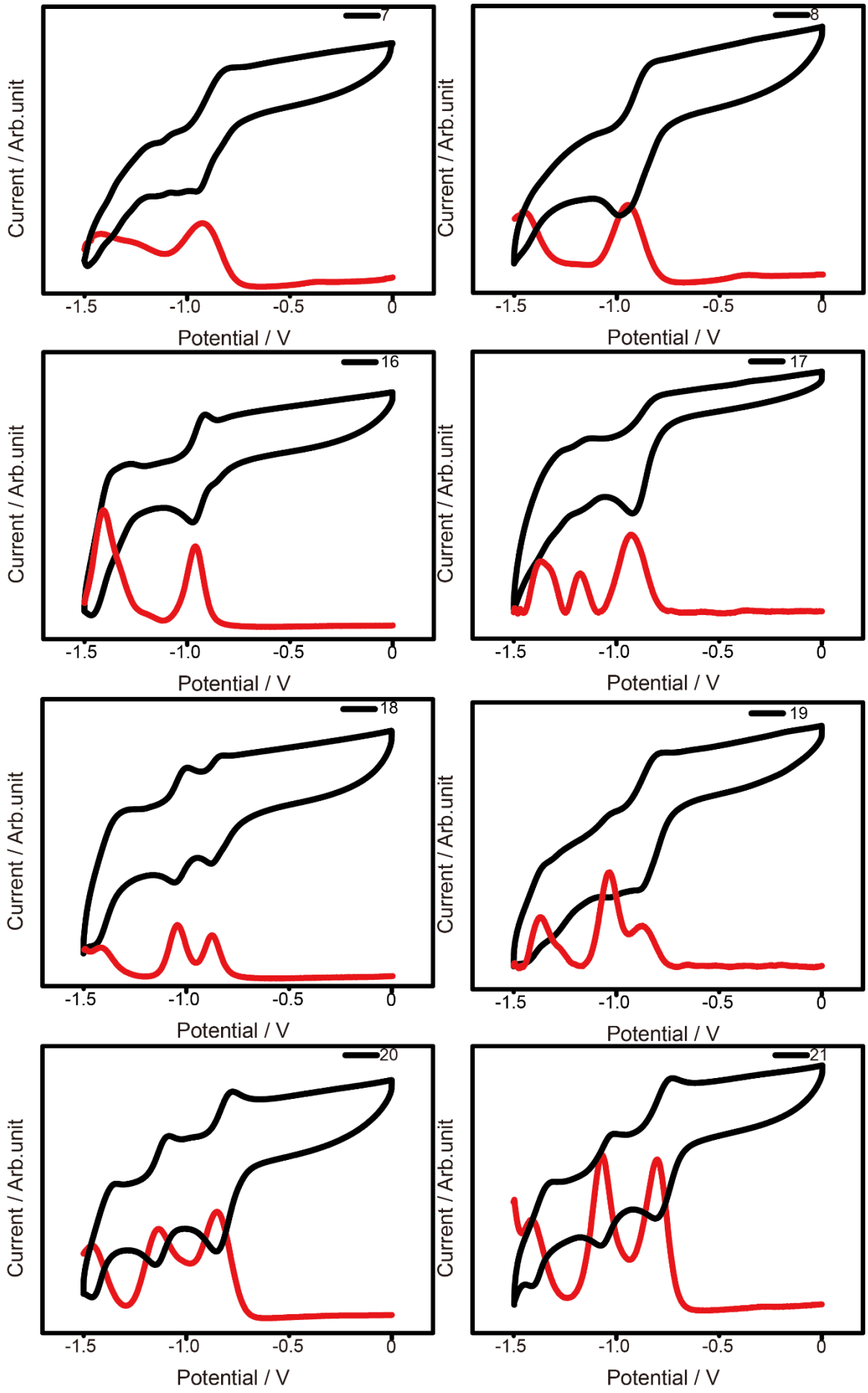

Figure S17. CV and DPV of **7-8** and **16-21** in CH_2Cl_2 (c = 10^{-4} mol L^{-1}) at RT. Reference electrode: SCE.

7. Theoretical calculations

All calculations were carried out with the Gaussian 16 programs. For DFT calculations, we used the hybrid gradient corrected exchange functional of Lee, Yang, and Parr. A standardized 6-31G basis set was used together with polarization (d) functions. The UV-Vis absorption spectra were calculated at TD-ωB97XD / IEFPCM(CH_2Cl_2) (nstates = 40, root = 1) level of theory using optimized structures. The optimized structures and molecular orbitals are displayed using Chemcraft.[S8] The calculated UV-Vis absorption spectra were displayed using Multiwfn software.[S9]

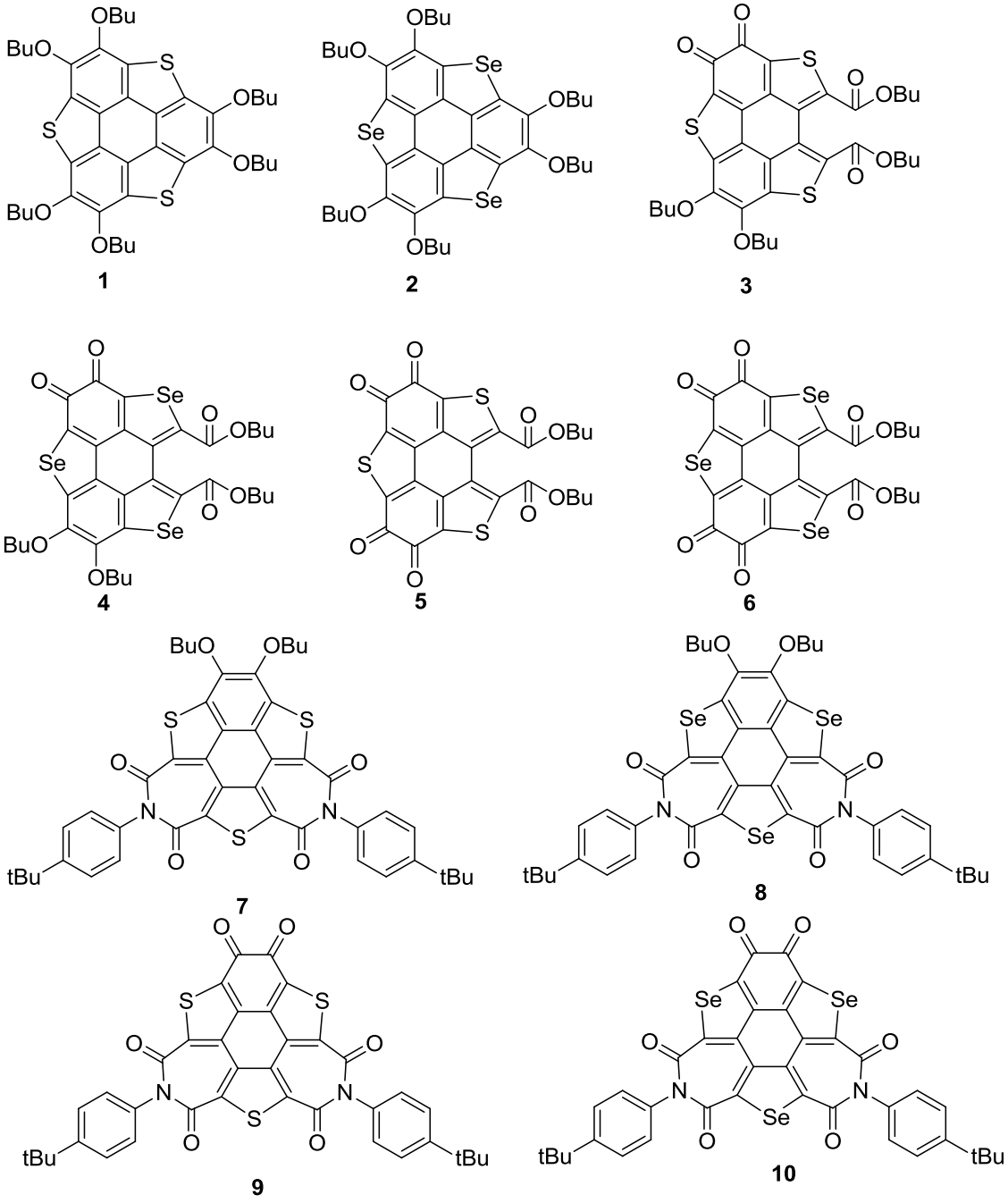

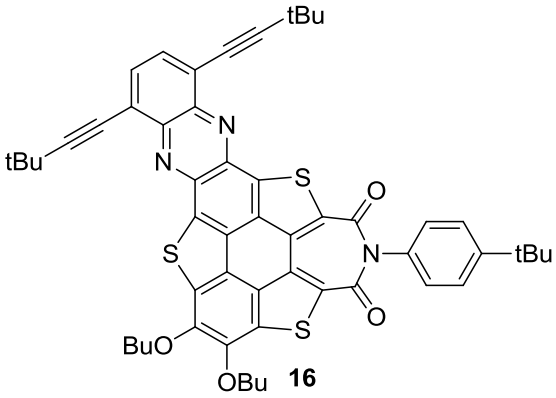

16

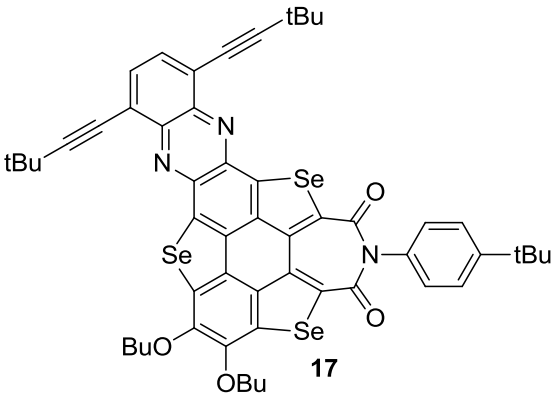

17

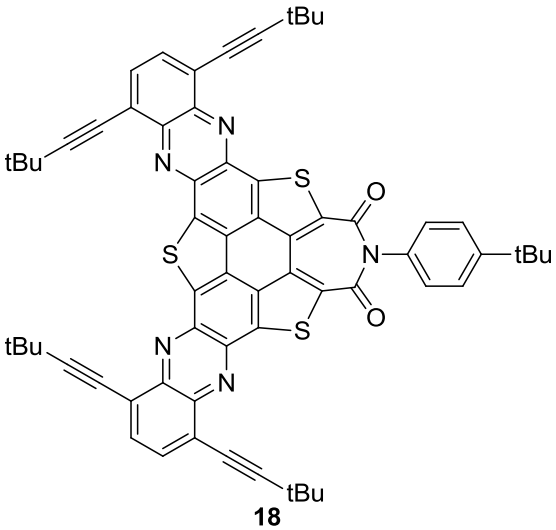

18

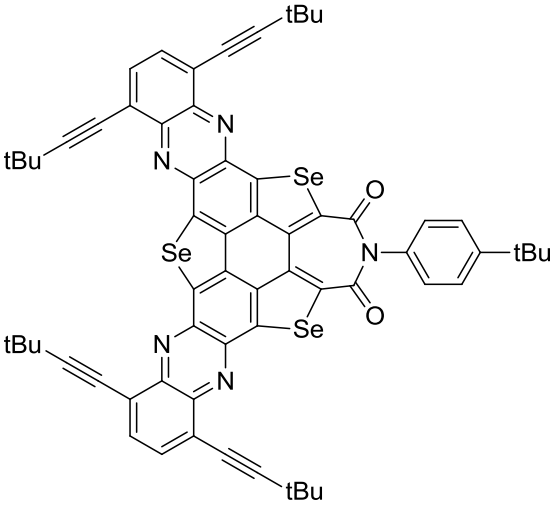

19

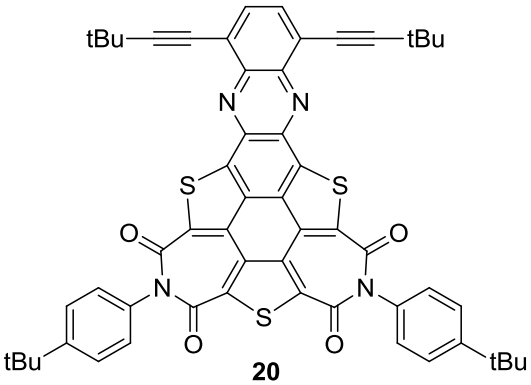

20

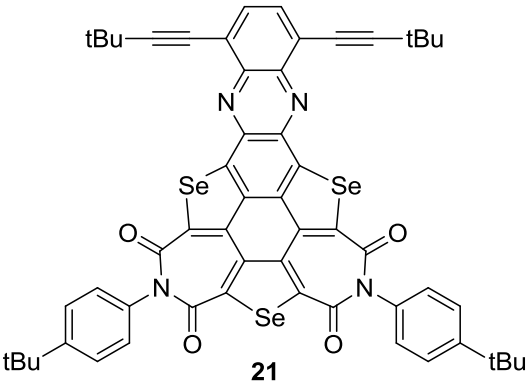

21

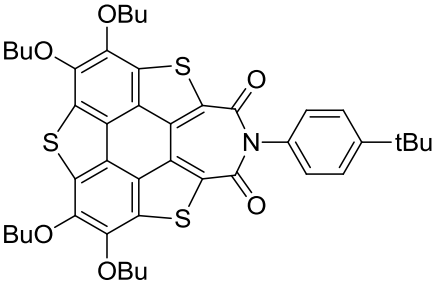

24

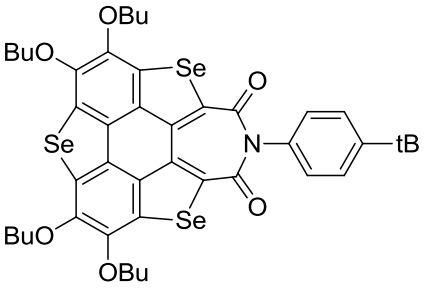

22

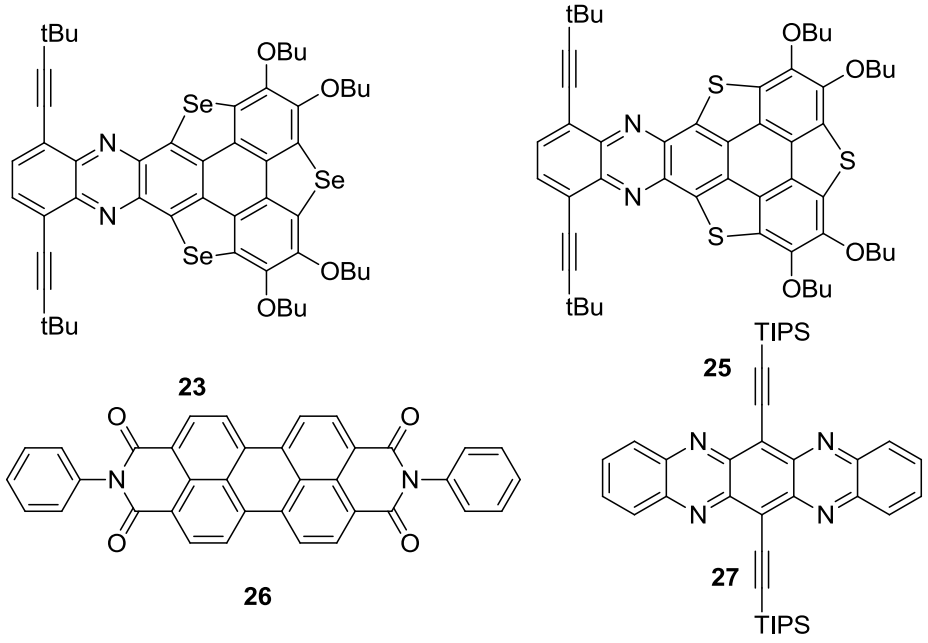

Scheme S3. The chemical structures of mentioned compounds **1-10 and 16-25.**

7.1 Optimized Structures, Molecular Orbitals and Corresponding Energies

Table S5. The calculated energy levels for the frontier orbitals for compounds **1-10** and **16-25.**

Compound	Energy levels / eV						
	HOMO-2	HOMO-1	HOMO	LUMO	LUMO+1	LUMO+2	E_g[a]
1	-6.22	-5.15	-5.01	-0.97	-0.86	-0.40	4.03
2	-6.18	-5.21	-5.03	-0.97	-0.87	-0.22	4.06
3	-6.81	-6.60	-6.01	-3.33	-2.57	-1.00	2.68
4	-6.74	-6.39	-5.85	-3.35	-2.56	-1.06	2.50
5	-7.31	7.19	-7.14	-4.16	-3.54	-2.90	2.98
6	-7.14	-6.99	-6.92	-4.15	-3.55	-2.89	2.77
7	-6.40	-6.40	-6.04	-2.73	-2.72	-1.55	3.31
8	-6.41	-6.28	-5.90	-2.72	-2.69	-1.52	3.17
9	-6.98	-6.69	-6.69	-3.94	-3.14	-2.99	2.75
10	-6.80	-6.69	-6.68	-3.89	-3.10	-2.93	2.79
16	-6.23	-5.82	-5.55	-2.77	-2.54	-1.44	2.78
17	-6.03	-5.74	-5.50	-2.77	-2.54	-1.43	2.72
18	-6.13	-5.70	-5.62	-2.93	-2.72	-2.55	2.69
19	-5.99	-5.68	-5.60	-2.96	-2.73	-2.57	2.65
20	-6.45	-6.44	-5.79	-3.05	-2.74	-2.71	2.74
21	-6.38	-6.23	-5.75	-3.03	-2.73	-2.67	2.72
22	-6.18	-5.89	-5.37	-2.49	-1.36	-0.88	2.88
23	-5.50	-5.40	-4.93	-2.49	-1.08	-0.95	2.44
24	-6.15	-6.08	-5.46	-2.50	-1.38	-0.89	2.96
25	-5.58	-5.50	-5.04	-2.48	-1.12	-1.07	2.57
26	-6.77	-6.77	-5.98	-.344	-1.84	-1.71	2.54
27	-6.67	-6.63	-5.29	-3.45	-1.88	-1.00	1.84

[a] $E_g = E_{LUMO} - E_{HOMO}$

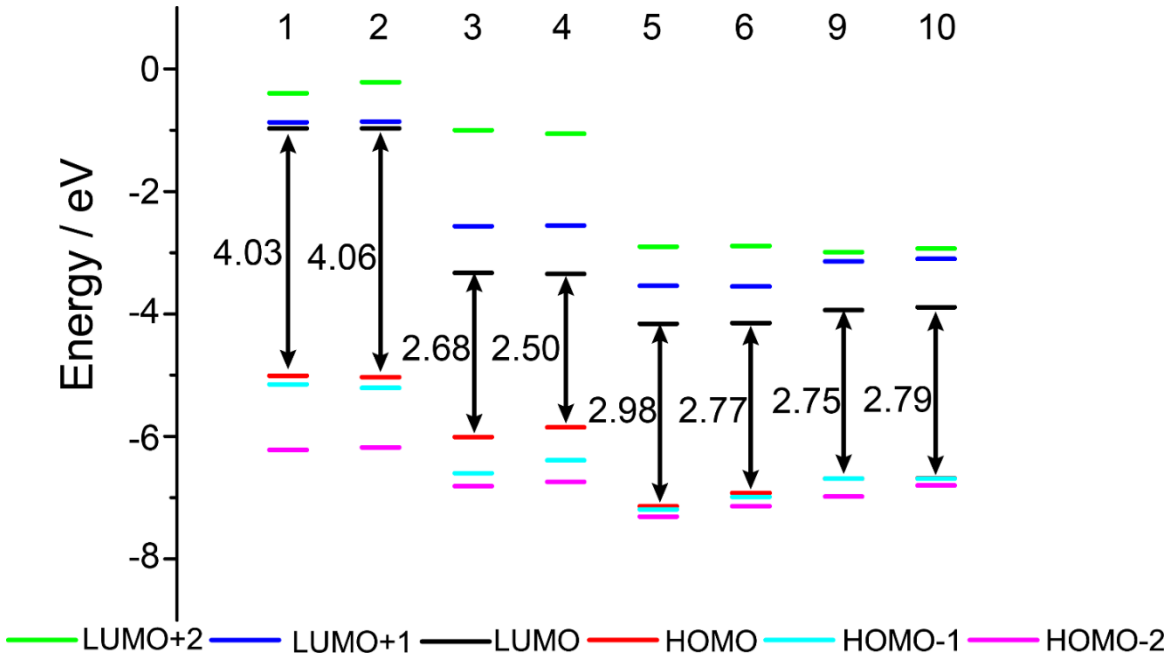

Figure S18. Schematic plot of HOMO-LUMO levels of compounds **1-6** and **9-10.**

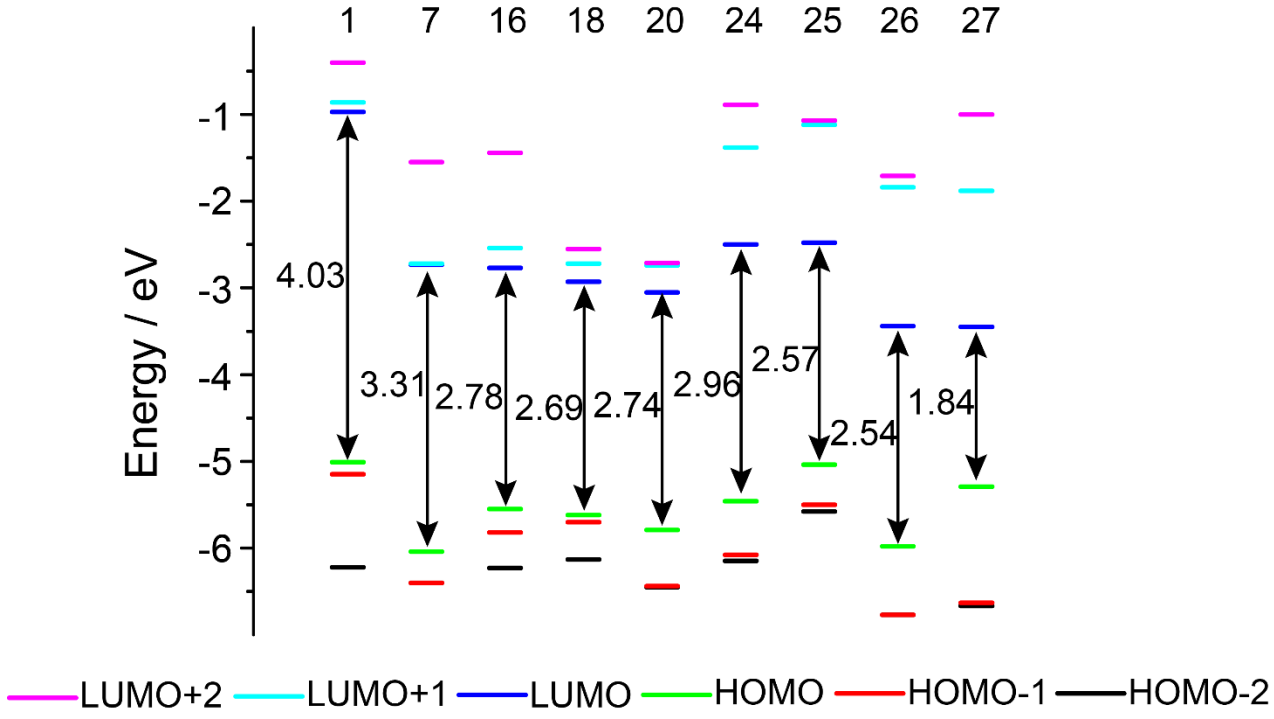

Figure S19. Schematic plot of HOMO-LUMO levels of compounds**1, 7, 16, 18, 20,** and **24-27.**

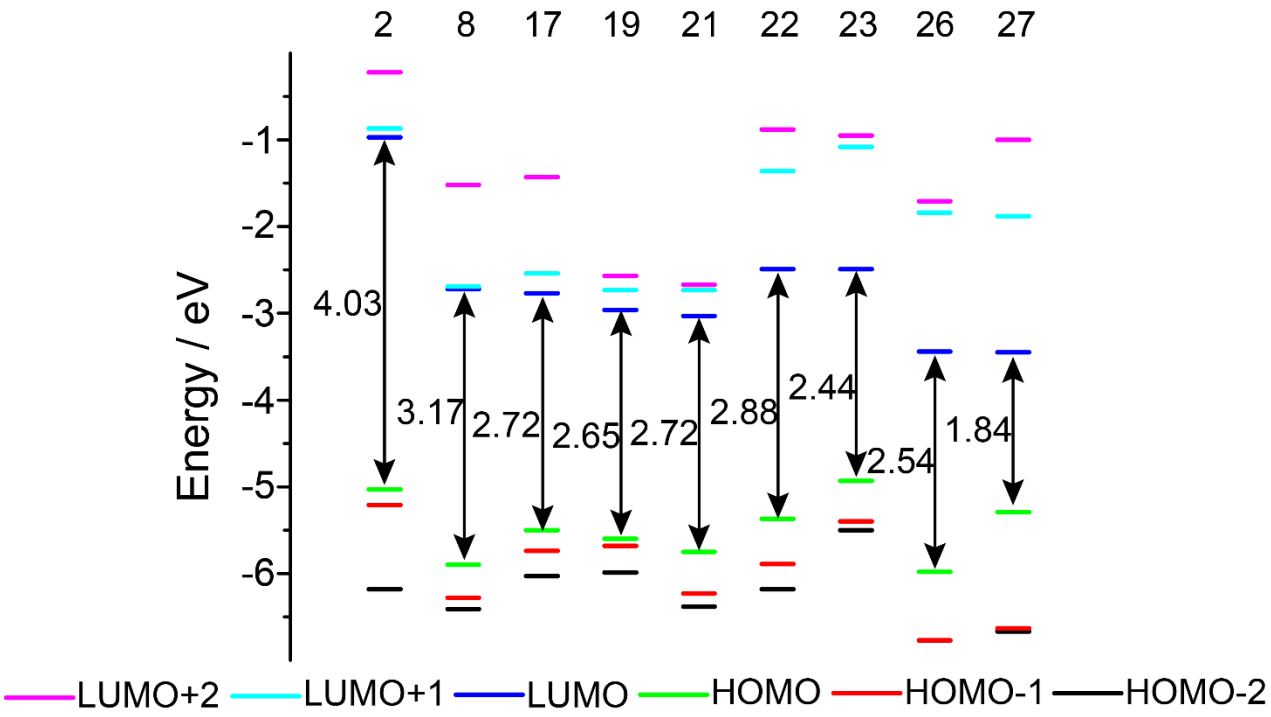

Figure S20. Schematic plot of HOMO-LUMO levels of compounds **2, 8, 17, 19, 21-23, 26,** and **27.**

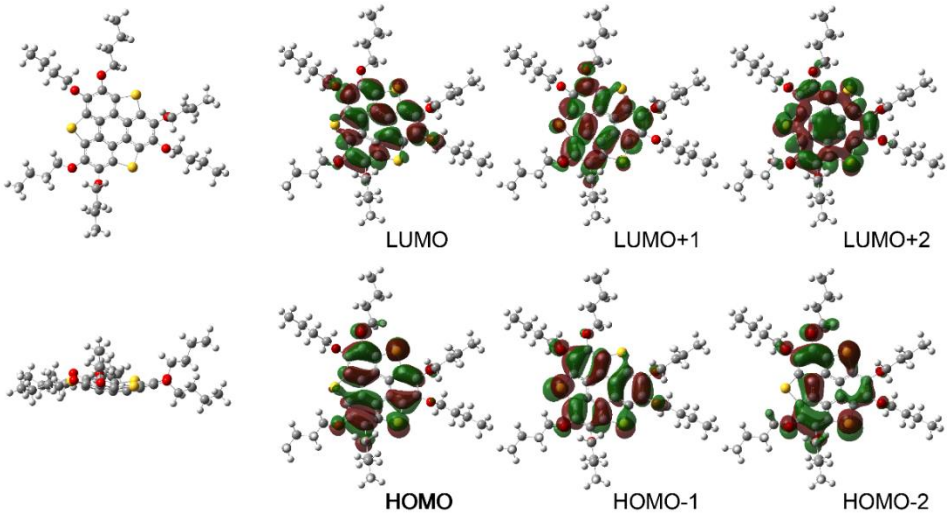

Figure S21. Calculated molecular orbitals of compound **1.**

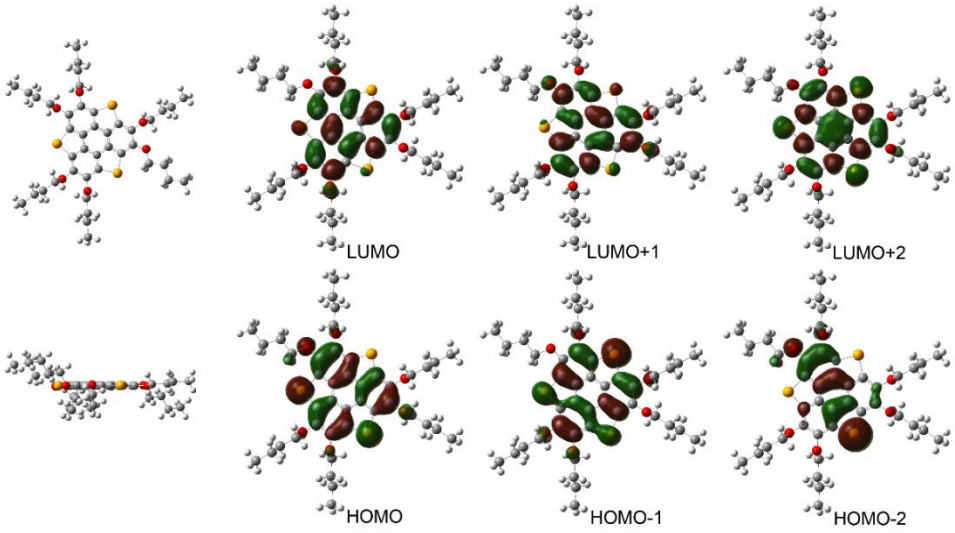

Figure S22. Calculated molecular orbitals of compound **2.**

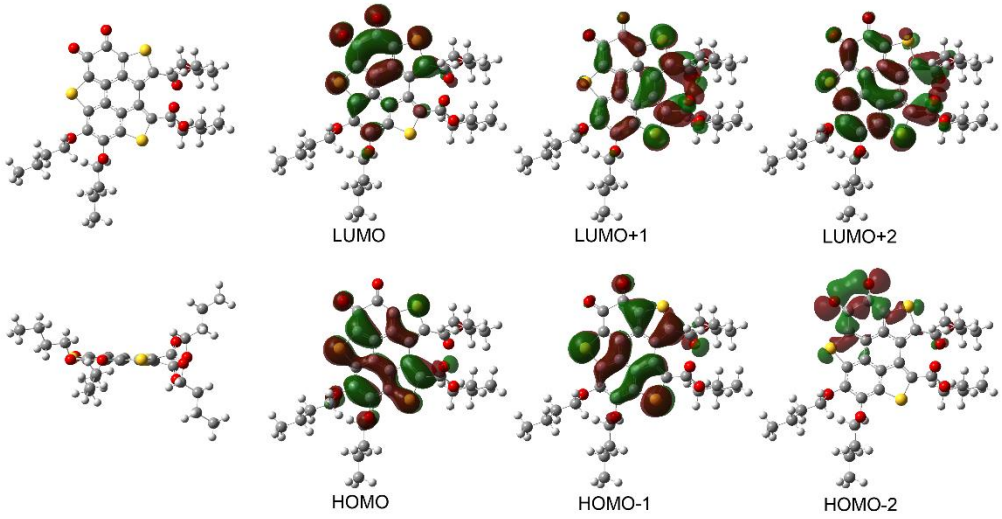

Figure S23. Calculated molecular orbitals of compound **3.**

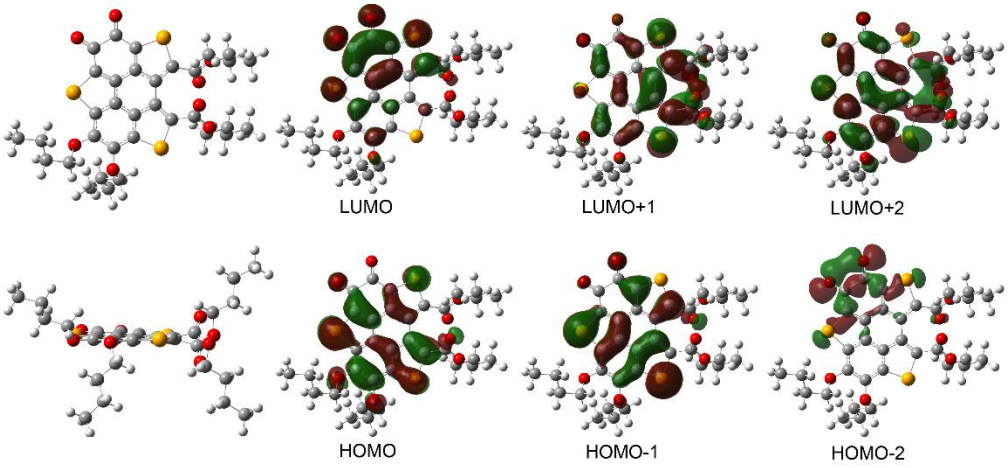

Figure S24. Calculated molecular orbitals of compound **4.**

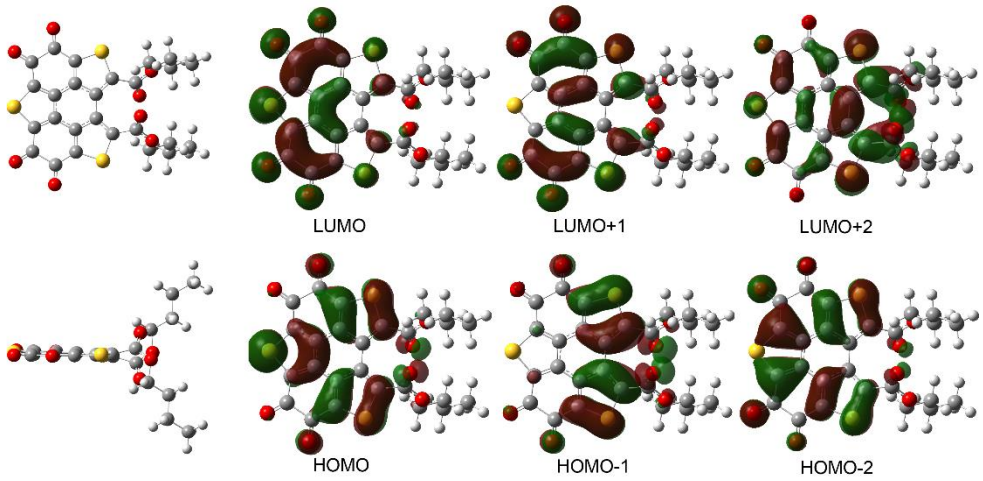

Figure S25. Calculated molecular orbitals of compound **5.**

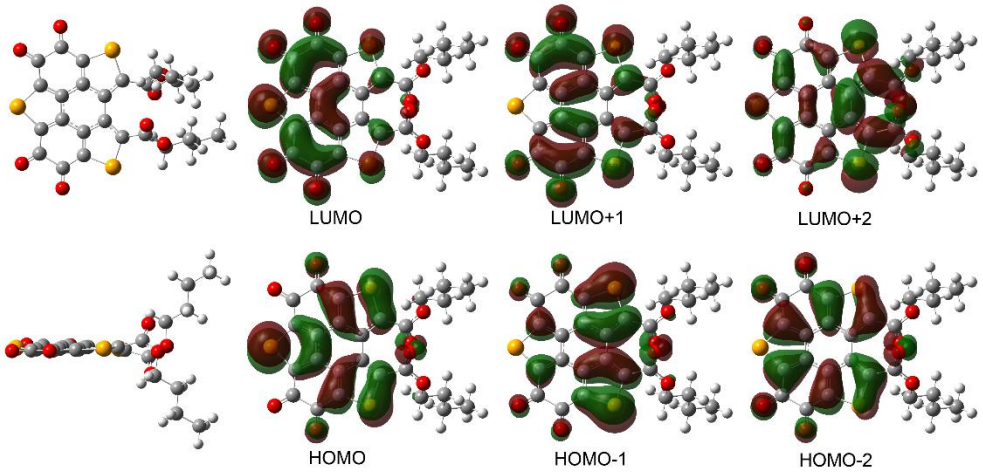

Figure S26. Calculated molecular orbitals of compound **6.**

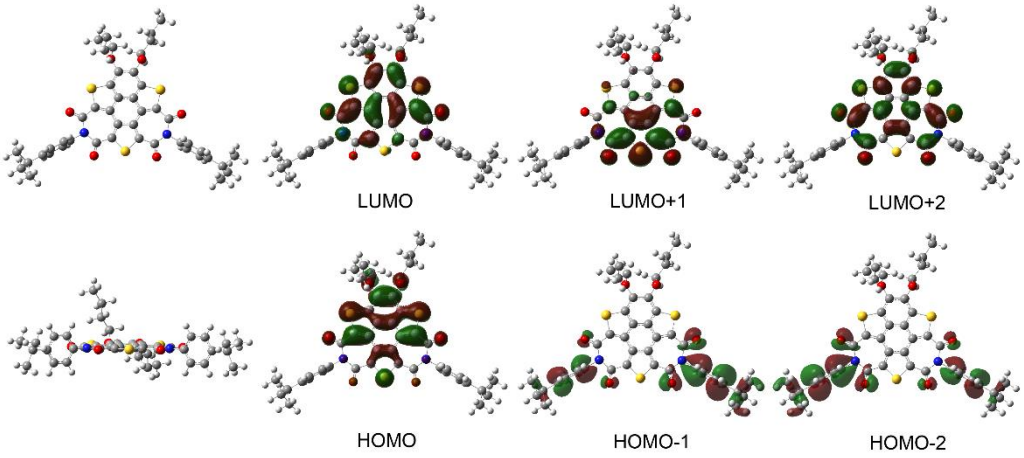

Figure S27. Calculated molecular orbitals of compound **7.**

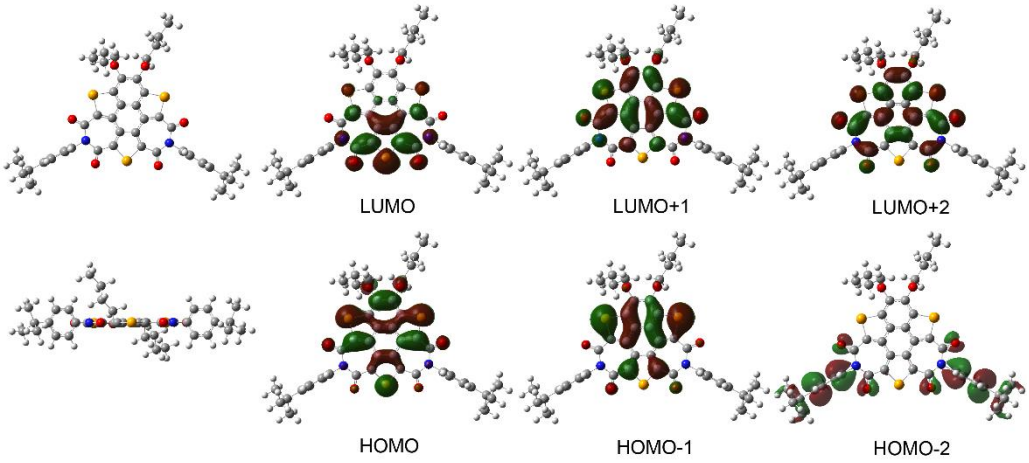

Figure S28. Calculated molecular orbitals of compound **8.**

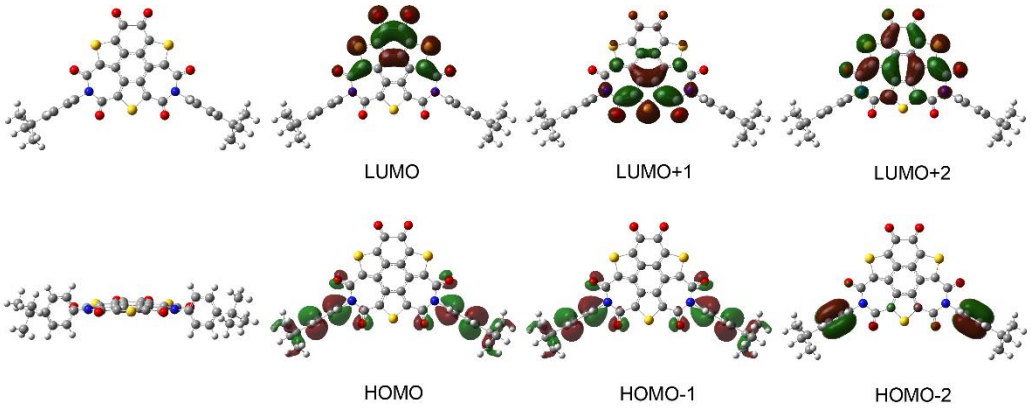

Figure S29. Calculated molecular orbitals of compound **9.**

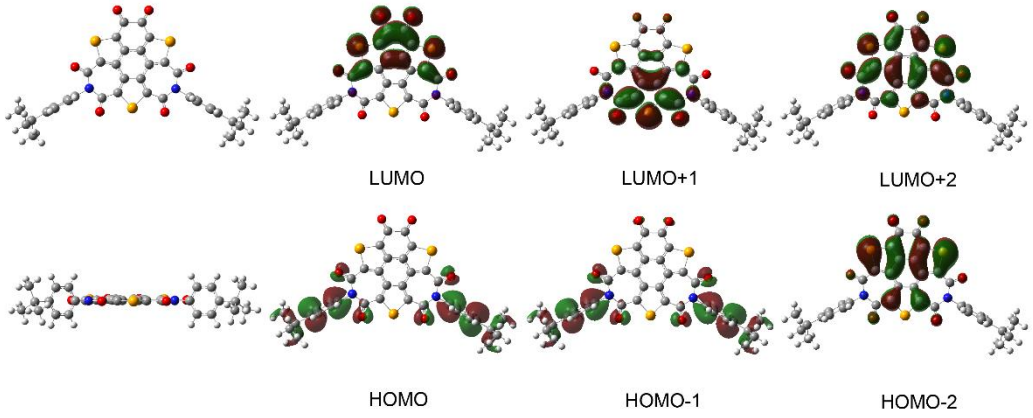

Figure S30. Calculated molecular orbitals of compound **10.**

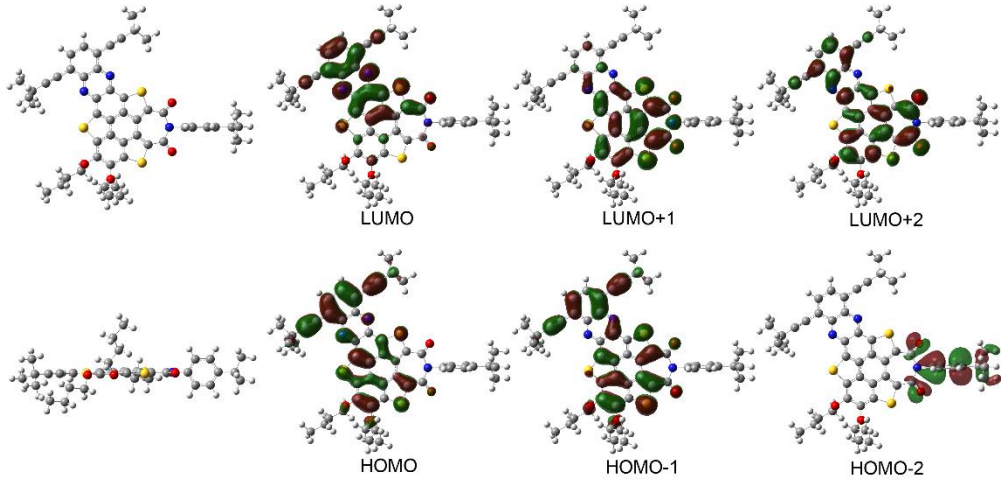

Figure S31. Calculated molecular orbitals of compound **16.**

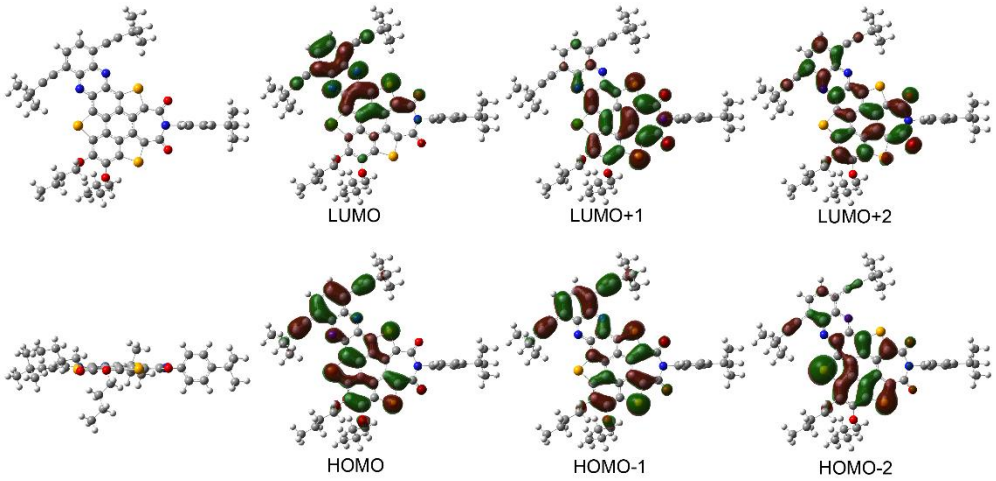

Figure S32. Calculated molecular orbitals of compound **17.**

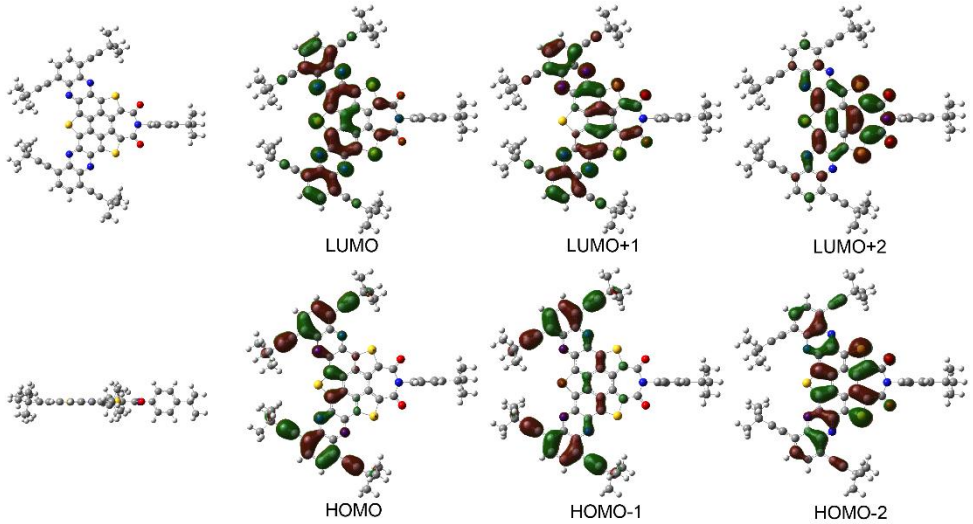

Figure S33. Calculated molecular orbitals of compound **18.**

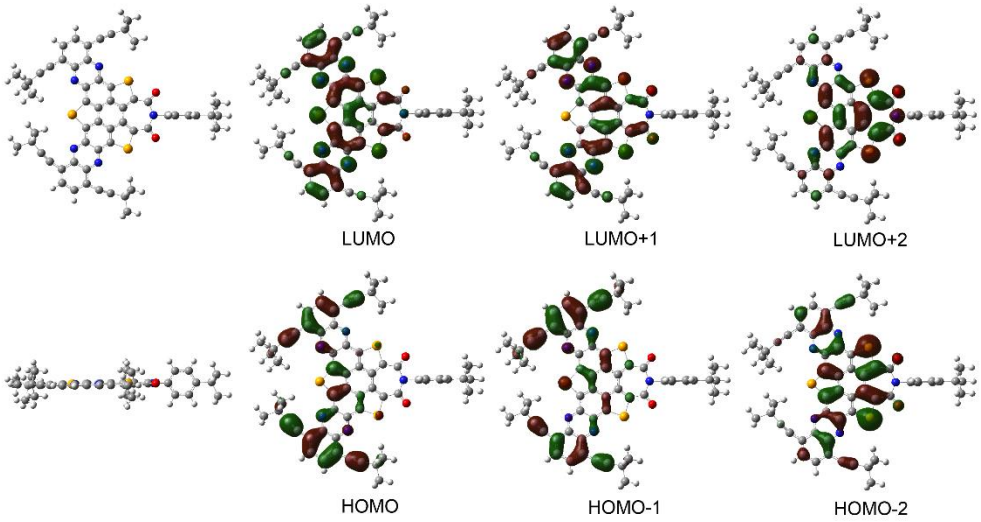

Figure S34. Calculated molecular orbitals of compound **19.**

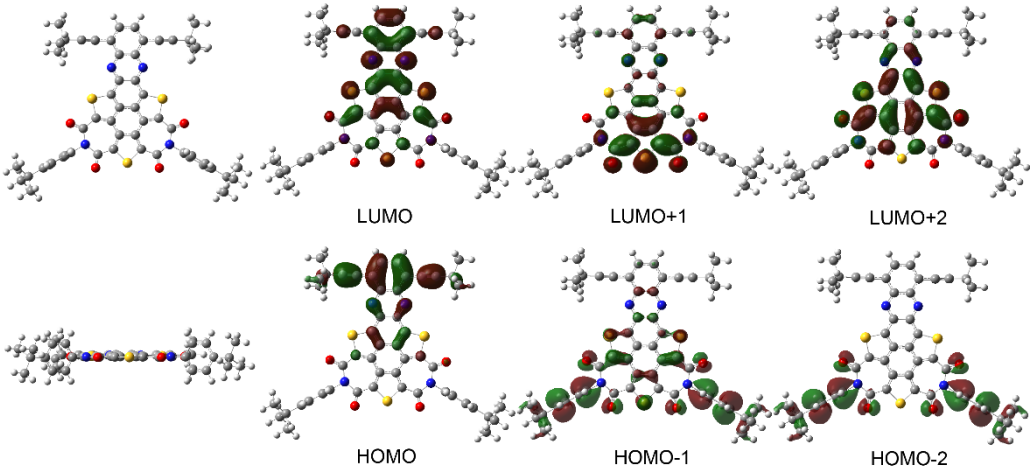

Figure S35. Calculated molecular orbitals of compound **20.**

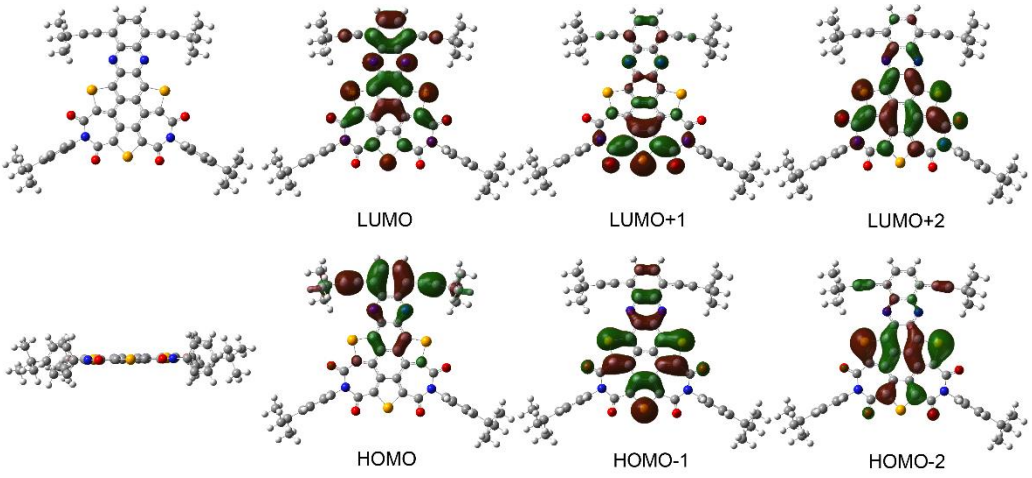

igure S36. Calculated molecular orbitals of compound **21.**

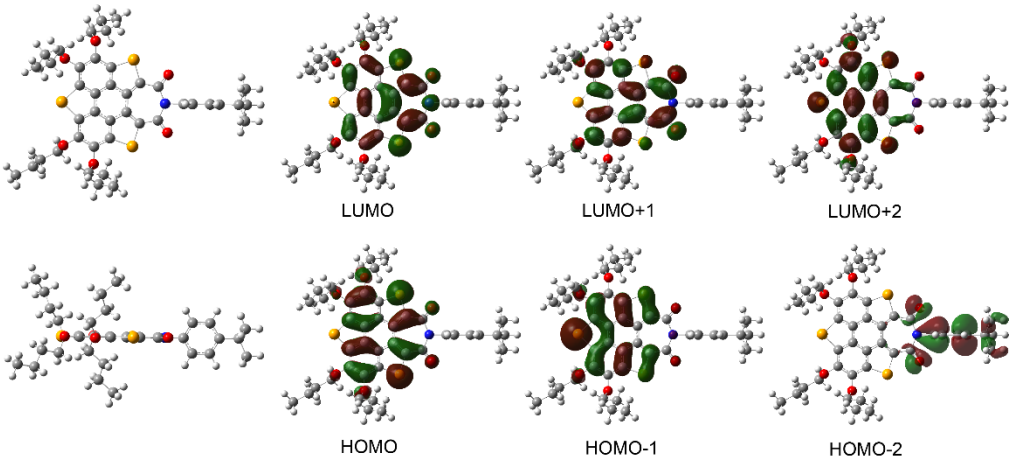

Figure S37. Calculated molecular orbitals of compound **22.**

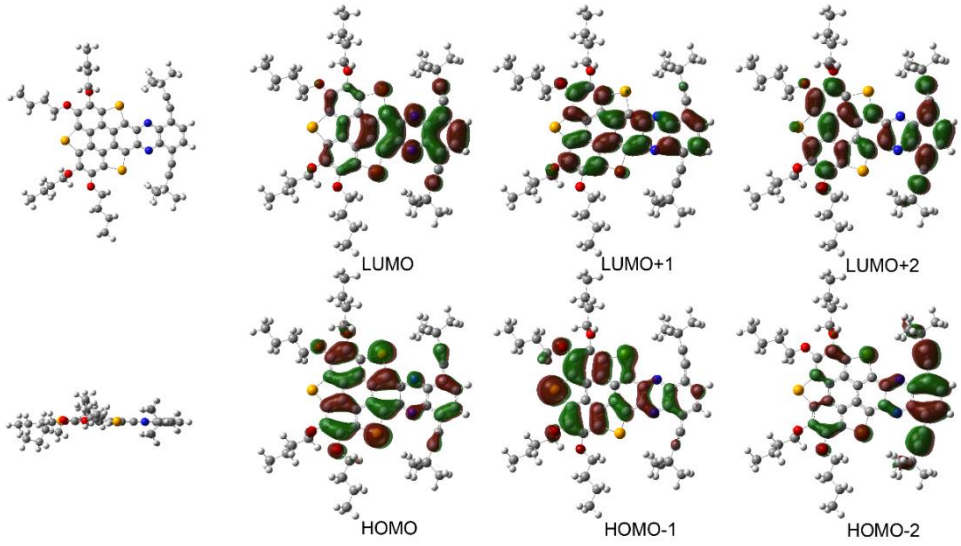

Figure S38. Calculated molecular orbitals of compound **23.**

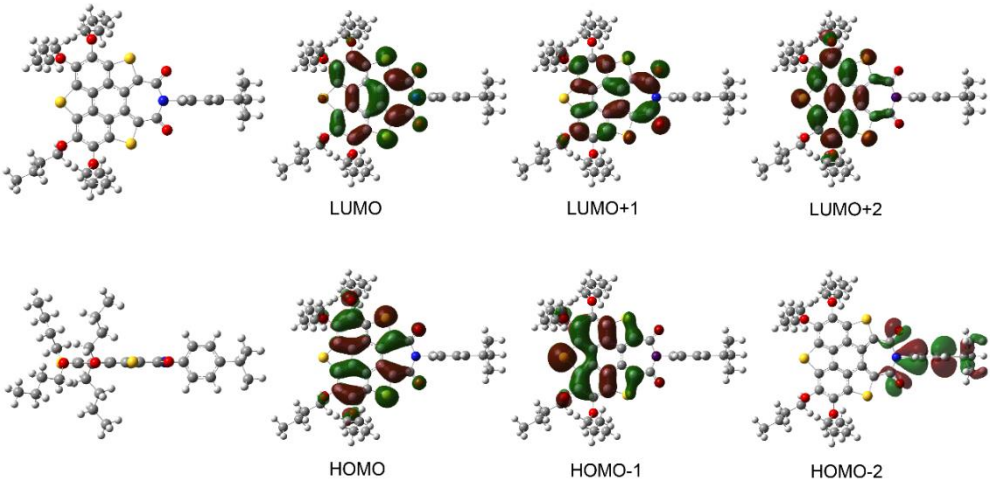

Figure S39. Calculated molecular orbitals of compound **24.**

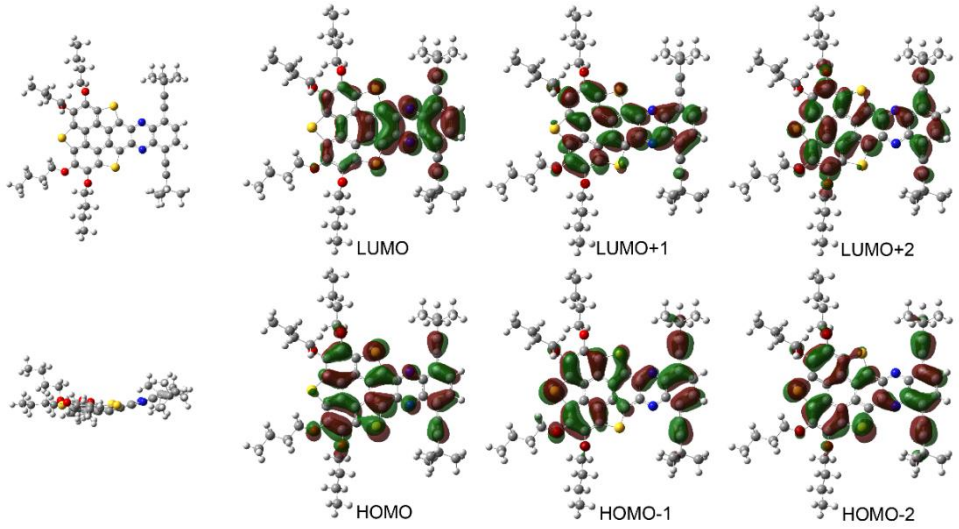

Figure S40. Calculated molecular orbitals of compound **25.**

7.2 UV-Vis Absorption Spectra Calculation

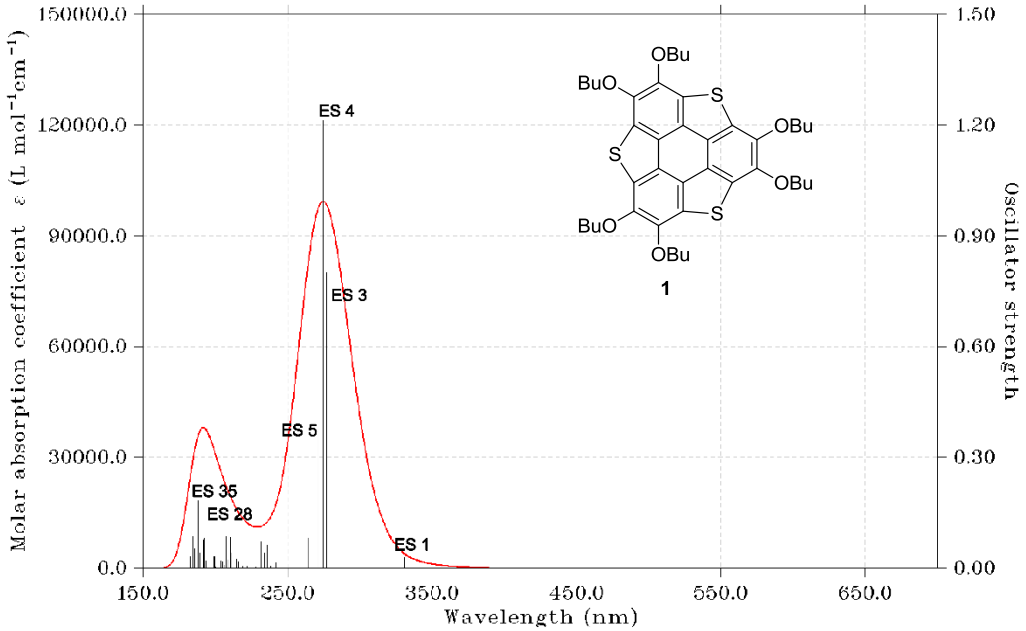

Figure S41. Calculated UV-Vis absorption spectra and corresponding excitation states (**ES**s) of **1.**

Table S6. Calculated excitation energy, excitation wavelength, oscillator strength, transition type and corresponding contribution of each excited state (**ES**) of **1.**

Excited State (**ES**)	Excitation Energy /eV	Excitation Wavelength / nm	Oscillator Strength	Transition Type	Contribution
1	3.7485	330.75	0.0285	HOMO-2→LUMO+2	2.39%
				HOMO-1→LUMO+1	**30.35%**
				HOMO→LUMO	**58.56%**
3	4.4802	276.74	0.7996	**HOMO-1→LUMO**	**20.54%**
				HOMO-1→LUMO+1	**19.63%**
				HOMO→LUMO	**11.13%**
				HOMO→LUMO+1	**18.06%**
				HOMO→LUMO+2	**17.97%**
4	4.5198	274.31	1.2134	**HOMO-1→LUMO**	**23.97%**
				HOMO-1→LUMO+1	**33.07%**
				HOMO→LUMO	**16.87%**
				HOMO→LUMO+1	**19.38%**
5	4.5700	271.30	0.3840	HOMO-3→LUMO+1	2.63%
				HOMO-2→LUMO	6.62%
				HOMO-1→LUMO	6.22%
				HOMO-1→LUMO+1	7.85%
				HOMO→LUMO	4.28%
				HOMO→LUMO+1	5.00%
				HOMO→LUMO+2	**53.96%**
28	6.2986	196.84	0.167	HOMO-11→LUMO	2.20%
				HOMO-5→LUMO+1	4.29%
				HOMO-4→LUMO+2	8.42%
				HOMO-3→LUMO+2	**21.94%**
				HOMO-2→LUMO+2	7.79%
				HOMO-1→LUMO+4	2.88%
				HOMO→LUMO+8	**14.31%**
				HOMO→LUMO+9	2.63%
				HOMO→LUMO+10	4.24%
35	6.5918	188.09	0.1821	HOMO-8→LUMO	7.73%
				HOMO-8→LUMO+2	2.03%
				HOMO-5→LUMO	2.32%
				HOMO-3→LUMO+7	2.13%
				HOMO-2→LUMO+2	5.24%
				HOMO-2→LUMO+4	3.18%
				HOMO-1→LUMO+4	2.54%
				HOMO-1→LUMO+8	**11.43%**
				HOMO-1→LUMO+9	**16.98%**
				HOMO→LUMO+9	2.74%
				HOMO→LUMO+10	2.26%
				HOMO→LUMO+11	**14.32%**

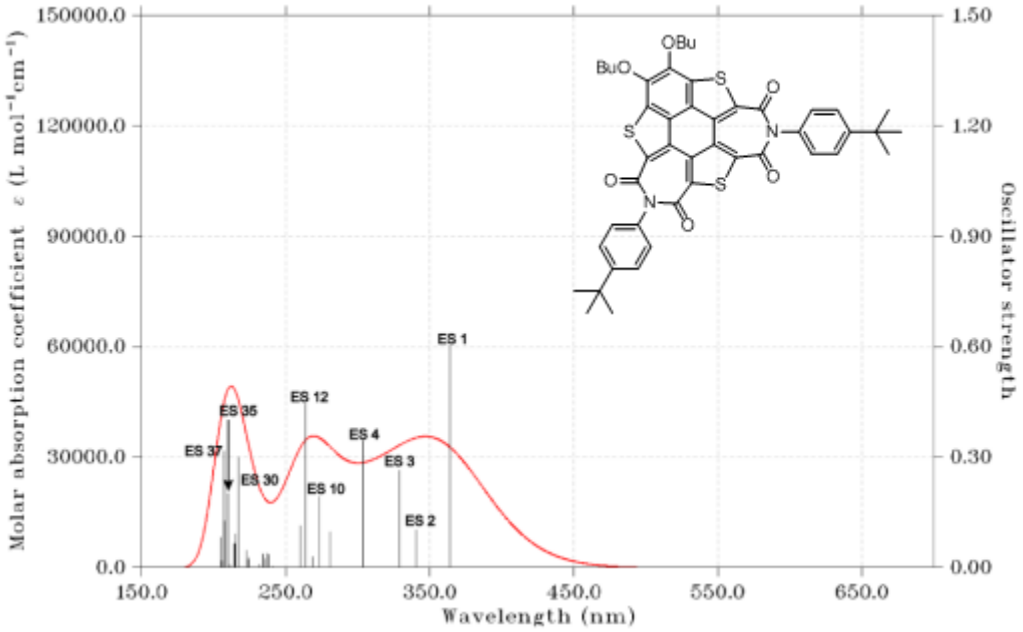

Figure S42. Calculated UV-Vis absorption spectra and corresponding excitation states (**ES**s) of **7.**

Table S7. Calculated excitation energy, excitation wavelength, oscillator strength, transition type and corresponding contribution of each excited state (**ES**) of **7.**

Excited State (**ES**)	Excitation Energy /eV	Excitation Wavelength / nm	Oscillator Strength	Transition Type	Contribution
1	3.4087	363.73	0.6009	HOMO-1→LUMO+1	2.05%
				HOMO→LUMO	**91.87%**
2	3.6437	340.27	0.1025	HOMO-7→LUMO+1	7.20%
				HOMO→LUMO+1	**88.08%**
3	3.7734	328.58	0.2630	**HOMO-1→LUMO**	**89.28%**
				HOMO→LUMO+2	4.00%
				HOMO→LUMO+4	2.32%
4	4.0818	303.75	0.3446	HOMO-7→LUMO	7.47%
				HOMO-6→LUMO+1	**15.74%**
				HOMO-4→LUMO	5.69%
				HOMO1→LUMO+2	**58.48%**
				HOMO→LUMO	3.67%
10	4.537	273.27	0.1922	HOMO-13→LUMO	3.39%
				HOMO-7→LUMO	**63.84%**
				HOMO-6→LUMO+1	9.61%
				HOMO-4→LUMO+1	4.91%
				HOMO-1→LUMO+2	8.15%
12	4.7044	263.55	0.443	HOMO-7→LUMO	2.40%
				HOMO-7→LUMO+1	**42.37%**
				HOMO-6→LUMO	5.21%

				HOMO-4→LUMO	2.49%
				HOMO-1→LUMO	3.19%
				HOMO→LUMO+1	3.02%
				HOMO→LUMO+2	**25.51%**
				HOMO→LUMO+4	3.48%
30	5.7106	217.11	0.2984	HOMO-19→LUMO	3.18%
				HOMO-13→LUMO+1	**22.74%**
				HOMO-6→LUMO+2	**26.44%**
				HOMO-5→LUMO	2.67%
				HOMO-4→LUMO+2	3.43%
				HOMO-1→LUMO+2	4.99%
				HOMO→LUMO+9	**13.90%**
35	5.9104	209.77	0.202	HOMO-17→LUMO	4.66%
				HOMO-15→LUMO	**45.72%**
				HOMO-14→LUMO	2.84%
				HOMO-13→LUMO	7.19%
				HOMO-7→LUMO+2	3.88%
				HOMO-6→LUMO+3	5.21%
				HOMO-1→LUMO+3	9.56%
37	5.9999	206.65	0.3159	HOMO-19→LUMO	2.19%
				HOMO-19→LUMO+1	3.00%
				HOMO-17→LUMO+1	2.71%
				HOMO12→LUMO+1	**15.798**%
				HOMO-12→LUMO+2	5.75%
				HOMO-11→LUMO	15.79%
				HOMO-7→LUMO+2	6.87%
				HOMO-1→LUMO+3	17.77%
				HOMO→LUMO+4	4.06%

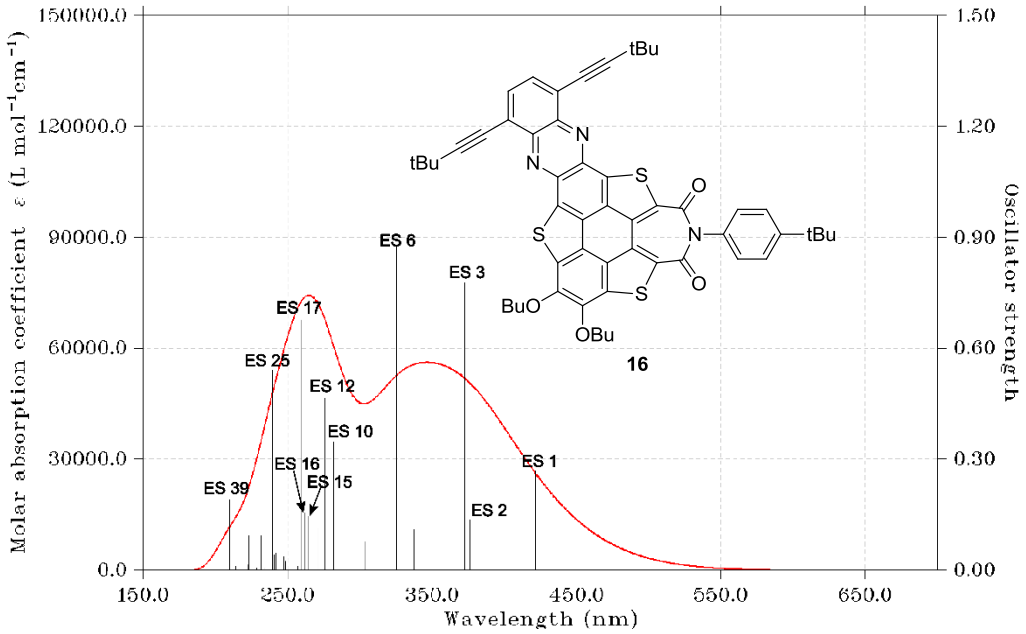

Figure S43. Calculated UV-Vis absorption spectra and corresponding excitation states (**ES**s) of **16.**

Table S8. Calculated excitation energy, excitation wavelength, oscillator strength, transition type and corresponding contribution of each excited state (**ES**) of **16.**

Excited State (**ES**)	Excitation Energy /eV	Excitation Wavelength / nm	Oscillator Strength	Transition Type	Contribution
1	2.9432	421.35	0.2686	**HOMO-1→LUMO**	**14.40%**
				HOMO→LUMO	**77.63%**
2	3.2945	376.33	0.1367	HOMO-2→LUMO	2.43%
				HOMO-1→LUMO	5.78%
				HOMO-1→LUMO+1	**17.31%**
				HOMO→LUMO	4.38%
				HOMO→LUMO+1	**59.59%**
6	3.8092	325.49	0.8741	HOMO-5→LUMO	4.77%
				HOMO-2→LUMO	**13.19%**
				HOMO-2→LUMO+1	**39.18%**
				HOMO-1→LUMO+1	**15.64%**
				HOMO→LUMO+1	9.75%
				HOMO→LUMO+2	2.35%
10	4.4027	281.61	0.3469	HOMO-9→LUMO	9.52%
				HOMO-9→LUMO+1	3.77%
				HOMO-6→LUMO+1	**31.86%**
				HOMO-5→LUMO	4.15%
				HOMO-5→LUMO+1	**12.80%**
				HOMO-1→LUMO+2	7.45%
				HOMO→LUMO+2	9.38%

				HOMO→LUMO+4	3.11%
12	4.5016	275.42	0.4646	HOMO-9→LUMO+1	8.01%
				HOMO-6→LUMO	2.06%
				HOMO-6→LUMO+1	**11.78%**
				HOMO-5→LUMO	3.28%
				HOMO-2→LUMO	2.18%
				HOMO-2→LUMO+1	2.65%
				HOMO-1→LUMO+2	**16.35%**
				HOMO-1→LUMO+3	2.61%
				HOMO→LUMO+2	**28.32%**
				HOMO→LUMO+3	5.11%
15	4.6906	264.33	0.1444	HOMO-6→LUMO+1	4.00%
				HOMO-5→LUMO	**28.09%**
				HOMO-5→LUMO+1	3.94%
				HOMO-4→LUMO	7.65%
				HOMO-4→LUMO+1	3.02%
				HOMO-2→LUMO	8.45%
				HOMO-2→LUMO+1	3.17%
				HOMO-2→LUMO+3	6.24%
				HOMO-1→LUMO+3	6.82%
				HOMO→LUMO+2	7.53%
				HOMO→LUMO+5	3.18%
16	4.7424	261.44	0.1549	**HOMO-11→LUMO**	**12.31%**
				HOMO-9→LUMO	**12.04%**
				HOMO-6→LUMO	**14.31%**
				HOMO-6→LUMO+1	6.44%
				HOMO-5→LUMO+1	2.30%
				HOMO-2→LUMO	2.19%
				HOMO-2→LUMO+2	2.53%
				HOMO-1→LUMO	3.10%
				HOMO-1→LUMO+1	7.05%
				HOMO→LUMO+1	6.00%
				HOMO→LUMO+3	**11.18%**
17	4.7754	259.63	0.6757	HOMO-11→LUMO	2.02%
				HOMO-9→LUMO	2.61%
				HOMO-5→LUMO	6.65%
				HOMO-2→LUMO+1	2.01%
				HOMO-1→LUMO+2	6.14%
				HOMO-1→LUMO+3	**11.28%**
				HOMO-1→LUMO+4	5.88%
				HOMO-1→LUMO+5	3.29%
				HOMO→LUMO+2	3.96%
				HOMO→LUMO+3	**31.75%**
				HOMO→LUMO+4	8.36%

25	5.1747	239.6	0.5404	**HOMO-9→LUMO**	**20.26%**
				HOMO-5→LUMO	3.84%
				HOMO-5→LUMO+1	3.09%
				HOMO-4→LUMO+1	2.91%
				HOMO-2→LUMO+2	6.11%
				HOMO-2→LUMO+3	2.27%
				HOMO-1→LUMO+2	**12.74%**
				HOMO→LUMO+3	**11.39%**
				HOMO→LUMO+4	**15.57%**
39	5.9101	209.78	0.1894	HOMO-19→LUMO	3.85%
				HOMO-15→LUMO+1	**25.36%**
				HOMO-14→LUMO	6.20%
				HOMO-14→LUMO+2	4.79%
				HOMO-5→LUMO+3	3.49%
				HOMO-2→LUMO+2	3.84%
				HOMO-2→LUMO+7	3.34%
				HOMO-1→LUMO+3	3.43%
				HOMO-1→LUMO+5	3.84%
				HOMO→LUMO+9	2.44%
				HOMO→LUMO+10	4.27%

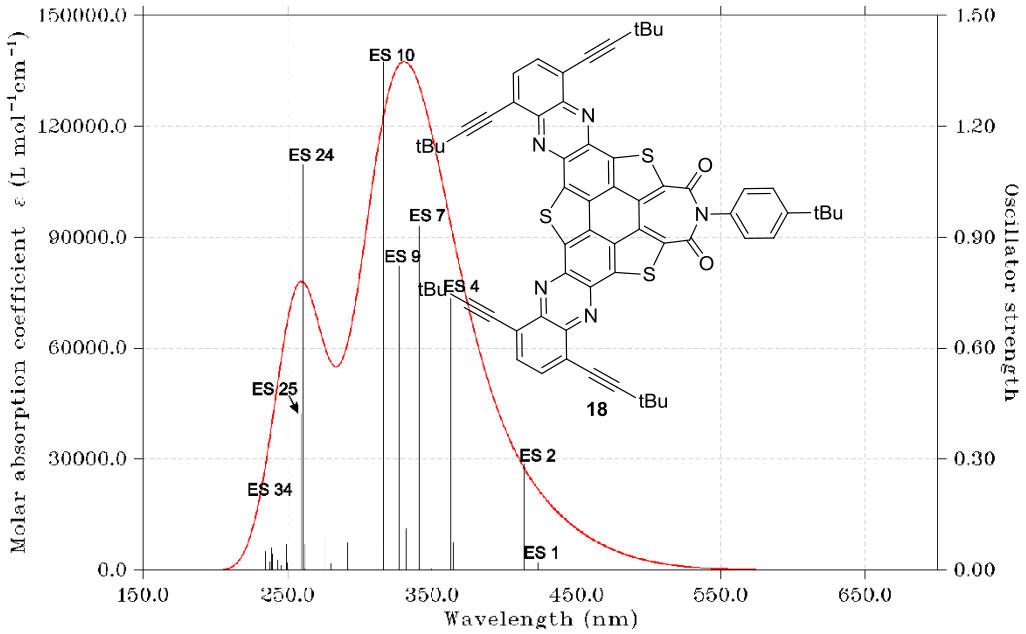

Figure S44. Calculated UV-Vis absorption spectra and corresponding excitation states (**ES**s) of **18.**

Table S9. Calculated excitation energy, excitation wavelength, oscillator strength, transition type and corresponding contribution of each excited state (**ES**) of **18.**

Excited State (**ES**)	Excitation Energy /eV	Excitation Wavelength / nm	Oscillator Strength	Transition Type	Contribution
1	2.9289	423.31	0.0195	**HOMO-1→LUMO+1**	**31.97%**
				HOMO→LUMO	**60.19%**
2	2.9982	413.52	0.2871	HOMO-2→LUMO+1	2.26%
				HOMO-1→LUMO	**53.66%**
				HOMO→LUMO+1	**38.21%**
4	3.4166	362.89	0.7348	HOMO-16→LUMO+1	4.01%
				HOMO-12→LUMO+1	5.06%
				HOMO-2→LUMO	**68.25%**
				HOMO-1→LUMO+1	6.33%
				HOMO→LUMO	4.51%
7	3.6353	341.05	0.9290	HOMO-6→LUMO	5.02%
				HOMO-5→LUMO	2.94%
				HOMO-3→LUMO+1	6.29%
				HOMO-2→LUMO+2	**42.83%**
				HOMO-1→LUMO+1	3.11%
				HOMO→LUMO+2	**28.48%**
				HOMO→LUMO+4	2.13%
9	3.7893	327.19	0.8219	HOMO-6→LUMO	6.43%

				HOMO-6→LUMO+2	3.97%
				HOMO-5→LUMO	3.58%
				HOMO-5→LUMO+2	2.30%
				HOMO-3→LUMO+1	**41.78%**
				HOMO-1→LUMO+1	7.01%
				HOMO-1→LUMO+3	4.41%
				HOMO→LUMO+2	**19.06%**
10	3.2900	316.29	1.3745	**HOMO-3→LUMO+2**	**29.90%**
				HOMO-2→LUMO+1	**23.15%**
				HOMO-1→LUMO+2	**34.14%**
24	4.7577	260.60	1.0976	HOMO-3→LUMO	2.34%
				HOMO-2→LUMO+6	2.27%
				HOMO-1→LUMO+4	**23.78%**
				HOMO-1→LUMO+5	**10.87%**
				HOMO→LUMO+3	**24.43%**
				HOMO→LUMO+6	**18.63%**
25	4.7750	259.65	0.4218	HOMO-16→LUMO+1	4.06%
				HOMO-13→LUMO	6.22%
				HOMO-11→LUMO	3.32%
				HOMO-6→LUMO	2.90%
				HOMO-2→LUMO+4	3.56%
				HOMO-1→LUMO+3	**14.80%**
				HOMO-1→LUMO+6	**14.80%**
				HOMO→LUMO+4	**17.00%**
				HOMO→LUMO+5	**11.61%**
34	5.1425	241.10	0.1966	HOMO-16→LUMO+1	2.56%
				HOMO-11→LUMO	7.91%
				HOMO-11→LUMO+2	2.29%
				HOMO-6→LUMO	7.99%
				HOMO-6→LUMO+2	**15.08%**
				HOMO-5→LUMO+2	3.00%
				HOMO-3→LUMO+1	5.49%
				HOMO-2→LUMO	4.51%
				HOMO-2→LUMO+4	2.19%
				HOMO-1→LUMO+1	**10.73%**
				HOMO-1→LUMO+3	2.12%
				HOMO-1→LUMO+7	2.92%
				HOMO-→LUMO	6.29%
				HOMO→LUMO+4	8.50%
				HOMO→LUMO+5	2.28%

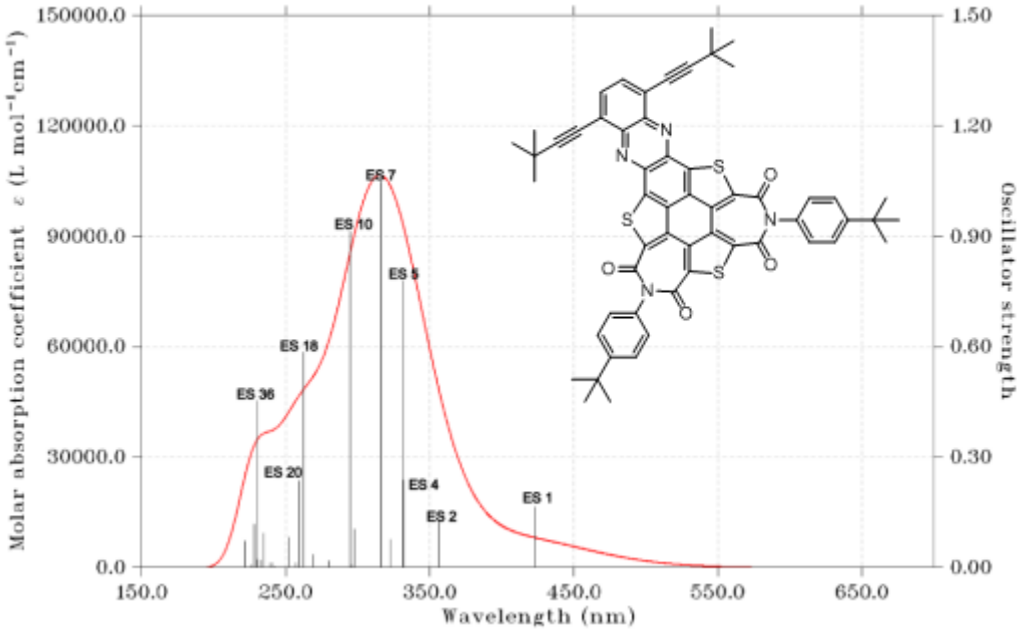

Figure S45. Calculated UV-Vis absorption spectra and corresponding excitation states (**ES**s) of **20.**

Table S10. Calculated excitation energy, excitation wavelength, oscillator strength, transition type and corresponding contribution of each excited state (**ES**) of **20.**

Excited State (**ES**)	Excitation Energy / eV	Excitation Wavelength / nm	Oscillator Strength	Transition Type	Contribution
1	2.932	422.86	0.1643	**HOMO→LUMO**	**90.43%**
				HOMO→LUMO+2	3.61%
2	3.6437	340.27	0.1025	HOMO-11→LUMO	5.09%
				HOMO-10→LUMO	5.09%
				HOMO-2→LUMO+1	9.17%
				HOMO-1→LUMO	**60.89%**
				HOMO-1→LUMO+2	2.20%
				HOMO→LUMO+1	**10.47%**
4	3.7404	331.47	0.2372	HOMO-7→LUMO	9.71%
				HOMO-5→LUMO	5.58%
				HOMO-2→LUMO	**33.70%**
				HOMO-2→LUMO+2	5.71%
				HOMO-1→LUMO+1	**34.43%**
5	3.7464	330.95	0.778	HOMO-7→LUMO+1	3.31%
				HOMO-2→LUMO+1	16.33%
				HOMO-1→LUMO	21.26%
				HOMO-1→LUMO	8.09%
				HOMO→LUMO+1	39.95%

7	3.927	315.72	1.0479	HOMO-11→LUMO	2.66%
				HOMO-11→LUMO+2	5.65%
				HOMO10→LUMO+2	4.52%
				HOMO-2→LUMO+1	2.33%
				HOMO-1→LUMO+2	**71.56%**
				HOMO→LUMO+1	8.19%
10	4.2068	294.72	0.9115	HOMO-7→LUMO+2	8.03%
				HOMO-5→LUMO+2	3.96%
				HOMO-2→LUMO+2	**47.97%**
				HOMO-1→LUMO+1	**24.29%**
				HOMO→LUMO+2	7.87%
18	4.728	262.24	0.5843	HOMO-17→LUMO	3.57%
				HOMO-7→LUMO	**17.77%**
				HOMO-5→LUMO	8.31%
				HOMO-2→LUMO	5.57%
				HOMO-2→LUMO+3	3.63%
				HOMO-1→LUMO+1	3.10%
				HOMO→LUMO+3	**22.36%**
				HOMO→LUMO+5	**24.19%**
20	4.7847	259.13	0.235	**HOMO-7→LUMO**	**26.20%**
				HOMO-5→LUMO	**14.57%**
				HOMO-1→LUMO+1	3.53%
				HOMO→LUMO+3	**22.8%**
				HOMO→LUMO+5	**16.53%**
36	5.3882	230.1	0.4525	HOMO26→LUMO+2	2.58%
				HOMO-15→LUMO+1	7.18%
				HOMO-11→LUMO	3.97%
				HOMO-11→LUMO+2	8.92%
				HOMO-10→LUMO	4.68%
				HOMO10→LUMO+2	3.86%
				HOMO-5→LUMO+1	2.25%
				HOMO-1→LUMO+3	8.02%
				HOMO→LUMO+1	6.77%
				HOMO→LUMO+4	**21.84%**
				HOMO→LUMO+6	6.35%

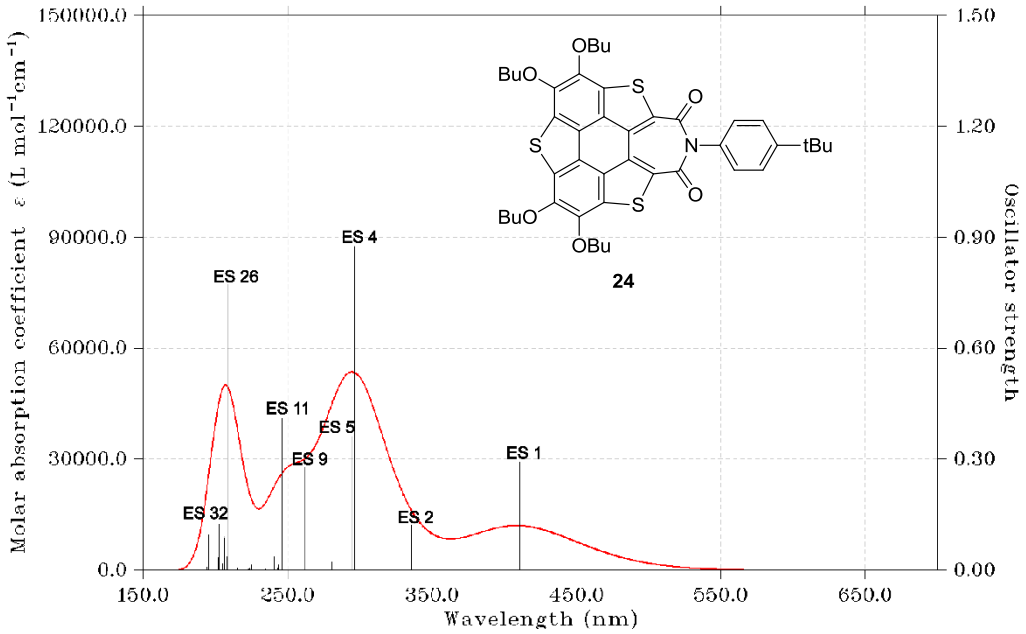

Figure S46. Calculated UV-Vis absorption spectra and corresponding excitation states (**ES**s) of **24.**

Table S11. Calculated excitation energy, excitation wavelength, oscillator strength, transition type and corresponding contribution of each excited state (**ES**) of **24.**

Excited State(**ES**)	Excitation Energy /eV	Excitation Wavelength / nm	Oscillator Strength	Transition Type	Contribution
1	3.0179	410.82	0.2919	**HOMO→LUMO**	**96.42%**
2	3.6942	335.61	0.1205	HOMO-4→LUMO	3.57%
				HOMO-1→LUMO	**74.15%**
				HOMO-1→LUMO+2	2.60%
				HOMO→LUMO+1	**12.36%**
9	4.7424	261.44	0.2767	HOMO-6→LUMO	2.41%
				HOMO-5→LUMO	8.81%
				HOMO-1→LUMO+1	3.32%
				HOMO→LUMO+2	**76.47%**
11	5.0351	246.24	0.4099	HOMO-5→LUMO+2	2.26%
				HOMO-3→LUMO	3.21%
				HOMO-1→LUMO+1	**72.85%**
				HOMO-1→LUMO+5	2.39%
				HOMO→LUMO+2	4.25%
				HOMO→LUMO+3	6.68%
26	5.9547	208.21	0.7727	**HOMO-12→LUMO**	**14.62%**
				HOMO-5→LUMO+1	7.52%
				HOMO-4→LUMO+2	7.99%
				HOMO-3→LUMO+1	**11.01%**

				HOMO-2→LUMO+4	2.44%
				HOMO-1→LUMO+2	**12.52%**
				HOMO→LUMO+5	**16.58%**
				HOMO→LUMO+10	5.01%
32	6.1167	202.70	0.1241	HOMO-14→LUMO	4.65%
				HOMO-13→LUMO	**14.60%**
				HOMO-12→LUMO	**12.00%**
				HOMO-9→LUMO+1	5.83%
				HOMO-6→LUMO+1	**12.72%**
				HOMO-5→LUMO+2	2.39%
				HOMO-4→LUMO+2	3.27%
				HOMO-2→LUMO+4	7.36%
				HOMO→LUMO+5	7.79%

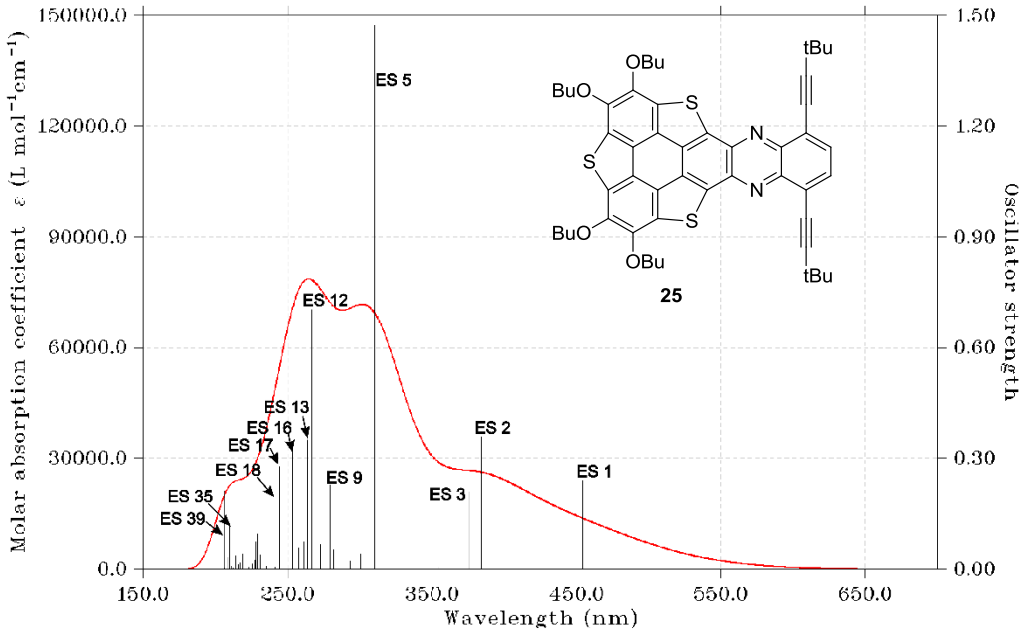

Figure S47. Calculated UV-Vis absorption spectra and corresponding excitation states (**ES**s) of **25.**

Table S12. Calculated excitation energy, excitation wavelength, oscillator strength, transition type and corresponding contribution of each excited state (**ES**) of **25.**

Excited State(**ES**)	Excitation Energy /eV	Excitation Wavelength / nm	Oscillator Strength	Transition Type	Contribution
1	2.7329	453.68	0.2416	HOMO-2→LUMO	2.12%
				HOMO→LUMO	**89.31%**

2	3.2315	383.67	0.3588	HOMO-6→LUMO	6.11%
				HOMO-2→LUMO	**16.62%**
				HOMO-1→LUMO	**61.49%**
				HOMO→LUMO	2.24%
				HOMO→LUMO+1	4.52%
3	3.3037	375.28	0.2090	HOMO-6→LUMO	4.67%
				HOMO-2→LUMO	**70.54%**
				HOMO-1→LUMO	**11.49%**
				HOMO-1→LUMO+2	2.20%
				HOMO→LUMO+1	2.48%
				HOMO→LUMO+2	2.17%
5	4.0015	309.84	1.4731	HOMO-1→LUMO	8.25%
				HOMO-1→LUMO+3	2.81%
				HOMO→LUMO+1	**74.13%**
9	4.4406	279.20	0.2278	**HOMO-8→LUMO**	**18.05%**
				HOMO-7→LUMO	2.48%
				HOMO-5→LUMO	**28.61%**
				HOMO-3→LUMO	9.12%
				HOMO-3→LUMO+1	2.29%
				HOMO-2→LUMO+2	2.53%
				HOMO-1→LUMO+1	3.86%
				HOMO→LUMO+2	5.18%
				HOMO→LUMO+4	4.87%
12	4.6445	266.95	0.7025	HOMO-4→LUMO	7.75%
				HOMO-3→LUMO	6.52%
				HOMO-2→LUMO+1	4.35%
				HOMO-2→LUMO+2	2.01%
				HOMO-2→LUMO+4	2.25%
				HOMO-1→LUMO+1	**36.78%**
				HOMO-1→LUMO+5	2.33%
				HOMO→LUMO+3	**20.13%**
				HOMO→LUMO+4	3.63%
13	4.7056	263.48	0.3505	HOMO-4→LUMO	9.82%
				HOMO-3→LUMO	**13.94%**
				HOMO-2→LUMO+2	**15.20%**
				HOMO-2→LUMO+3	6.03%
				HOMO-2→LUMO+4	2.97%
				HOMO-1→LUMO+1	2.78%
				HOMO-1→LUMO+3	2.13%
				HOMO→LUMO+2	**10.56%**
				HOMO→LUMO+3	**21.04%**
16	4.8914	253.47	0.3219	**HOMO-10→LUMO**	**28.81%**
				HOMO-6→LUMO	**23.37%**
				HOMO-1→LUMO	5.45%

				HOMO-1→LUMO+2	2.26%
				HOMO-1→LUMO+3	**12.64%**
17	5.0806	244.03	0.2793	**HOMO-10→LUMO**	**28.57%**
				HOMO-10→LUMO+2	2.32%
				HOMO-6→LUMO	**22.64%**
				HOMO-5→LUMO	3.64%
				HOMO-2→LUMO+1	**12.59%**
				HOMO-1→LUMO+1	6.40%
				HOMO→LUMO+4	5.47%
35	5.9059	209.93	0.1246	HOMO-16→LUMO	2.71%
				HOMO-13→LUMO	2.32%
				HOMO-12→LUMO	6.86%
				HOMO-5→LUMO+2	8.72%
				HOMO-5→LUMO+3	2.54%
				HOMO-3→LUMO+1	**16.79%**
				HOMO-3→LUMO+2	**12.21%**
				HOMO-3→LUMO+3	9.27%
				HOMO-2→LUMO+2	2.31%
				HOMO→LUMO+6	2.32%
				HOMO→LUMO+7	2.79%
39	6.0069	206.40	0.2112	HOMO-14→LUMO	3.32%
				HOMO-12→LUMO	2.97%
				HOMO-4→LUMO+1	**25.76%**
				HOMO-4→LUMO+2	**15.75%**
				HOMO-4→LUMO+3	7.45%
				HOMO→LUMO+3	2.20%
				HOMO→LUMO+4	4.29%
				HOMO→LUMO+6	2.74%
				HOMO→LUMO+7	3.55%

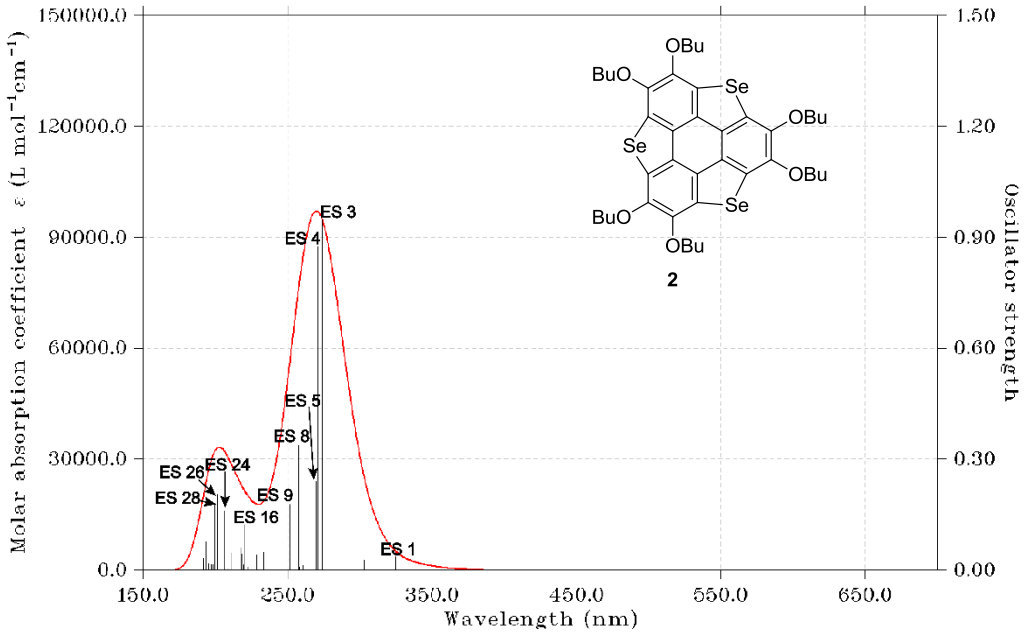

Figure S48. Calculated UV-Vis absorption spectra and corresponding excitation states (**ES**s) of **2.**

Table S13. Calculated excitation energy, excitation wavelength, oscillator strength, transition type and corresponding contribution of each excited state (**ES**) of **2.**

Excited State (**ES**)	Excitation Energy /eV	Excitation Wavelength / nm	Oscillator Strength	Transition Type	Contribution
1	3.8158	324.93	0.0368	HOMO-1→LUMO	3.31%
				HOMO-1→LUMO+1	**27.15%**
				HOMO→LUMO	**59.57%**
				HOMO→LUMO+1	3.20%
3	4.5231	274.11	0.9475	**HOMO-1→LUMO**	**35.79%**
				HOMO-1→LUMO+1	**18.51%**
				HOMO→LUMO	6.46%
				HOMO→LUMO+1	**22.23%**
				HOMO→LUMO+2	4.80%
4	4.5820	270.59	0.8759	**HOMO-1→LUMO**	**11.78%**
				HOMO-1→LUMO+1	**34.68%**
				HOMO-1→LUMO+3	2.05%
				HOMO→LUMO	**17.40%**
				HOMO→LUMO+1	9.20%
				HOMO→LUMO+3	**11.38%**
5	4.5963	269.75	0.2413	HOMO-4→LUMO+3	7.40%
				HOMO-4→LUMO+5	2.45%
				HOMO-3→LUMO+3	4.79%

				HOMO-1→LUMO	3.26%
				HOMO-1→LUMO+1	8.55%
				HOMO-1→LUMO+3	8.90%
				HOMO→LUMO	4.15%
				HOMO→LUMO+1	2.74%
				HOMO→LUMO+3	**42.45%**
				HOMO→LUMO+5	5.85%
8	4.8087	257.83	0.3375	HOMO-3→LUMO	3.31%
				HOMO-3→LUMO+1	3.01%
				HOMO-2→LUMO	9.75%
				HOMO-2→LUMO+1	2.96%
				HOMO-1→LUMO	5.69%
				HOMO-1→LUMO+2	2.75%
				HOMO→LUMO+1	3.48%
				HOMO→LUMO+2	**52.17%**
9	4.9268	251.65	0.1771	HOMO-4→LUMO	3.86%
				HOMO-4→LUMO+1	4.33%
				HOMO-3→LUMO	4.93%
				HOMO-3→LUMO+1	5.33%
				HOMO-2→LUMO	7.03%
				HOMO-2→LUMO+1	2.81%
				HOMO-1→LUMO+1	3.29%
				HOMO-1→LUMO+2	**47.11%**
				HOMO→LUMO+2	5.57%
16	5.6227	220.51	0.1224	HOMO-5→LUMO+1	3.10%
				HOMO-3→LUMO	**18.16%**
				HOMO-2→LUMO+1	**22.08%**
				HOMO-1→LUMO+2	**11.28%**
				HOMO-1→LUMO+3	7.30%
				HOMO→LUMO+2	9.63%
				HOMO→LUMO+5	5.26%
				HOMO→LUMO+6	2.99%
				HOMO→LUMO+7	2.54%
24	6.0019	206.57	0.1601	**HOMO-5→LUMO**	**23.71%**
				HOMO-4→LUMO	6.44%
				HOMO-4→LUMO+1	**32.96%**
				HOMO-3→LUMO+1	5.39%
				HOMO-3→LUMO+2	2.75%
				HOMO-1→LUMO+2	4.07%
				HOMO→LUMO+7	3.18%
				HOMO→LUMO+11	6.01%
26	6.1695	200.96	0.2038	**HOMO-5→LUMO**	**22.07%**
				HOMO-4→LUMO+2	9.82%
				HOMO-3→LUMO+2	**14.17%**

				HOMO-2→LUMO+2	7.36%
				HOMO-1→LUMO+6	**20.48%**
				HOMO-1→LUMO+7	8.54%
28	6.2169	199.43	0.1787	HOMO-7→LUMO	3.57%
				HOMO-6→LUMO+1	2.01%
				HOMO-5→LUMO+1	**30.84%**
				HOMO-4→LUMO+2	2.33%
				HOMO-3→LUMO+2	5.86%
				HOMO-2→LUMO+2	5.54%
				HOMO-1→LUMO+6	2.51%
				HOMO-1→LUMO+7	6.37%
				HOMO→LUMO+7	4.58%
				HOMO→LUMO+9	4.54%
				HOMO→LUMO+10	7.31%

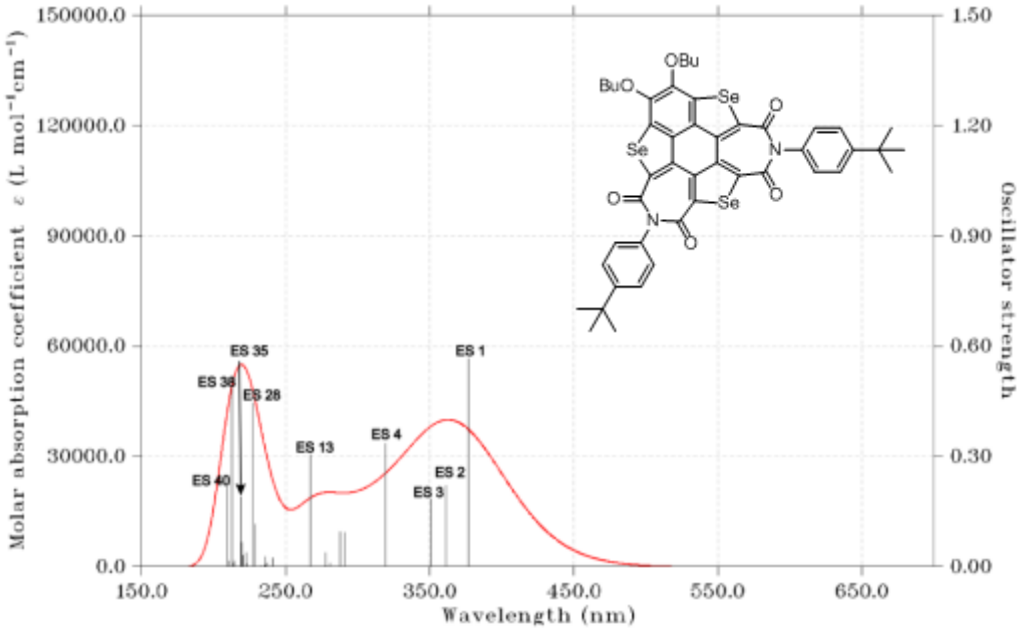

Figure S49. Calculated UV-Vis absorption spectra and corresponding excitation states (**ES**s) of **8.**

Table S14. Calculated excitation energy, excitation wavelength, oscillator strength, transition type and corresponding contribution of each excited state (**ES**) of **8.**

Excited State (**ES**)	Excitation Energy / eV	Excitation Wavelength / nm	Oscillator Strength	Transition Type	Contribution
1	3.292	376.62	0.5651	HOMO-1→LUMO+1	4.04%
				HOMO→LUMO	**89.43%**

2	3.4377	360.67	0.2208	HOMO-6→LUMO+1	7.20%
				HOMO-→LUMO+1	**85.51%**
3	3.5384	350.4	0.1854	**HOMO-1→LUMO**	**89.28%**
				HOMO→LUMO+2	3.13%
4	3.8838	319.23	0.3355	HOMO-7→LUMO+1	6.18%
				HOMO-6→LUMO	4.78%
				HOMO-4→LUMO+1	9.22%
				HOMO-1→LUMO+1	**65.4%**
				HOMO→LUMO	6.03%
13	4.6477	266.77	0.304	HOMO-7→LUMO	2.92%
				HOMO-4→LUMO	5.26%
				HOMO-1→LUMO	4.73%
				HOMO→LUMO+2	**73.58%**
				HOMO→LUMO+4	3.79%
28	5.4586	227.13	0.4454	**HOMO-13→LUMO**	**27.12%**
				HOMO-11→LUMO	6.93%
				HOMO7→LUMO+2	5.53%
				HOMO-5→LUMO	3.86%
				HOMO4→LUMO+1	3.44%
				HOMO-4→LUMO+2	**19.61%**
				HOMO-1→LUMO+2	**12.51%**
				HOMO→LUMO+11	6.90%
35	5.6596	219.07	0.1897	**HOMO-15→LUMO**	**22.16%**
				HOMO-15→LUMO+1	3.45%
				HOMO-14→LUMO	7.82%
				HOMO-13→LUMO	6.78%
				HOMO13→LUMO+2	2.81%
				HOMO-7→LUMO+2	6.09%
				HOMO-4→LUMO+2	5.10%
				HOMO-4→LUMO+3	2.47%
				HOMO-1→LUMO+3	**17.49%**
				HOMO-1→LUMO+4	5.83%
38	5.8293	212.69	0.4823	HOMO13→LUMO+2	4.63%
				HOMO-12→LUMO	**24.37%**
				HOMO11→LUMO+1	**28.35%**
				HOMO-7→LUMO+2	5.46%
				HOMO-6→LUMO+2	**36.40%**
				HOMO→LUMO+4	8.19%
40	5.9306	209.06	0.2172	HOMO16→LUMO+1	6.88%
				HOMO-15→LUMO	4.52%
				HOMO15→LUMO+1	**10.12%**
				HOMO-14→LUMO	6.01%
				HOMO14→LUMO+1	3.16%
				HOMO12→LUMO+1	7.00%

				HOMO-11→LUMO	**10.10%**
				HOMO-9→LUMO+1	2.14%
				HOMO-7→LUMO+2	3.98%
				HOMO-6→LUMO+3	3.24%
				HOMO-4→LUMO+2	7.86%
				HOMO-1→LUMO+4	7.23%
				HOMO→LUMO+3	2.54%

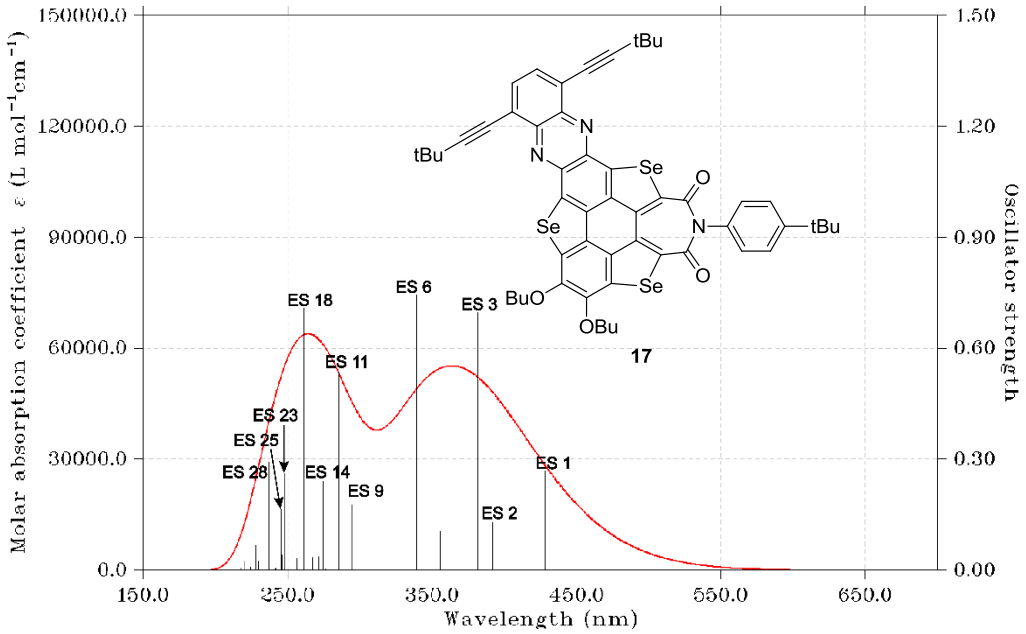

Figure S50. Calculated UV-Vis absorption spectra and corresponding excitation states (**ES**s) of **17.**

Table S15. Calculated excitation energy, excitation wavelength, oscillator strength, transition type and corresponding contribution of each excited state (**ES**) of **17.**

Excited State(**ES**)	Excitation Energy /eV	Excitation Wavelength / nm	Oscillator Strength	Transition Type	Contribution
1	2.8966	428.04	0.2664	**HOMO-1→LUMO**	**20.29%**
				HOMO→LUMO	**70.73%**
2	3.1615	392.17	0.1286	HOMO-7→LUMO	2.71%
				HOMO-1→LUMO	9.17%
				HOMO-1→LUMO+1	**10.76%**
				HOMO→LUMO	8.57%
				HOMO→LUMO+1	**59.87%**
3	3.2519	381.26	0.6967	HOMO-7→LUMO	5.36%
				HOMO-1→LUMO	**53.88%**
				HOMO-1→LUMO+1	**11.11%**

				HOMO→LUMO	7.03%
				HOMO→LUMO+1	**10.92%**
				HOMO→LUMO+2	3.10%
4	3.487	355.56	0.1065	HOMO-4→LUMO	4.03%
				HOMO-2→LUMO	**57.22%**
				HOMO-2→LUMO+1	**18.20%**
				HOMO-1→LUMO+1	5.23%
				HOMO→LUMO+3	2.70%
6	3.6532	339.38	0.7449	HOMO-4→LUMO	4.60%
				HOMO-2→LUMO	**18.73%**
				HOMO-2→LUMO+1	**36.29%**
				HOMO-1→LUMO	2.62%
				HOMO-1→LUMO+1	**14.14%**
				HOMO→LUMO+1	8.67%
9	4.057	294.8	0.1762	HOMO-7→LUMO	6.39%
				HOMO-7→LUMO+1	2.47%
				HOMO-5→LUMO+1	**20.67%**
				HOMO-4→LUMO+1	**44.10%**
				HOMO-1→LUMO+2	2.03%
				HOMO→LUMO+2	3.10%
				HOMO→LUMO+4	2.70%
11	4.3407	285.63	0.5361	HOMO-7→LUMO	2.43%
				HOMO-7→LUMO+1	8.69%
				HOMO-6→LUMO	7.64%
				HOMO-5→LUMO	7.08%
				HOMO-4→LUMO	5.39%
				HOMO-2→LUMO+1	2.16%
				HOMO-1→LUMO+2	**14.67%**
				HOMO→LUMO+2	**29.42%**
				HOMO→LUMO+3	2.84%
14	4.5147	274.62	0.2408	HOMO-11→LUMO	2.13%
				HOMO-7→LUMO	2.43%
				HOMO-7→LUMO+1	2.39%
				HOMO-6→LUMO	**12.84%**
				HOMO-5→LUMO	7.81%
				HOMO-4→LUMO	**12.46%**
				HOMO-4→LUMO+1	2.52%
				HOMO-2→LUMO	3.75%
				HOMO-2→LUMO+1	7.01%
				HOMO-2→LUMO+3	3.85%
				HOMO-1→LUMO+4	2.75%
				HOMO→LUMO+2	**21.69%**
				HOMO→LUMO+5	2.62%
18	4.7494	261.05	0.7087	HOMO-2→LUMO+4	2.35%

				HOMO-1→LUMO+2	7.63%
				HOMO-1→LUMO+3	**17.62%**
				HOMO-1→LUMO+4	8.34%
				HOMO-1→LUMO+5	3.18%
				HOMO→LUMO+2	5.66%
				HOMO→LUMO+3	**35.52%**
				HOMO→LUMO+4	5.11%
23	4.9939	248.27	0.2618	**HOMO-11→LUMO**	**18.99%**
				HOMO-7→LUMO	4.90%
				HOMO-7→LUMO+1	**11.32%**
				HOMO-4→LUMO+1	5.19%
				HOMO-2→LUMO+2	**23.60%**
				HOMO-1→LUMO+2	7.52%
				HOMO-1→LUMO+3	5.02%
25	5.0585	245.00	0.1642	HOMO-7→LUMO	9.42%
				HOMO-4→LUMO	2.47%
				HOMO-2→LUMO+3	3.89%
				HOMO-2→LUMO+7	8.62%
				HOMO-2→LUMO+8	2.57%
				HOMO-1→LUMO+2	2.66%
				HOMO-1→LUMO+3	5.79%
				HOMO→LUMO+3	**10.11%**
				HOMO→LUMO+4	**16.59%**
				HOMO→LUMO+5	2.45%
				HOMO→LUMO+7	5.07%
28	5.2249	239.29	0.2915	HOMO-15→LUMO	7.73%
				HOMO-7→LUMO	5.51%
				HOMO-4→LUMO+2	**10.15%**
				HOMO-2→LUMO+3	9.88%
				HOMO-1→LUMO+1	7.32%
				HOMO-1→LUMO+2	5.26%
				HOMO→LUMO+1	3.72%
				HOMO→LUMO+2	2.89%
				HOMO→LUMO+3	2.47%
				HOMO→LUMO+4	3.24%
				HOMO→LUMO+5	11.54%

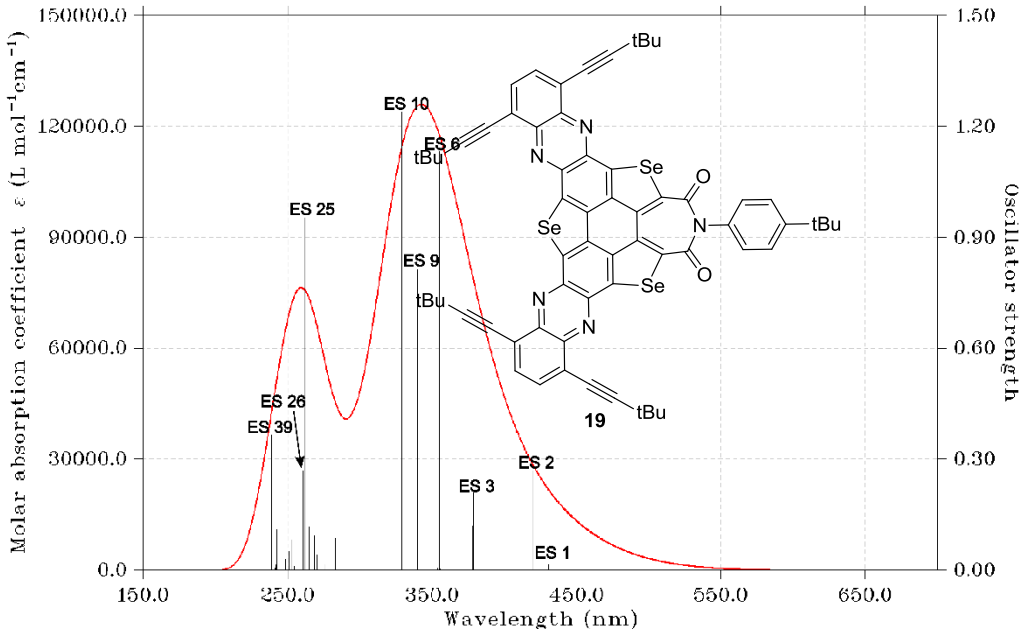

Figure S51. Calculated UV-Vis absorption spectra and corresponding excitation states (**ES**s) of **19.**

Table S16. Calculated excitation energy, excitation wavelength, oscillator strength, transition type and corresponding contribution of each excited state (**ES**) of **19.**

Excited State (**ES**)	Excitation Energy / eV	Excitation Wavelength / nm	Oscillator strength	Transition Type	Contribution
1	2.8814	430.29	0.0162	**HOMO-1→LUMO+1**	**30.71%**
				HOMO→LUMO	**58.90%**
				HOMO→LUMO+2	2.52%
2	2.9565	419.36	0.2683	HOMO-2→LUMO+1	4.33%
				HOMO-1→LUMO	**54.59%**
				HOMO→LUMO+1	**34.52%**
3	3.2769	378.36	0.2093	HOMO-11→LUMO	3.26%
				HOMO-11→LUMO+1	4.97%
				HOMO-3→LUMO	2.43%
				HOMO-3→LUMO+2	3.34%
				HOMO-2→LUMO	**42.49%**
				HOMO-2→LUMO+1	9.37%
				HOMO-2→LUMO+2	2.36%
				HOMO-1→LUMO+1	2.72%
				HOMO-1→LUMO+2	3.82%
				HOMO→LUMO	5.73%
				HOMO→LUMO+1	6.28%
				HOMO→LUMO+2	2.12%
6	3.4927	354.99	1.1322	HOMO-5→LUMO	5.32%

				HOMO-3→LUMO+1	4.15%
				HOMO-2→LUMO	4.84%
				HOMO-2→LUMO+2	**45.46%**
				HOMO-1→LUMO+1	3.43%
				HOMO→LUMO+2	**26.02%**
9	3.6507	339.61	0.8121	HOMO-7→LUMO	3.42%
				HOMO-5→LUMO	**10.16%**
				HOMO-5→LUMO+2	2.99%
				HOMO-3→LUMO+1	**51.78%**
				HOMO-1→LUMO+1	8.89%
				HOMO-1→LUMO+3	2.36%
				HOMO→LUMO+2	9.63%
10	3.7743	328.50	1.2390	**HOMO-3→LUMO+2**	**33.95%**
				HOMO-2→LUMO+1	**16.50%**
				HOMO-1→LUMO+2	**35.11%**
				HOMO→LUMO+1	4.31%
25	4.7317	262.03	0.9522	HOMO-5→LUMO+1	2.18%
				HOMO-3→LUMO	4.28%
				HOMO-3→LUMO+4	2.61%
				HOMO-2→LUMO+6	2.64%
				HOMO-1→LUMO	3.35%
				HOMO-1→LUMO+4	**22.17%**
				HOMO-1→LUMO+5	9.46%
				HOMO→LUMO+3	**18.29%**
				HOMO→LUMO+6	**15.91%**
26	4.7586	260.55	0.2697	HOMO-7→LUMO+2	4.32%
				HOMO-5→LUMO	7.26%
				HOMO-2→LUMO+4	4.04%
				HOMO-1→LUMO+3	**15.98%**
				HOMO-1→LUMO+6	**16.74%**
				HOMO→LUMO+4	**21.21%**
				HOMO→LUMO+5	**11.75%**
39	5.1895	238.91	0.3645	HOMO-19→LUMO+1	2.07%
				HOMO-11→LUMO+1	5.11%
				HOMO-7→LUMO+2	7.21%
				HOMO-6→LUMO+2	4.23%
				HOMO-3→LUMO+3	**27.98%**
				HOMO-3→LUMO+8	2.31%
				HOMO-1→LUMO+3	**17.81%**
				HOMO-1→LUMO+6	7.98%
				HOMO→LUMO+4	2.16%

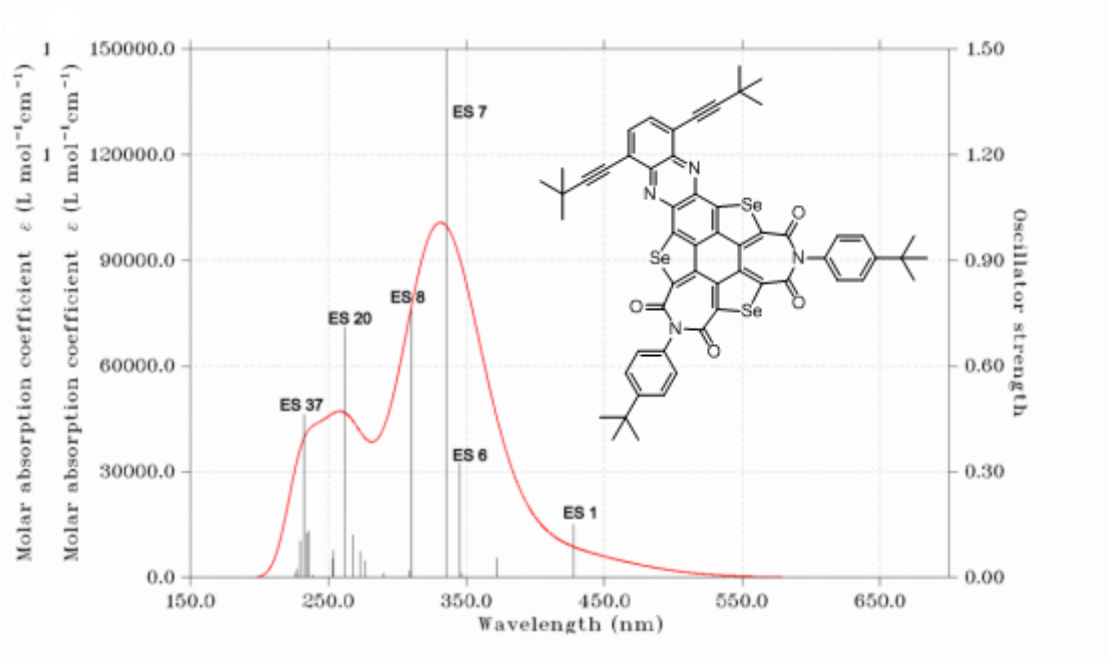

Figure S52. Calculated UV-Vis absorption spectra and corresponding excitation states (**ES**s) of **21.**

Table S17. Calculated excitation energy, excitation wavelength, oscillator strength, transition type and corresponding contribution of each excited state (**ES**) of **21.**

Excited State (**ES**)	Excitation Energy / eV	Excitation Wavelength / nm	Oscillator Strength	Transition Type	Contribution
1	2.8015	427.31	0.1511	**HOMO→LUMO**	**88.25%**
				HOMO→LUMO+2	5.41%
6	3.5925	345.12	0.323	HOMO-7→LUMO	2.84%
				HOMO-5→LUMO	8.96%
				HOMO-5→LUMO+2	3.89%
				HOMO-2→LUMO+2	**14.33%**
				HOMO-1→LUMO+1	**59.90%**
7	3.6969	335.37	1.6814	HOMO-8→LUMO	5.04%
				HOMO-8→LUMO+2	3.34%
				HOMO-5→LUMO+1	2.25%
				HOMO-2→LUMO+1	**19.57%**
				HOMO-1→LUMO	6.00%
				HOMO-1→LUMO+2	**32.44%**
				HOMO→LUMO+1	**24.77%**
8	3.7961	309.81	0.7583	HOMO-7→LUMO+2	2.31%
				HOMO-5→LUMO+2	7.91%
				HOMO-2→LUMO+2	**51.30%**
				HOMO-1→LUMO+1	**23.33%**
				HOMO→LUMO+2	8.58%
20	4.7442	261.34	0.7095	HOMO-5→LUMO	4.02%

				HOMO-2→LUMO+5	2.66%
				HOMO→LUMO+3	**46.06%**
				HOMO→LUMO+5	**32.08%**
37	5.3406	232.15	0.4616	HOMO-8→LUMO	5.25%
				HOMO-8→LUMO+3	3.37%
				HOMO-2→LUMO+4	2.84%
				HOMO-1→LUMO+3	3.56%
				HOMO-1→LUMO+5	5.26%
				HOMO→LUMO+1	9.65%
				HOMO→LUMO+4	**39.83%**
				HOMO→LUMO+6	**15.09%**

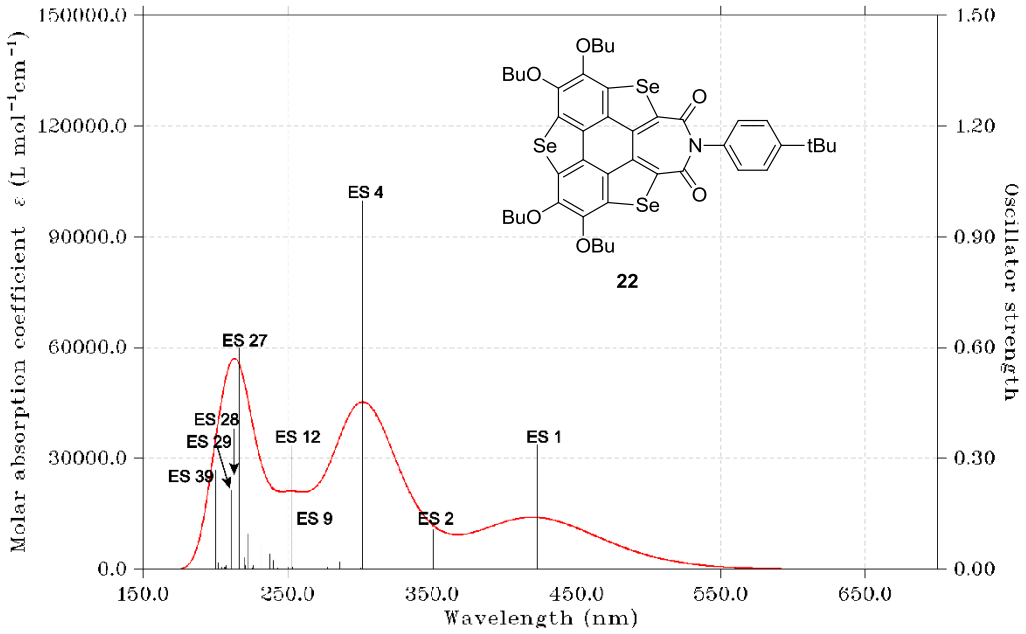

Figure S53. Calculated UV-Vis absorption spectra and corresponding excitation states (**ES**s) of **22.**

Table S18. Calculated excitation energy, excitation wavelength, oscillator strength, transition type and corresponding contribution of each excited state (**ES**) of **22.**

Excited State(**ES**)	Excitation Energy /eV	Excitation Wavelength / nm	Oscillator Strength	Transition Type	Contribution
1	2.9344	422.52	0.3376	**HOMO→LUMO**	**96.55%**
2	3.5355	350.68	0.1073	HOMO-4→LUMO	2.74%
				HOMO-1→LUMO	**78.56%**
				HOMO-1→LUMO+2	2.12%
				HOMO→LUMO+1	9.62%
4	4.1076	301..84	0.9967	HOMO-4→LUMO	6.52%
				HOMO-1→LUMO	**13.45%**
				HOMO→LUMO+1	**73.50%**

9	4.6518	266.53	0.1134	HOMO-4→LUMO	2.16%
				HOMO-3→LUMO	6.04%
				HOMO-1→LUMO+1	**11.32%**
				HOMO→LUMO+2	**72.54%**
12	4.9119	252.42	0.3354	HOMO-6→LUMO	2.94%
				HOMO-1→LUMO+1	**67.80%**
				HOMO→LUMO+2	**13.12%**
27	5.7277	216.46	0.5991	HOMO-12→LUMO	3.46%
				HOMO-11→LUMO	**35.79%**
				HOMO-10→LUMO	**12.34%**
				HOMO-3→LUMO+1	4.46%
				HOMO-1→LUMO+2	**10.97%**
				HOMO-1→LUMO+3	6.52%
				HOMO-1→LUMO+5	5.37%
				HOMO→LUMO+6	4.19%
				HOMO→LUMO+10	4.66%
28	5.8667	211.34	0..2132	HOMO-16→LUMO	5.22%
				HOMO-13→LUMO	**19.45%**
				HOMO-12→LUMO	5.24%
				HOMO-11→LUMO	2.34%
				HOMO-10→LUMO	4.03%
				HOMO-8→LUMO+1	2.52%
				HOMO-6→LUMO+1	8.51%
				HOMO-5→LUMO+1	2.25%
				HOMO-4→LUMO+2	6.92%
				HOMO-3→LUMO+1	**12.14%**
				HOMO→LUMO+6	**10.67%**
				HOMO→LUMO+10	2.07%
29	5.8667	211.34	0.2132	HOMO-6→LUMO+2	6.18%
				HOMO-4→LUMO+1	**13.35%**
				HOMO-4→LUMO+2	2.89%
				HOMO-3→LUMO+1	3.17%
				HOMO-3→LUMO+2	**10.82%**
				HOMO-1→LUMO+6	**29.95%**
				HOMO-1→LUMO+8	6.38%
				HOMO→LUMO+3	5.62%
				HOMO→LUMO+5	5.26%
39	6.1902	200.29	0.2677	HOMO-17→LUMO	9.66%
				HOMO-16→LUMO	5.36%
				HOMO-12→LUMO	2.72%
				HOMO-6→LUMO+2	**30.35%**
				HOMO-5→LUMO+2	**10.55%**
				HOMO-3→LUMO+2	9.36%

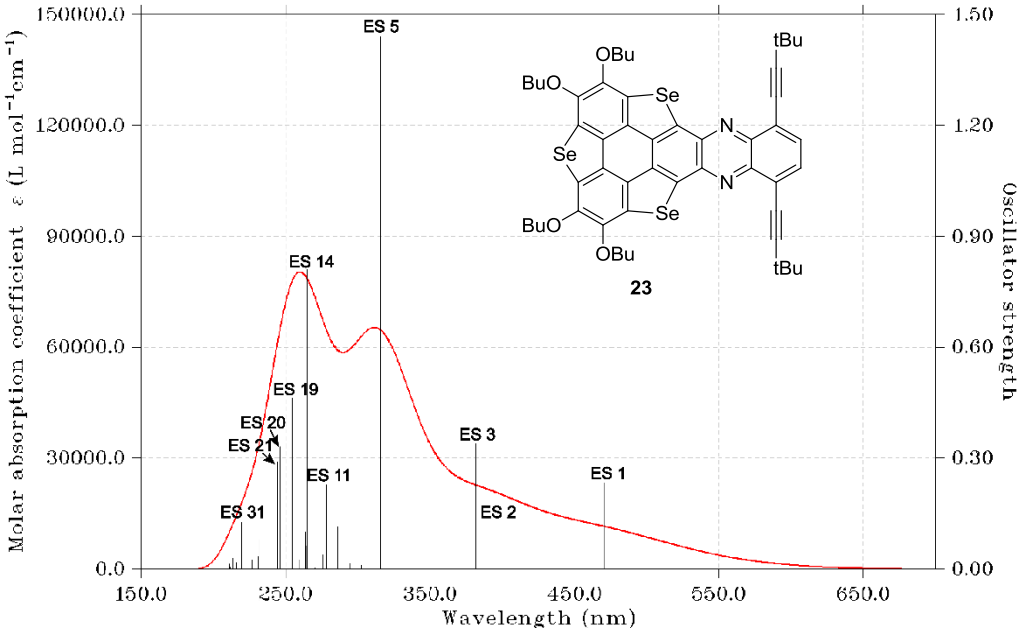

Figure S54. Calculated UV-Vis absorption spectra and corresponding excitation states (**ES**s) of **23.**

Table S19. Calculated excitation energy, excitation wavelength, oscillator strength, transition type and corresponding contribution of each excited state (**ES**) of **23.**

Excited State (**ES**)	Excitation Energy /eV	Excitation Wavelength / nm	Oscillator Strength	Transition Type	Contribution
1	2.6372	470.13	0.2343	HOMO-2→LUMO	3.50%
				HOMO→LUMO	**89.85%**
2	3.1660	391.61	0.1256	HOMO-6→LUMO	2.95%
				HOMO-2→LUMO	**71.59%**
				HOMO-1→LUMO	**14.33%**
				HOMO→LUMO	2.32%
				HOMO→LUMO+1	2.25%
3	3.2500	381.49	0.3381	HOMO-6→LUMO	4.13%
				HOMO-5→LUMO	7.84%
				HOMO-3→LUMO	2.25%
				HOMO-2→LUMO	**17.27%**
				HOMO-1→LUMO	**54.28%**
				HOMO-1→LUMO+2	3.22%
				HOMO→LUMO+1	5.90%
5	3.9277	315.66	1.4411	HOMO-1→LUMO	9.96%
				HOMO-1→LUMO+3	2.17%
				HOMO→LUMO+1	**74.70%**

11	4.4516	278.51	0.2285	HOMO-6→LUMO	5.54%
				HOMO-5→LUMO	4.60%
				HOMO-4→LUMO	**25.58**
				HOMO-4→LUMO+2	2.57%
				HOMO-3→LUMO	**13.60%**
				HOMO→LUMO+2	**29.22%**
				HOMO→LUMO+3	4.43%
14	4.6768	265.11	0.8102	HOMO-2→LUMO+2	3.69%
				HOMO-1→LUMO+1	**33.12%**
				HOMO-1→LUMO+5	2.14%
				HOMO→LUMO+3	**31.09%**
				HOMO→LUMO+5	3.31%
				HOMO→LUMO+7	3.08%
19	4.8717	254.50	0.4618	HOMO-15→LUMO	2.455%
				HOMO-13→LUMO	3.89%
				HOMO-6→LUMO	7.62%
				HOMO-5→LUMO	8.53%
				HOMO-4→LUMO+1	4.03%
				HOMO-1→LUMO	6.35%
				HOMO-1→LUMO+2	**11.16%**
				HOMO-1→LUMO+3	**32.33%**
				HOMO→LUMO+1	3.90%
20	5.0361	246.17	0.3308	**HOMO-10→LUMO**	**42.04%**
				HOMO-6→LUMO	**12.41%**
				HOMO-5→LUMO	3.56%
				HOMO-2→LUMO+1	**20.39%**
				HOMO-2→LUMO+5	2.66%
				HOMO→LUMO+5	2.10%
21	5.0717	244.46	0.2889	**HOMO-6→LUMO**	**10.62%**
				HOMO-5→LUMO	**10.55%**
				HOMO-3→LUMO+1	6.09%
				HOMO-2→LUMO+2	**12.63%**
				HOMO-2→LUMO+3	6.88%
				HOMO-1→LUMO+1	6.21%
				HOMO→LUMO+2	4.74%
				HOMO→LUMO+5	**10.77%**
				HOMO→LUMO+7	**10.77%**
31	5.6479	219.52	0.1270	HOMO-15→LUMO	2.52%
				HOMO-13→LUMO	3.80%
				HOMO-6→LUMO+1	5.77%
				HOMO-5→LUMO+2	2.27%
				HOMO-4→LUMO+1	**39.38%**
				HOMO-1→LUMO+3	**12.19%**
				HOMO-1→LUMO+5	**10.36%**

8. Complexation measurements of 18-21 with HBT

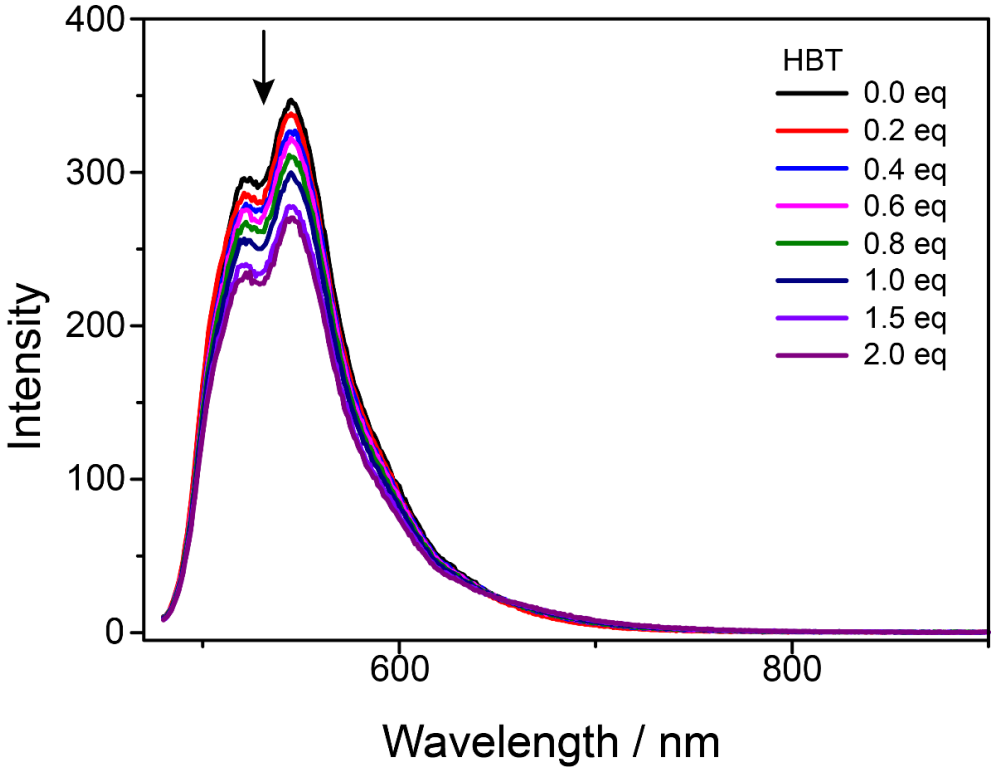

Figure S55. Emission spectra of **18** in toluene (1×10^{-4} mol L^{-1}) in the presence of **HBT**.

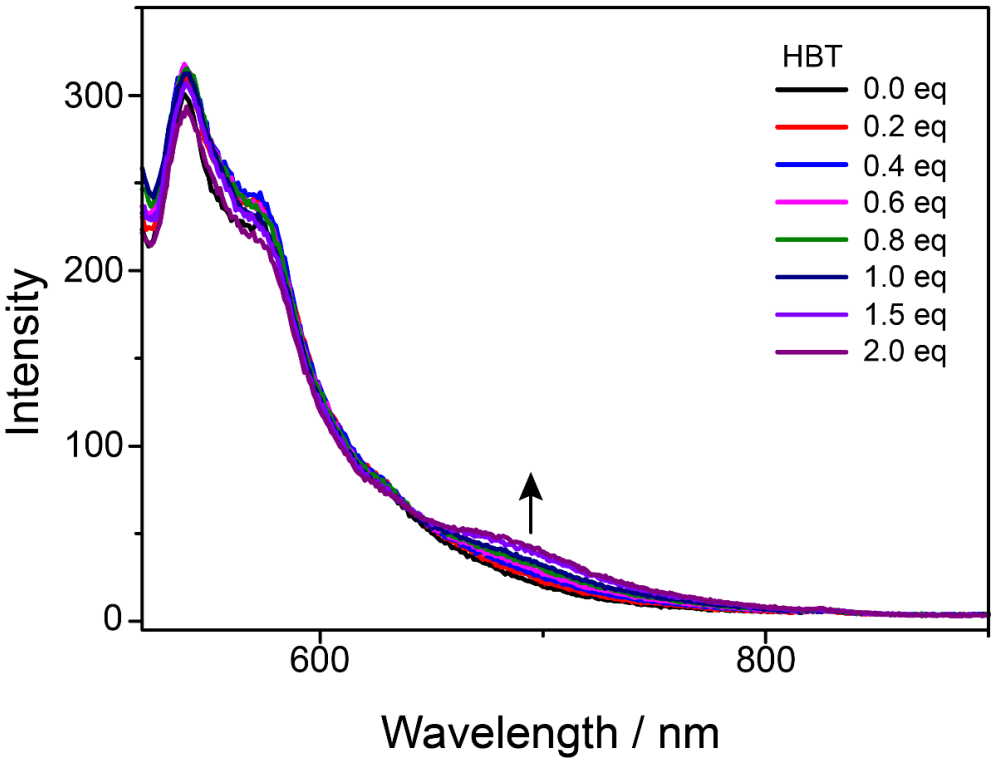

Figure S56. Emission spectra of **19** in toluene (1×10^{-4} mol L^{-1}) in the presence of **HBT**.

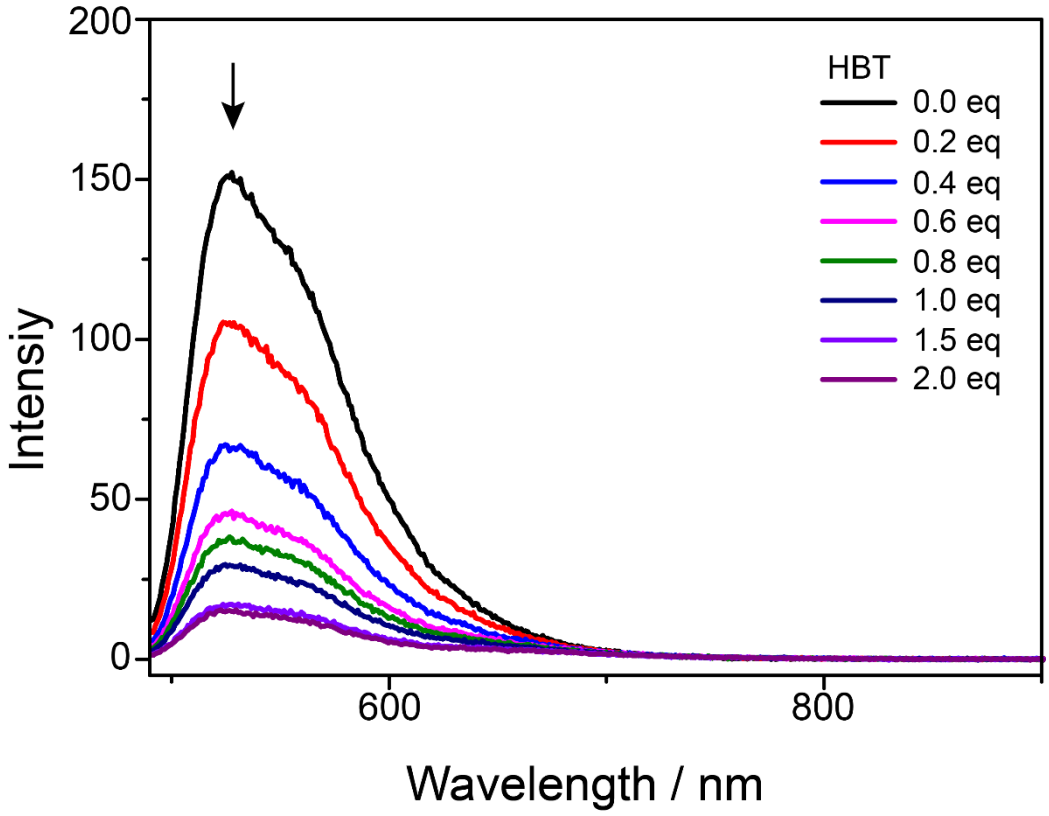

Figure S57. Emission spectra of **20** in toluene (1×10^{-4} mol L^{-1}) in the presence of **HBT**.

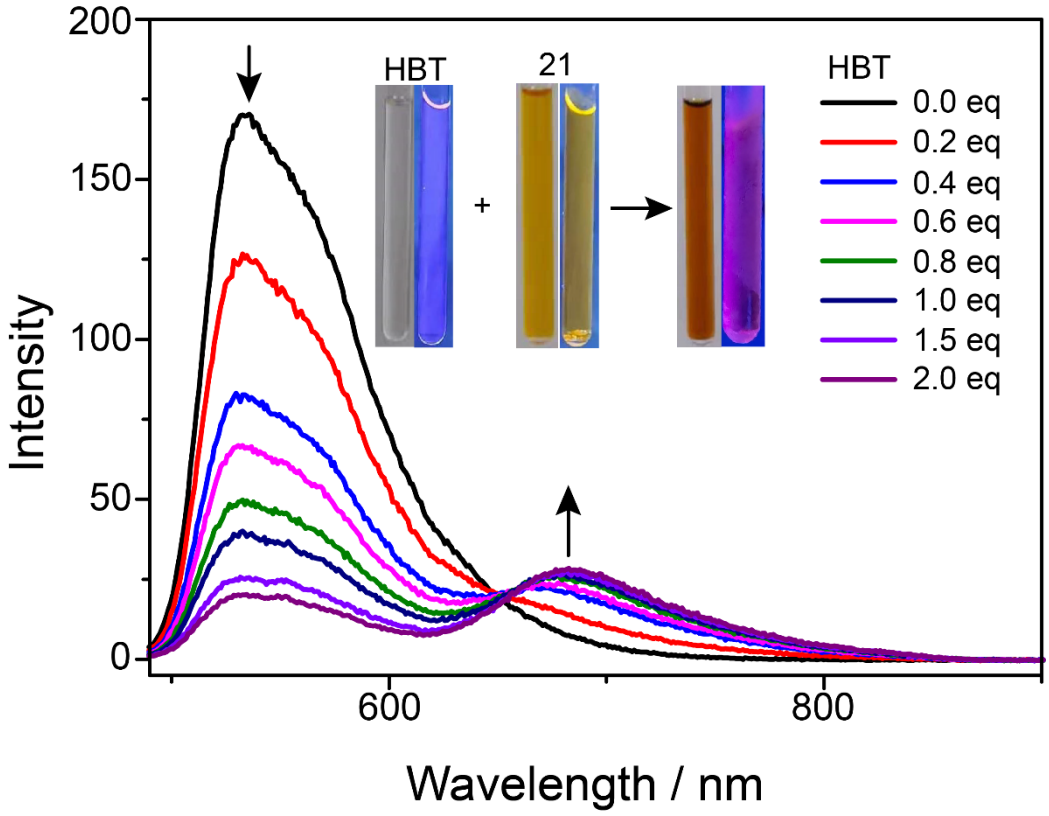

Figure S58. Emission spectra of **21** in toluene (1×10^{-4} mol L^{-1}) in the presence of **HBT**.

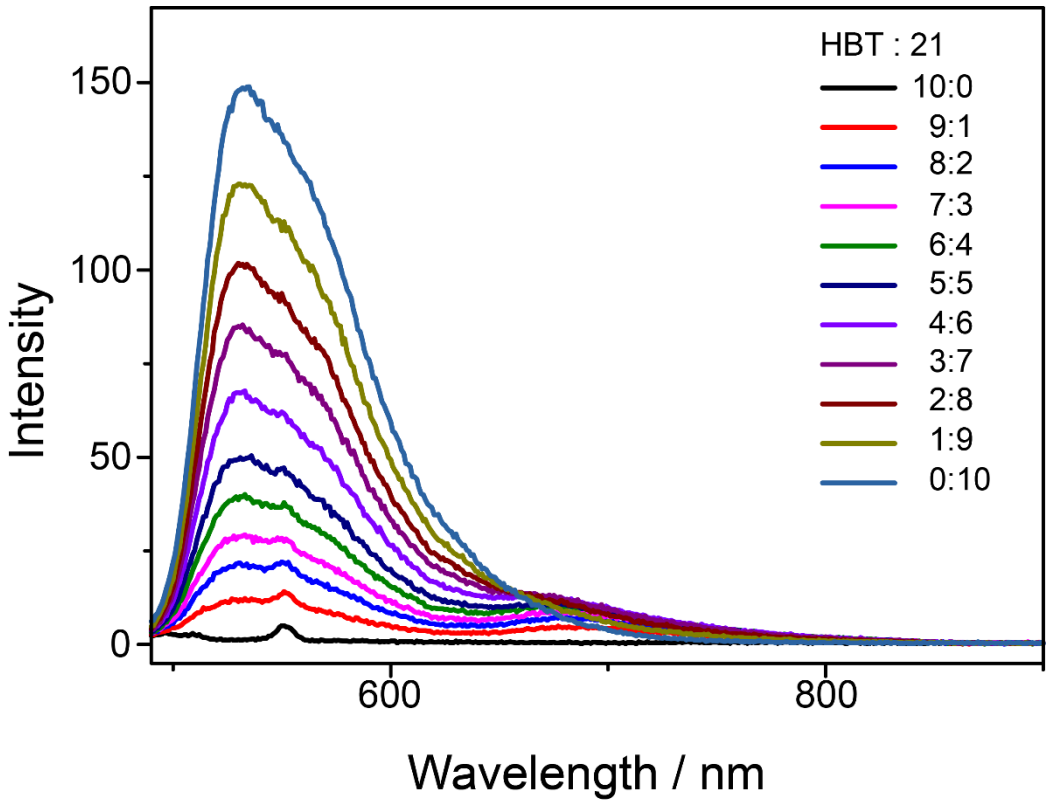

Figure S59. The Job-plot for complex **21**·**HBT** in toluene solution (c[**21**]+c[**HBT**]=1×10^{-4} mol L^{-1}) .

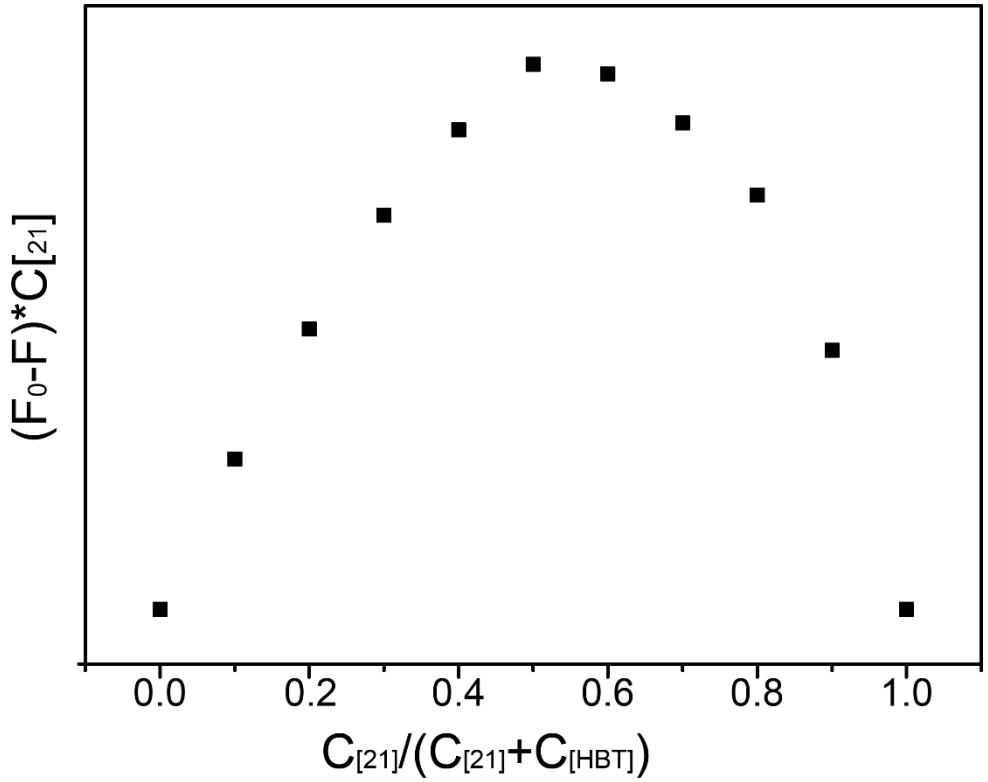

Figure S60. The combination ratio of **21** and **HBT** is 1 : 1.

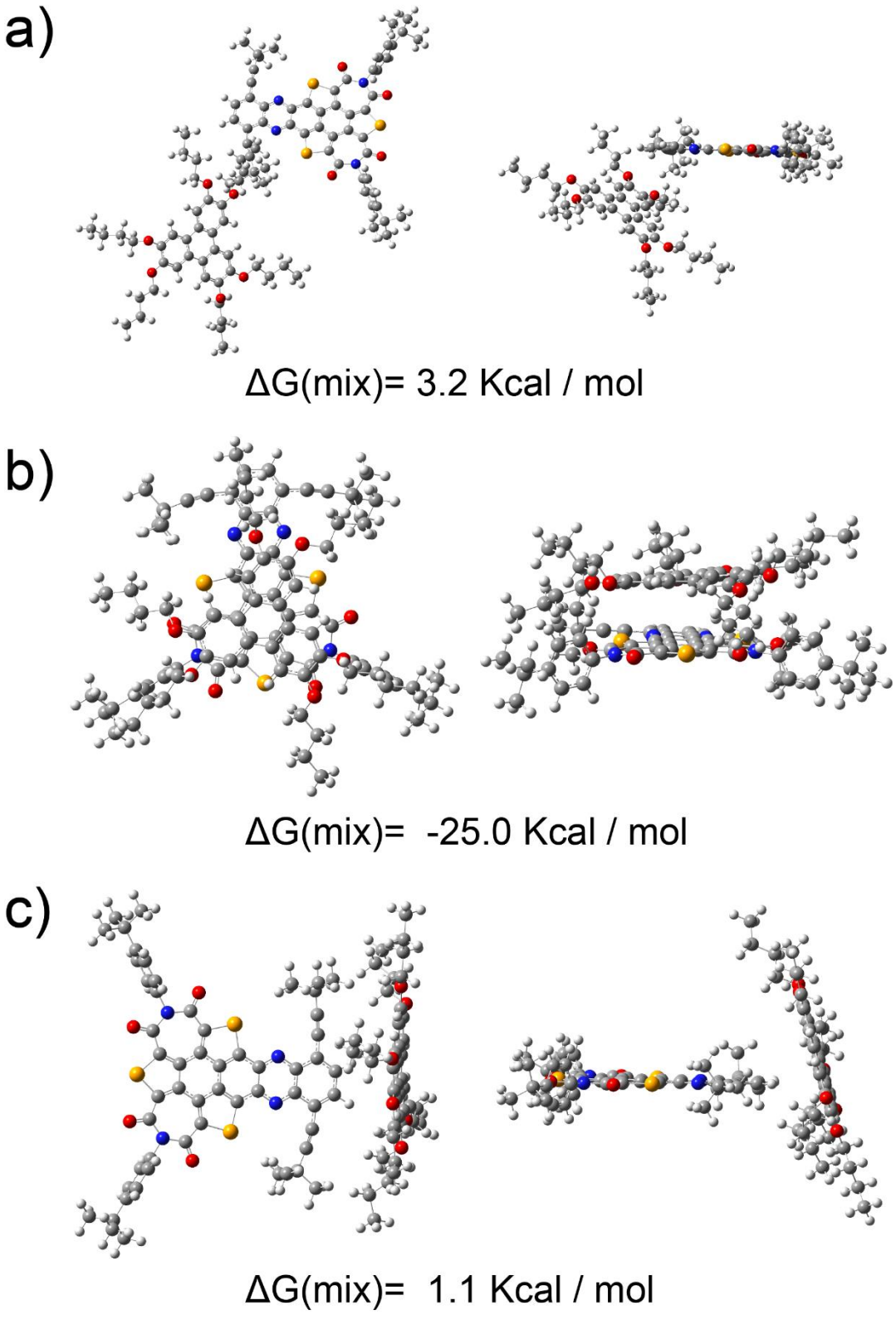

Figure S61. Optimized geometries of three possible structures of **21•HBT**

Table S20. The calculated energy levels for the frontier orbitals for compounds **HBT, 21, 21-HBT.**

Compound	Energy levels / eV				
	HOMO-1	HOMO	LUMO	LUMO+1	E_g[a]
HBT	-5.08	-5.08	-0.49	-0.49	4.59
21	-6.23	-5.75	-3.03	-2.73	2.72
21•HBT	5.19	-5.18	-2.84	-2.53	2.34

[a]E_g= E_{LUMO} - E_{HOMO}

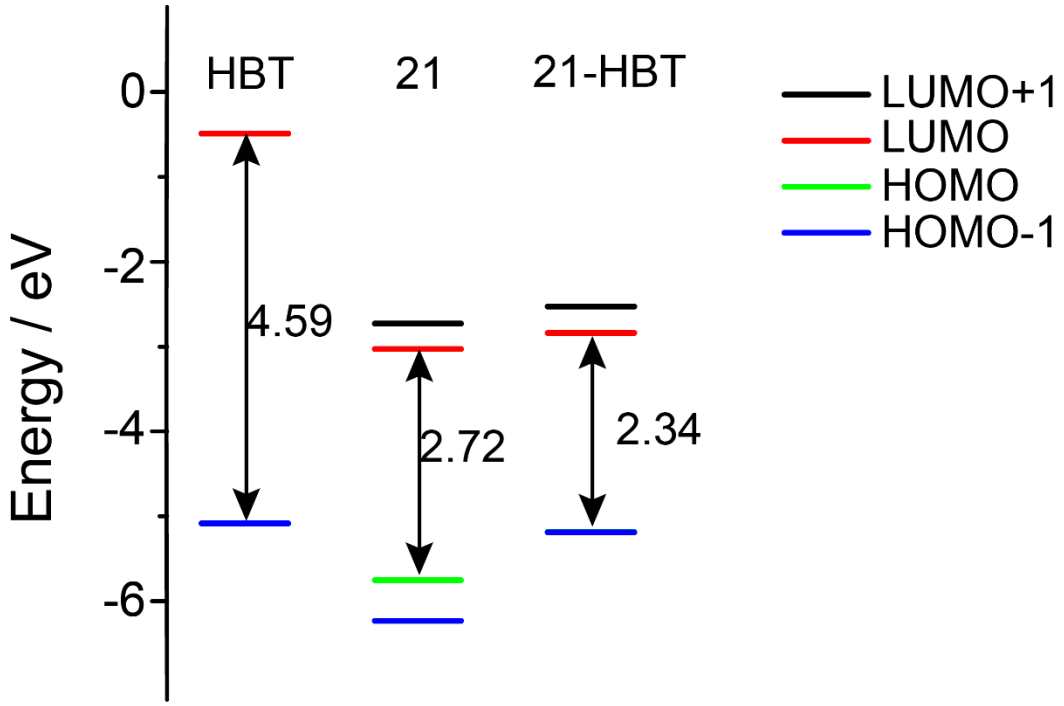

Figure S62. Schematic plot of HOMO-LUMO levels of compounds **HBT, 21, 21•HBT.**

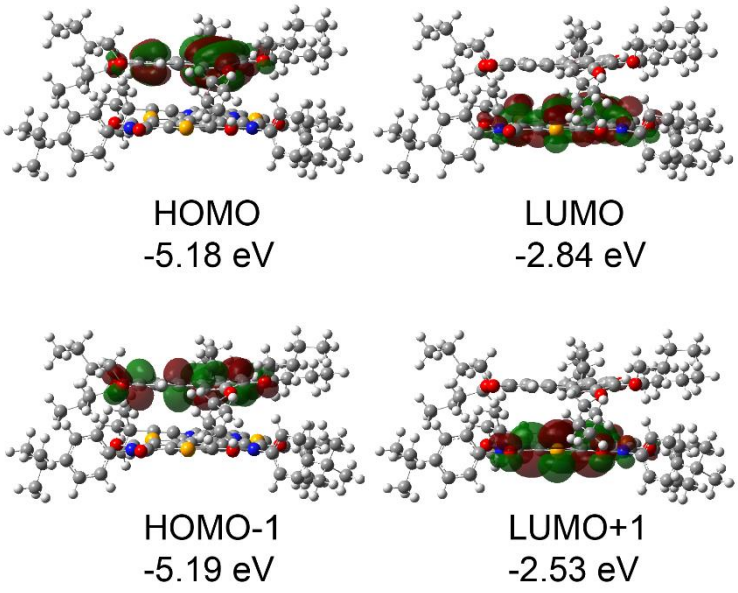

Figure S63. Calculated molecular orbitals of compounds **21•HBT.**

9. References:

[S1] W. L. F. Armarege, C. L. L. Chai., Purification of Laboratory Chemicals, 5th ed.

[S2] a) X. Li, Y. Zhu, J. Shao, B. Wang, S. Zhang, Y. Shao, X. Jin, X. Yao, R. Fang, X. Shao, *Angew. Chem. Int. Ed.*, **2014**, *53*, 535; b) X. Hou, J. Sun, Z. Liu, C. Yan, W. Song, H. Zhang, S. Zhou, X. Shao, *Chem. Commun.* **2018**, *54*, 10981.c) X. Li, Y. Zhu, J. Shao, L.Chen, S. Zhao, B. wang, S. Zhang,Y . Shao, H. Zhang, X. Shao, *Angew. Chem. Int. Ed.*, **2015**, *54*, 267;d) Y. Sun, X. Li, C. Sun, X. Hou, D. Lin, H. Zhang, C. Di, D. Zhu, X. Shao, *Angew. Chem. Int. Ed.*, **2017**, *56*, 13470.

[S3] M. C. Burla, R Caliandro., M. Camalli, B. Carrozzini, G. L. Cascarano, L. de Caro, C. Giacovazzo, G. Polidori, R. Spagna, *J. Appl. Cryst.* **2005**, *38*, 381.

[S4] G. M. Sheldrick, *SHELXL-97, A Program for Crystal Structure Refinement*, University of Göttingen, Göttingen, Germany, **1997**.

[S5] M. J. Frisch, G. W. Trucks, H. B. Schlegel, G. E. Scuseria, M. A. Robb, J. R. Cheeseman, G. Scalmani, V. Barone, G. A. Petersson, H. Nakatsuji, X. Li, M. Caricato, A. V. Marenich, J. Bloino, B. G. Janesko, R. Gomperts, B. Mennucci, H. P. Hratchian, J. V. Ortiz, A. F. Izmaylov, J. L. Sonnenberg, D. Williams-Young, F. Ding, F. Lipparini, F. Egidi, J. Goings, B. Peng, A. Petrone, T. Henderson, D. Ranasinghe, V. G. Zakrzewski, J. Gao, N. Rega, G. Zheng, W. Liang, M. Hada, M. Ehara, K. Toyota, R. Fukuda, J. Hasegawa, M. Ishida, T. Nakajima, Y. Honda, O. Kitao, H. Nakai, T. Vreven, K. Throssell, J. A. Montgomery, Jr., J. E. Peralta, F. Ogliaro, M. J. Bearpark, J. J. Heyd, E. N. Brothers, K. N. Kudin, V. N. Staroverov, T. A. Keith, R. Kobayashi, J. Normand, K. Raghavachari, A. P. Rendell, J. C. Burant, S. S. Iyengar, J. Tomasi, M. Cossi, J. M. Millam, M. Klene, C. Adamo, R. Cammi, J. W. Ochterski, R. L. Martin, K. Morokuma, O. Farkas, J. B. Foresman, D. J. Fox, *Gaussian 16, Revision A.03*, Gaussian, Inc., Wallingford CT, **2016**.

[S6] a) A. D. Becke, *J. Chem. Phys.* **1993**, *98*, 5648; b) C. Lee, W. Yang, R. G. Parr, *Phys. Rev. B.* **1988**, *37*, 785.

[S7] J. Tomasi, B. Mennucci, R. Cammi, *Chem. Rev*. **2005**, *105*, 2999.

[S8] G. A. Andrienko, Chemcraft, Version 1.8 (built 523b);

[S9] T. Lu, F. Chen, *J. Comput. Chem.* **2012**, *33*, 580.

10. ^{1}H NMR, ^{13}C NMR and IR Spectra of Products

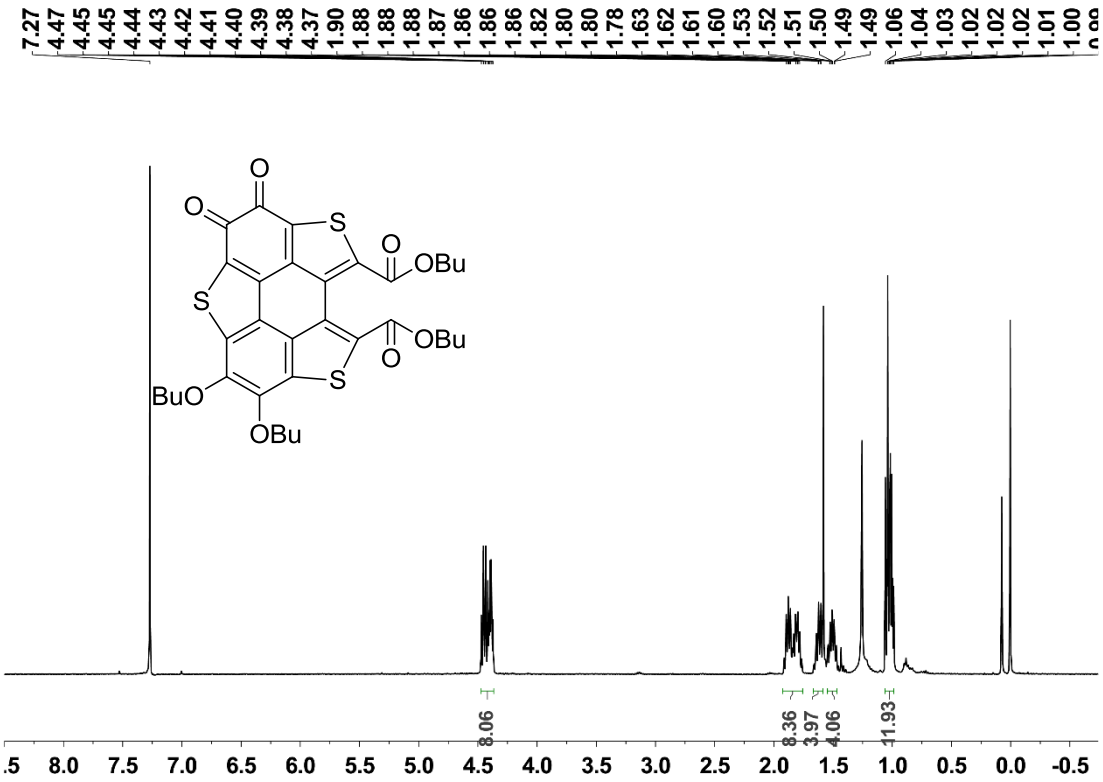

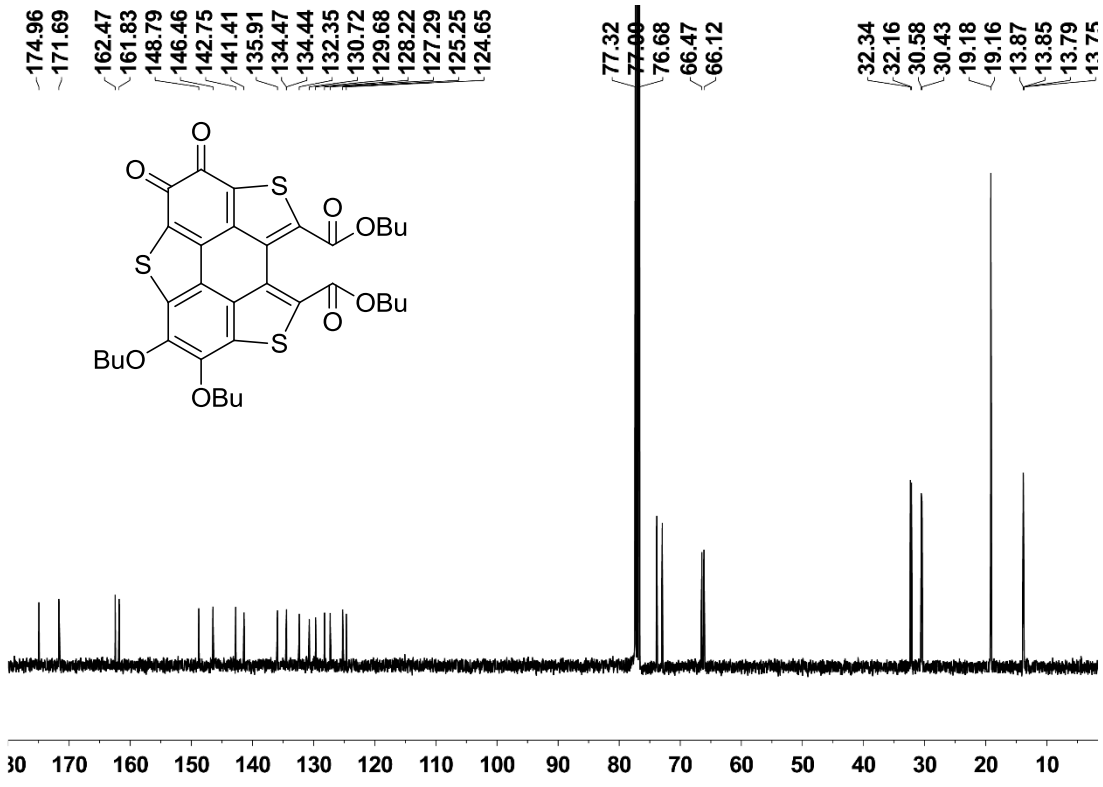

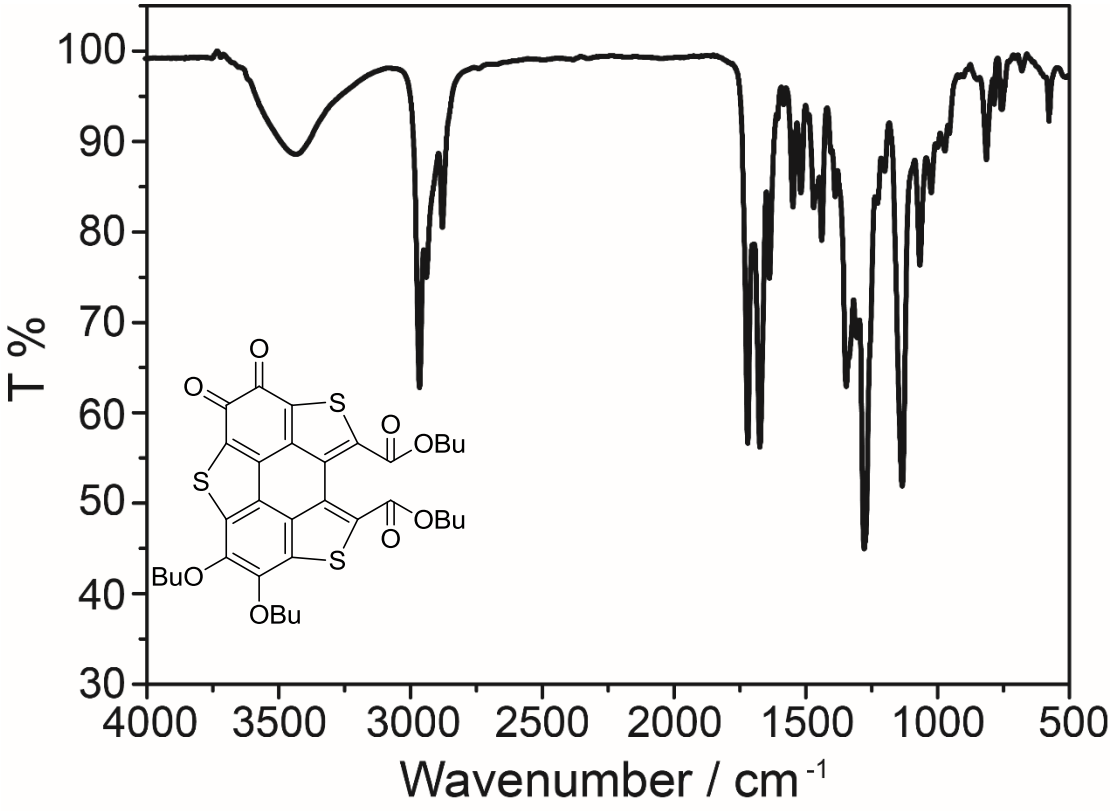
T %
Wavenumber / cm -1
100
90
80
70
60
50
40
30
4000
3500
3000
2500
2000
1500
1000
500
O
S
OBu
BuO

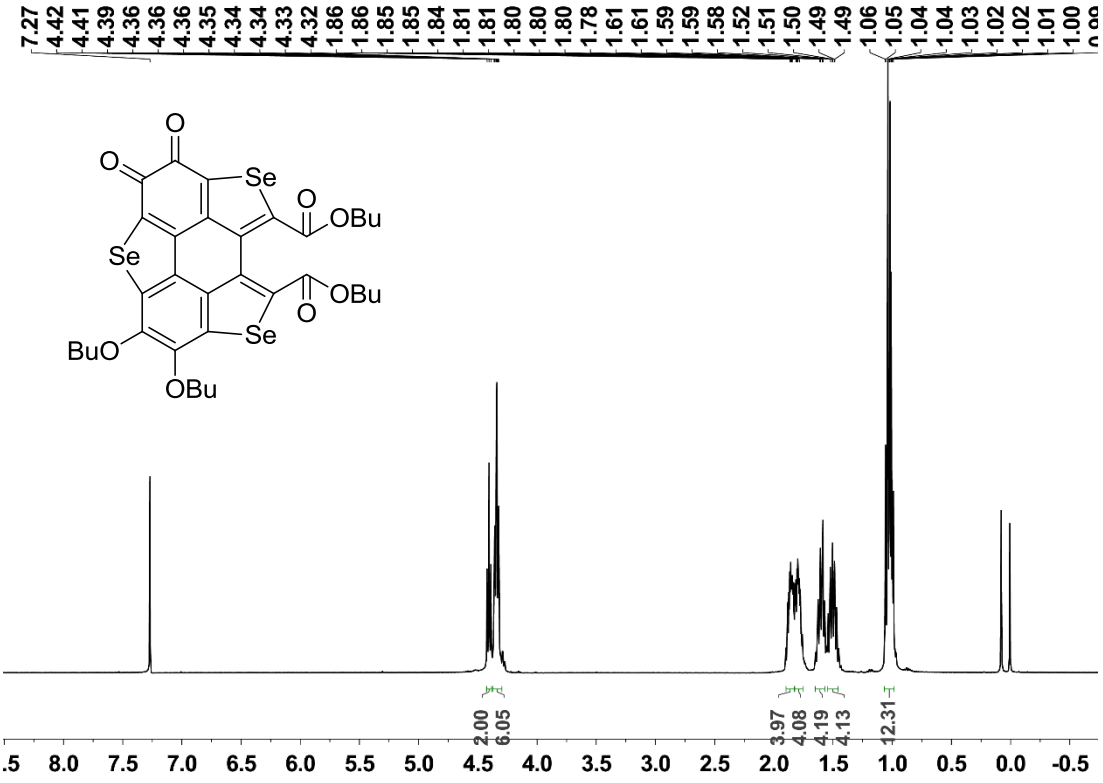
Se
OBu
BuO
2.00
6.05
3.97
4.08
4.19
4.13
12.31

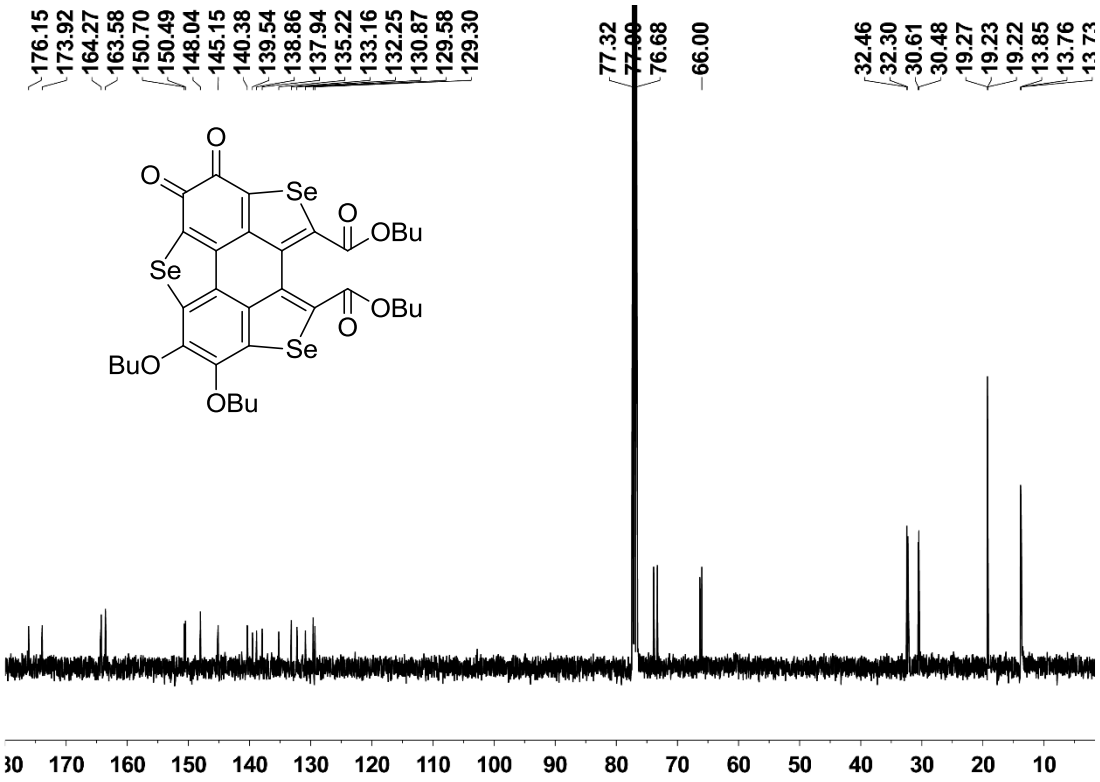
176.15
173.92
164.27
163.58
150.70
150.49
148.04
145.15
140.38
139.54
138.86
137.94
135.22
133.16
132.25
130.87
129.58
129.30
77.32
77.00
76.68
66.00
32.46
32.30
30.61
30.48
19.27
19.23
19.22
13.85
13.76
O
O
Se
O
OBu
Se
OBu
O
Se
BuO
OBu
170
160
150
140
130
120
110
100
90
80
70
60
50
40
30
20
10

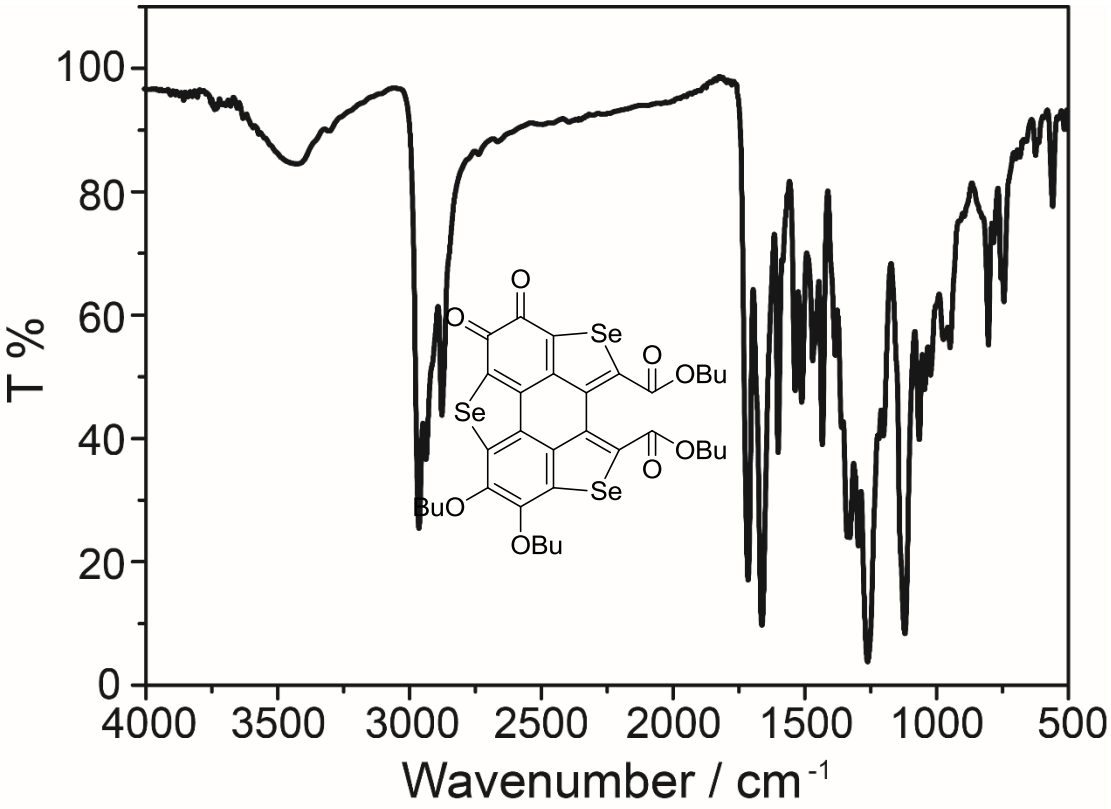
T %
100
80
60
40
20
0
4000
3500
3000
2500
2000
1500
1000
500
Wavenumber / cm-1
O
O
Se
O
OBu
Se
OBu
O
Se
BuO
OBu

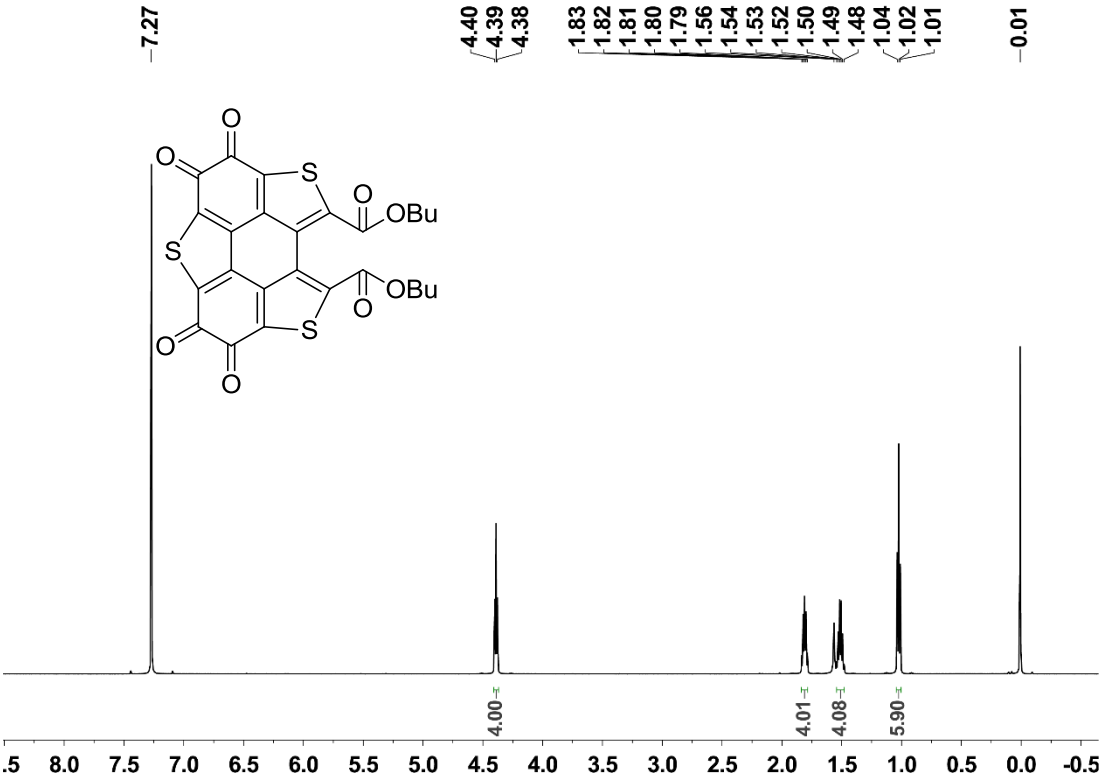
7.27
4.40
4.39
4.38
1.83
1.82
1.81
1.80
1.79
1.56
1.54
1.53
1.52
1.50
1.49
1.48
1.04
1.02
1.01
0.01
O
O
S
O
OBu
S
O
OBu
O
S
O
O
4.00
4.01
4.08
5.90
8.0
7.5
7.0
6.5
6.0
5.5
5.0
4.5
4.0
3.5
3.0
2.5
2.0
1.5
1.0
0.5
0.0
-0.5

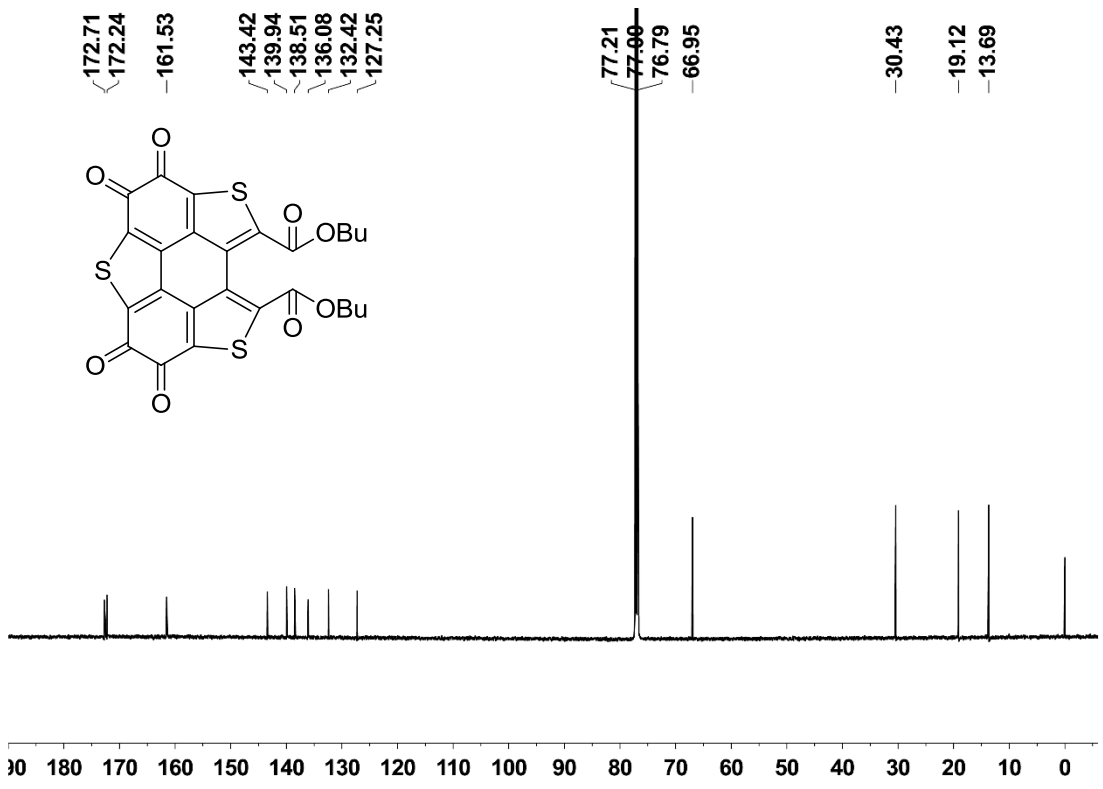
172.71
172.24
161.53
143.42
139.94
138.51
136.08
132.42
127.25
77.21
77.00
76.79
66.95
30.43
19.12
13.69
O
O
S
O
OBu
S
O
OBu
O
S
O
O
180
170
160
150
140
130
120
110
100
90
80
70
60
50
40
30
20
10
0

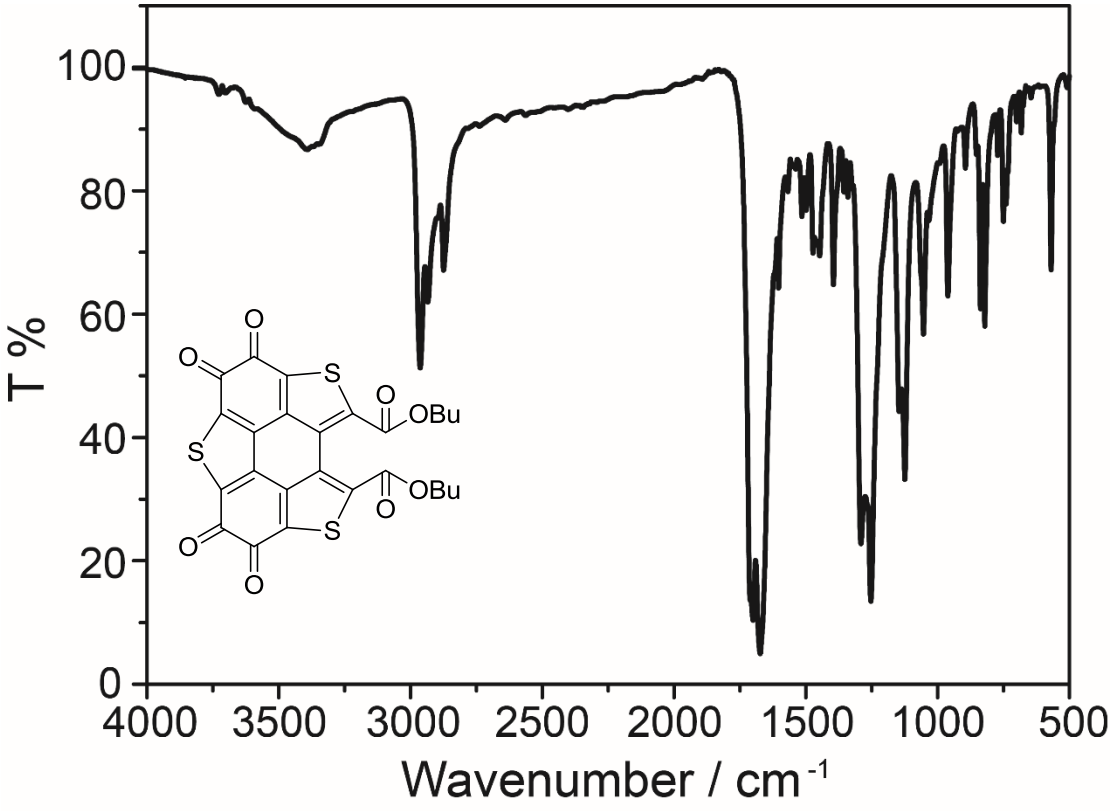
100
80
60
40
20
0
T %
4000
3500
3000
2500
2000
1500
1000
500
Wavenumber / cm -1
O
S
OBu
O

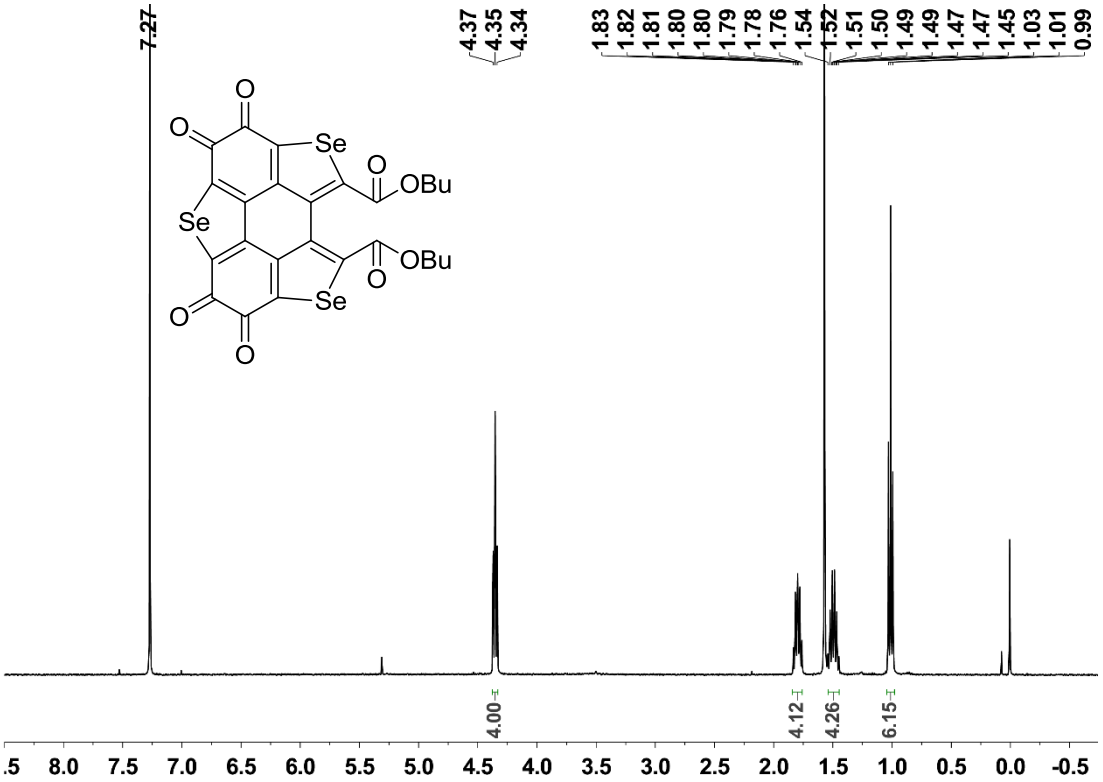
7.27
4.37
4.35
4.34
1.83
1.82
1.81
1.80
1.80
1.79
1.78
1.76
1.54
1.52
1.51
1.50
1.49
1.49
1.47
1.47
1.45
1.03
1.01
0.99
Se
OBu
O
4.00
4.12
4.26
6.15
8.0
7.5
7.0
6.5
6.0
5.5
5.0
4.5
4.0
3.5
3.0
2.5
2.0
1.5
1.0
0.5
0.0
-0.5

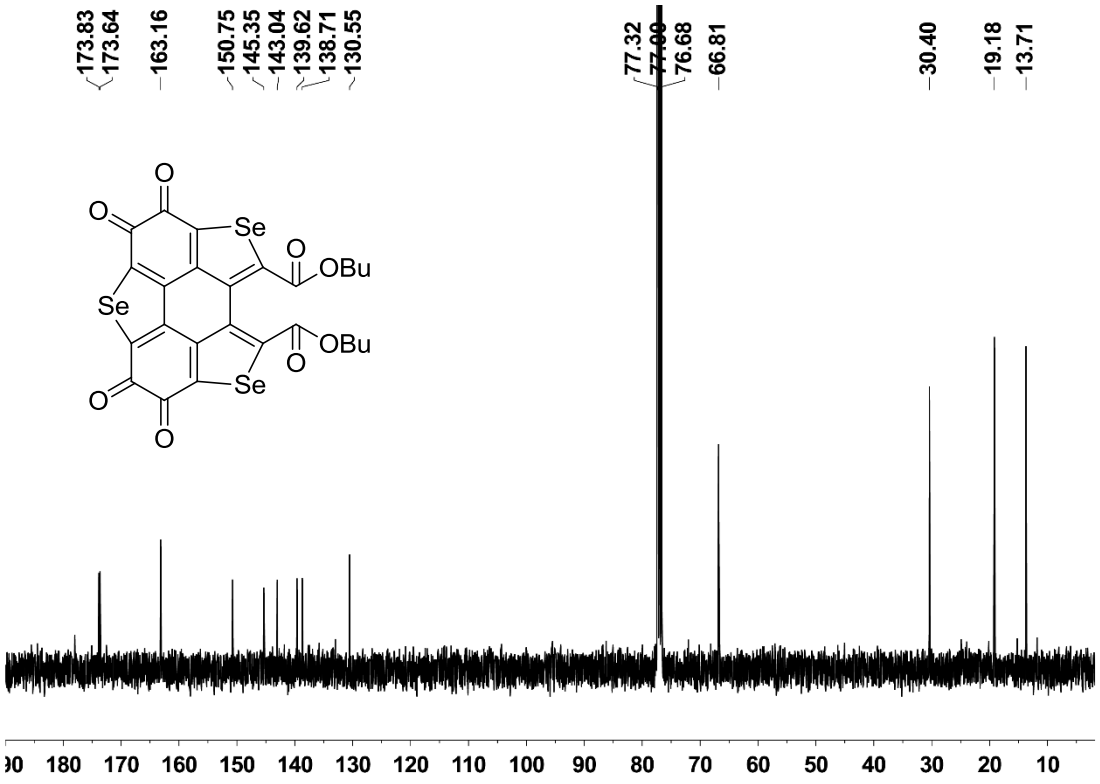
173.83
173.64
163.16
150.75
145.35
143.04
139.62
138.71
130.55
77.32
77.00
76.68
66.81
30.40
19.18
13.71
O
Se
OBu
180
170
160
150
140
130
120
110
100
90
80
70
60
50
40
30
20
10

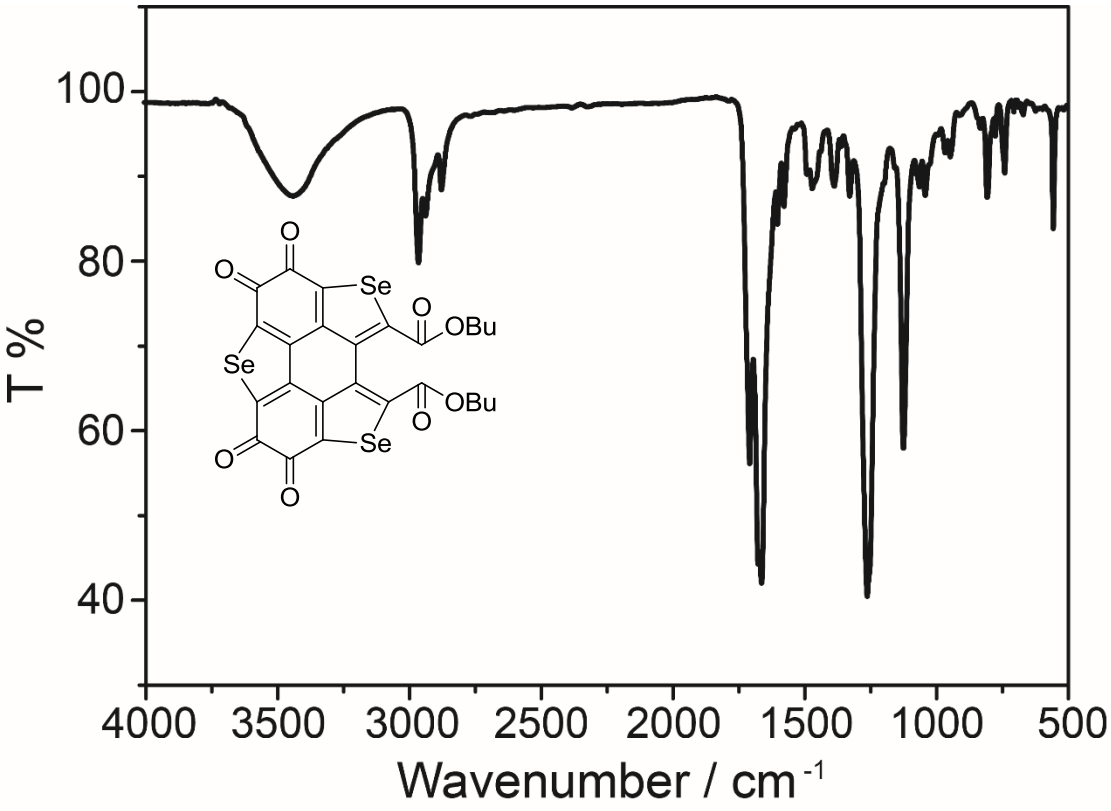
100
80
60
40
T %
4000
3500
3000
2500
2000
1500
1000
500
Wavenumber / cm -1
O
Se
OBu

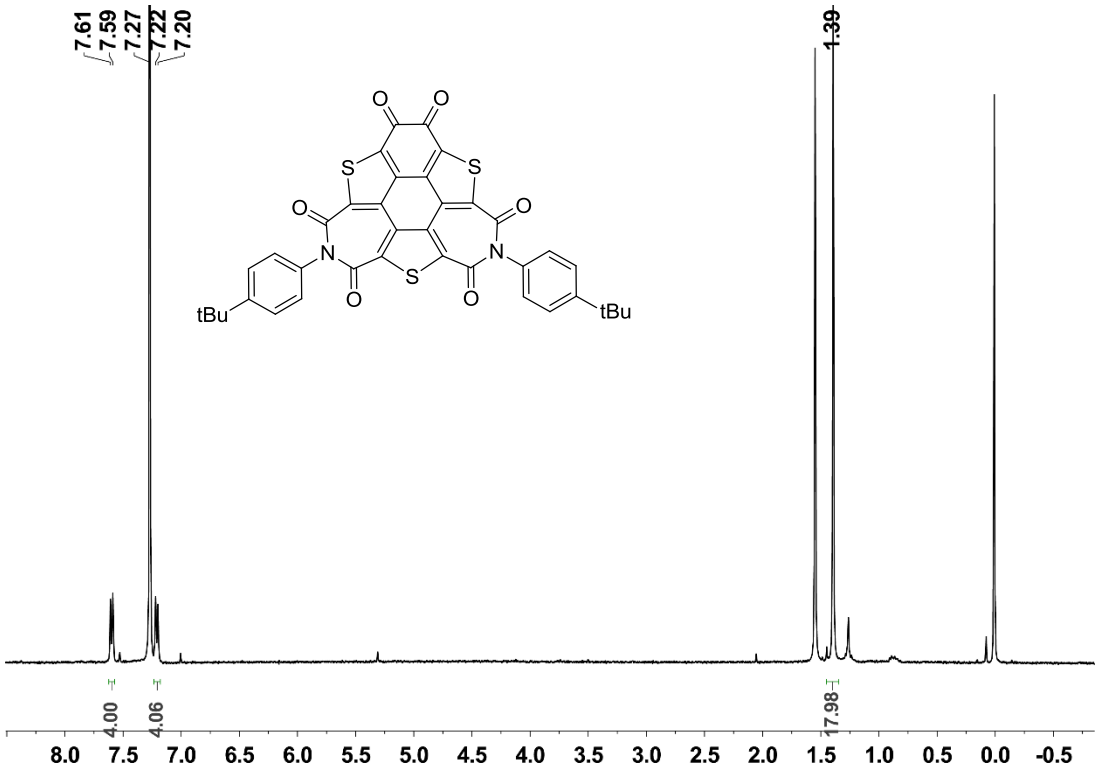
7.61
7.59
7.27
7.22
7.20
1.39
4.00
4.06
17.98
8.0 7.5 7.0 6.5 6.0 5.5 5.0 4.5 4.0 3.5 3.0 2.5 2.0 1.5 1.0 0.5 0.0 -0.5
tBu
tBu

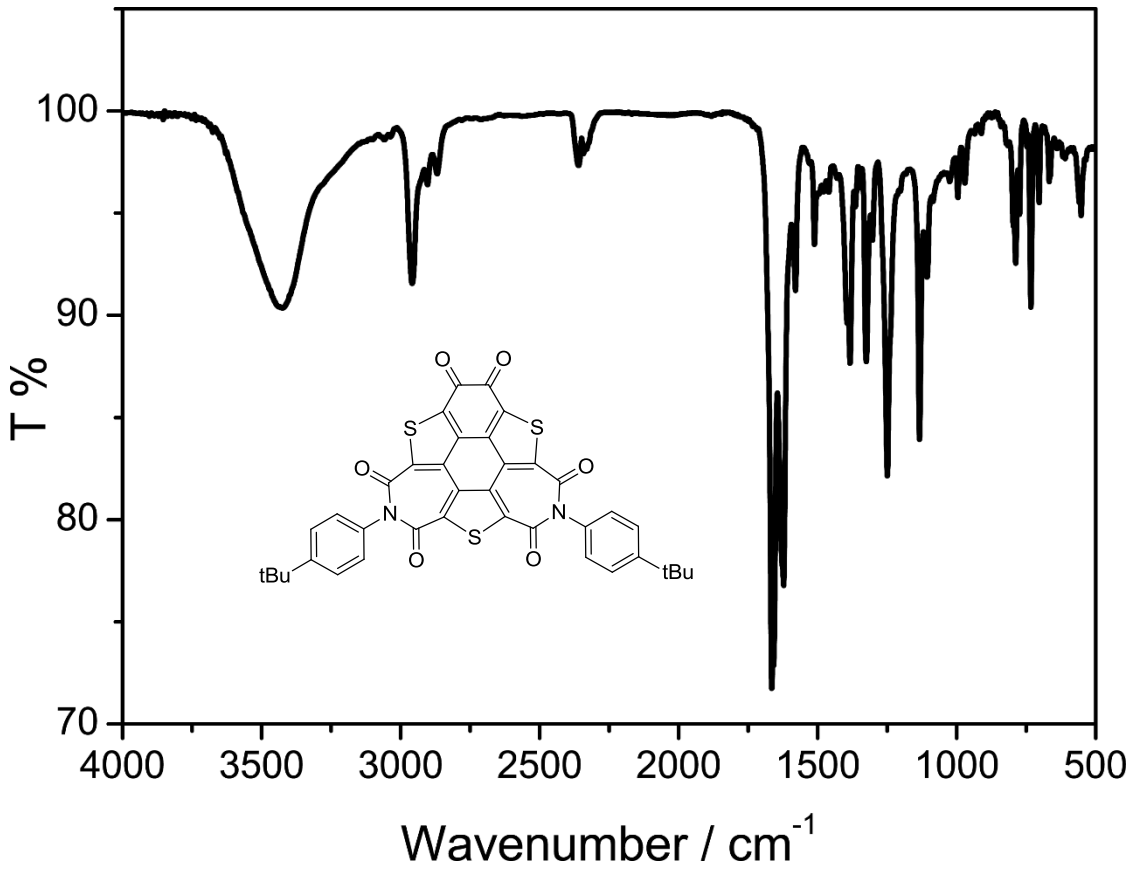
100
90
80
70
T %
4000 3500 3000 2500 2000 1500 1000 500
Wavenumber / cm-1
tBu
tBu

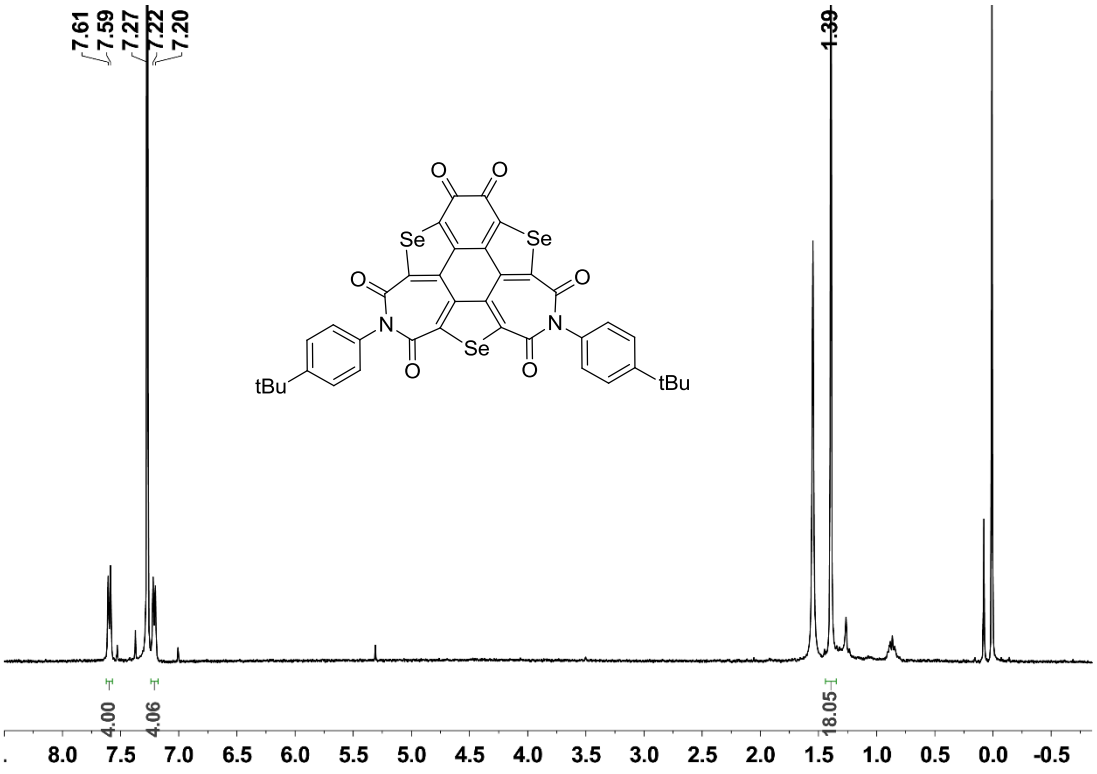
7.61
7.59
7.27
7.22
7.20
1.39
4.00
4.06
18.05
8.0 7.5 7.0 6.5 6.0 5.5 5.0 4.5 4.0 3.5 3.0 2.5 2.0 1.5 1.0 0.5 0.0 -0.5
O
O
Se
Se
O
O
N
N
Se
O
O
tBu
tBu

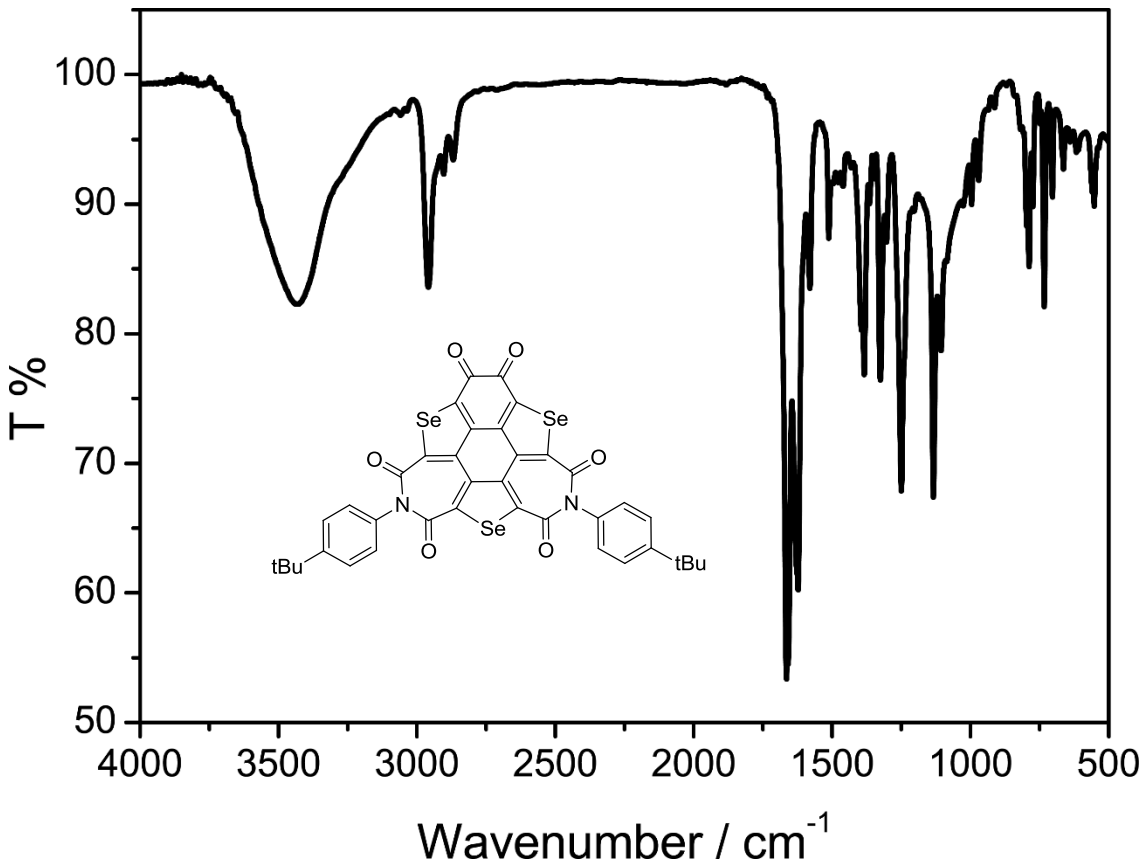
T %
100
90
80
70
60
50
4000 3500 3000 2500 2000 1500 1000 500
Wavenumber / cm-1
O
O
Se
Se
O
O
N
N
Se
O
O
tBu
tBu

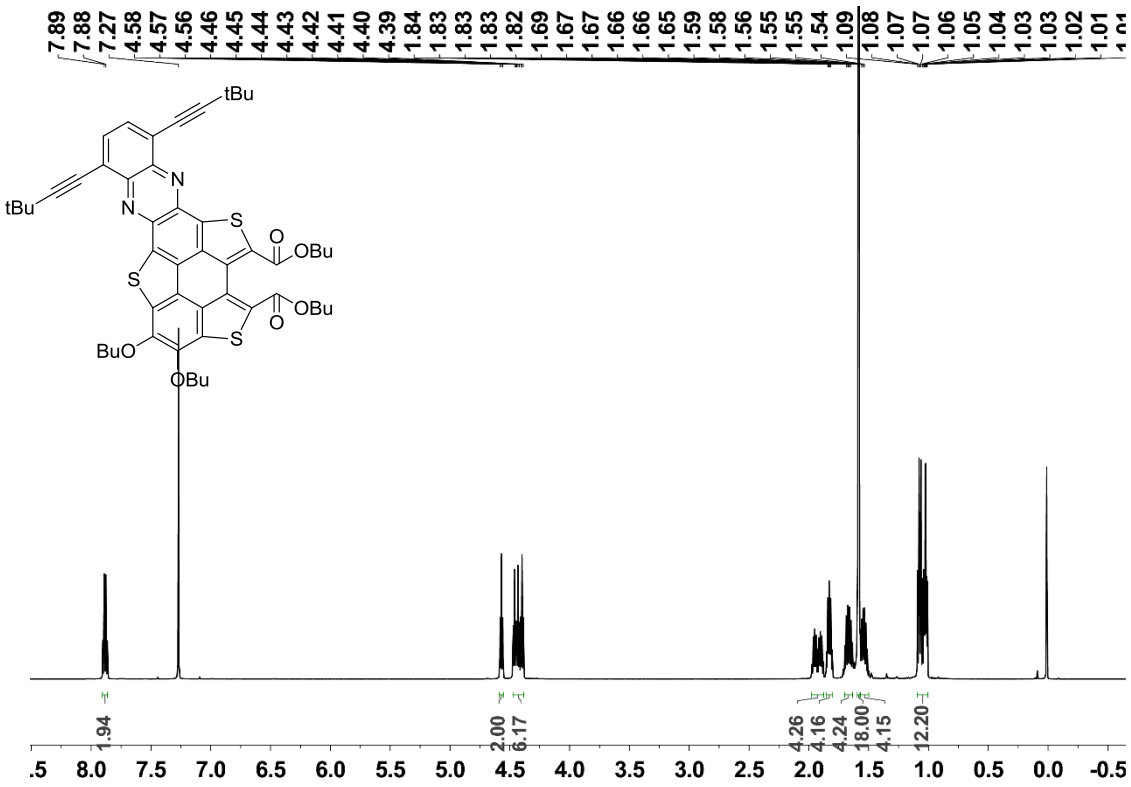
tBu
tBu
N
N
S
S
S
O
OBu
O
OBu
BuO
OBu

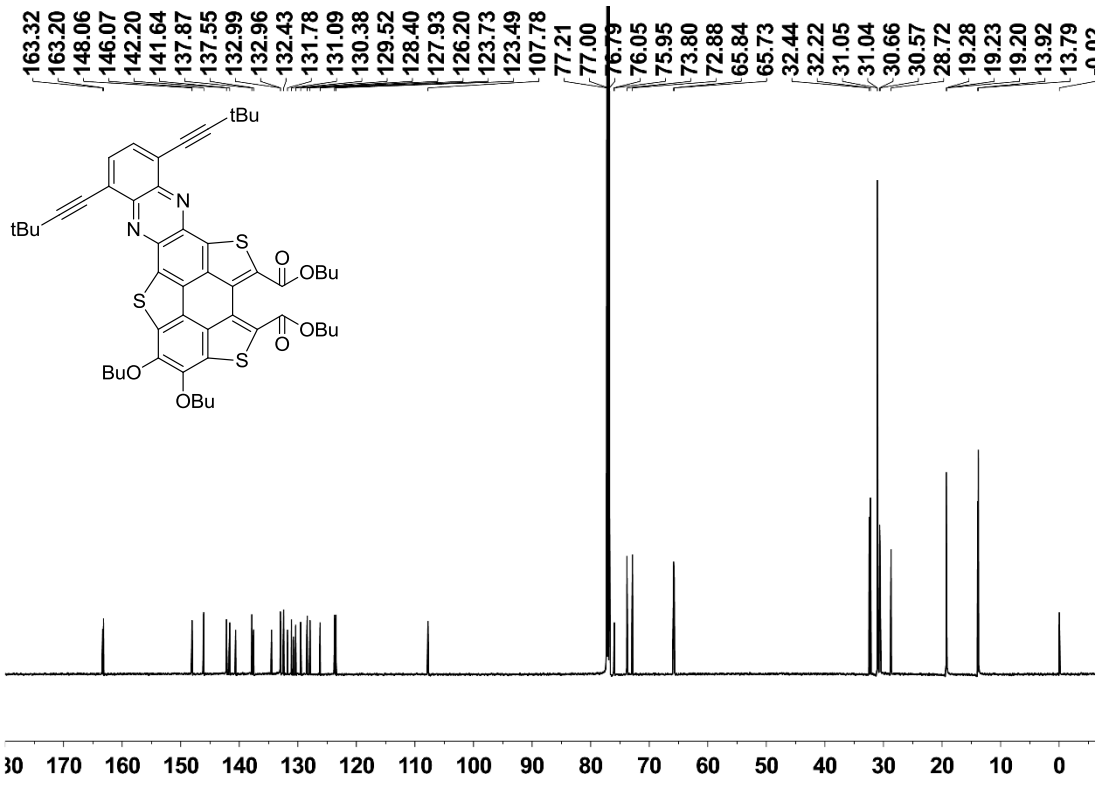
tBu
tBu
N
N
S
S
S
O
OBu
O
OBu
BuO
OBu

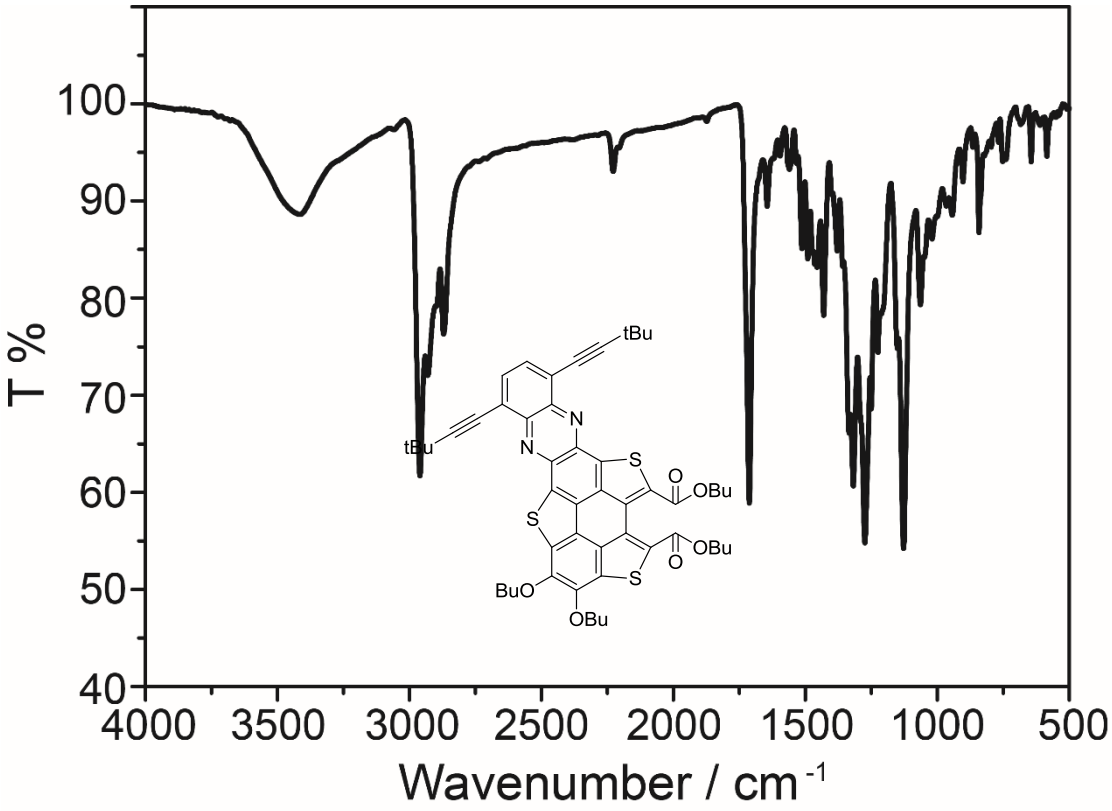
T %
100
90
80
70
60
50
40
4000 3500 3000 2500 2000 1500 1000 500
Wavenumber / cm -1
tBu
tBu
N
N
S
S
S
O
OBu
O
OBu
BuO
OBu

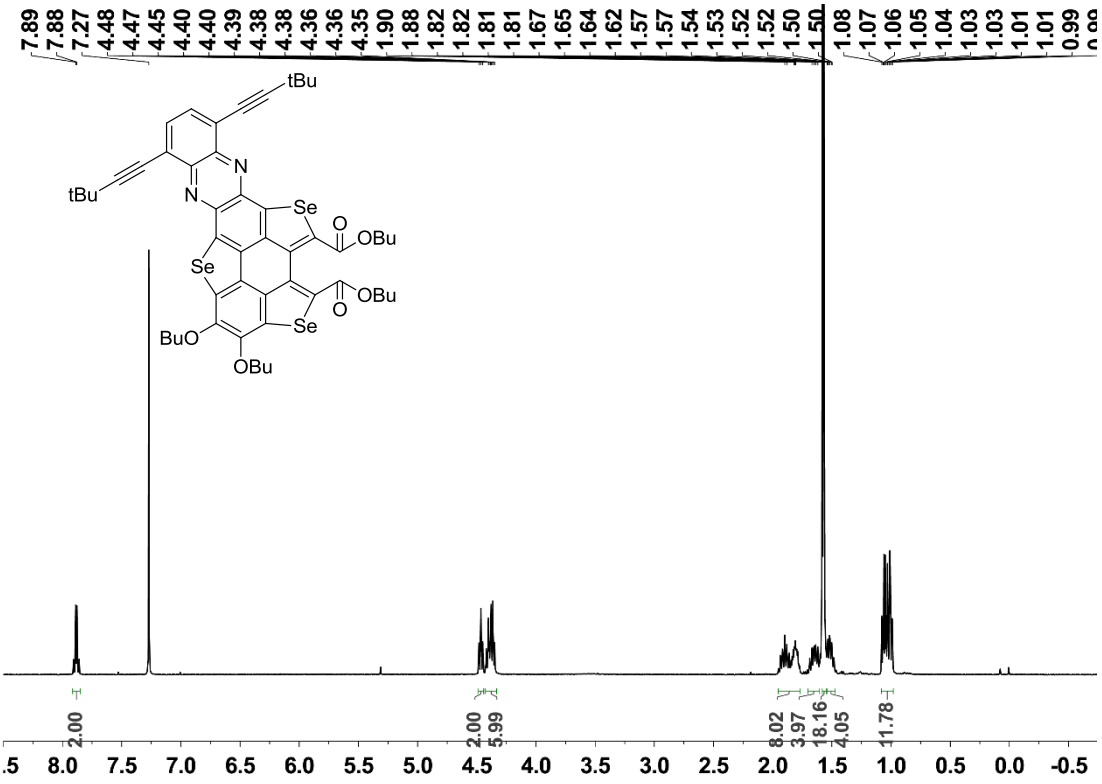
tBu
tBu
N
N
Se
Se
Se
O
OBu
O
OBu
BuO
OBu
2.00
2.00
5.99
8.02
3.97
18.16
4.05
11.78
8.0 7.5 7.0 6.5 6.0 5.5 5.0 4.5 4.0 3.5 3.0 2.5 2.0 1.5 1.0 0.5 0.0 -0.5

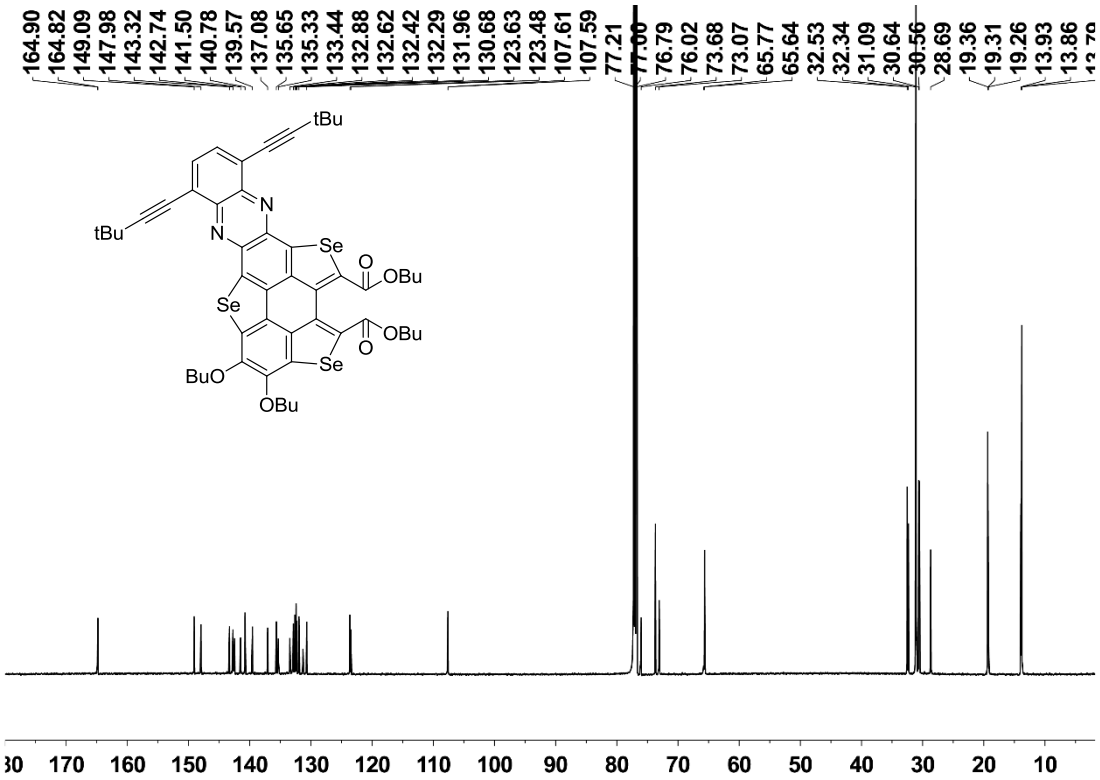
164.90
164.82
149.09
147.98
143.32
142.74
141.50
140.78
139.57
137.08
135.65
135.33
133.44
132.88
132.62
132.42
132.29
131.96
130.68
123.63
123.48
107.61
107.59
77.21
77.00
76.79
76.02
73.68
73.07
65.77
65.64
32.53
32.34
31.09
30.64
30.56
28.69
19.36
19.31
19.26
13.93
13.86
tBu
tBu
N
N
Se
Se
Se
O
OBu
O
OBu
BuO
OBu
170
160
150
140
130
120
110
100
90
80
70
60
50
40
30
20
10

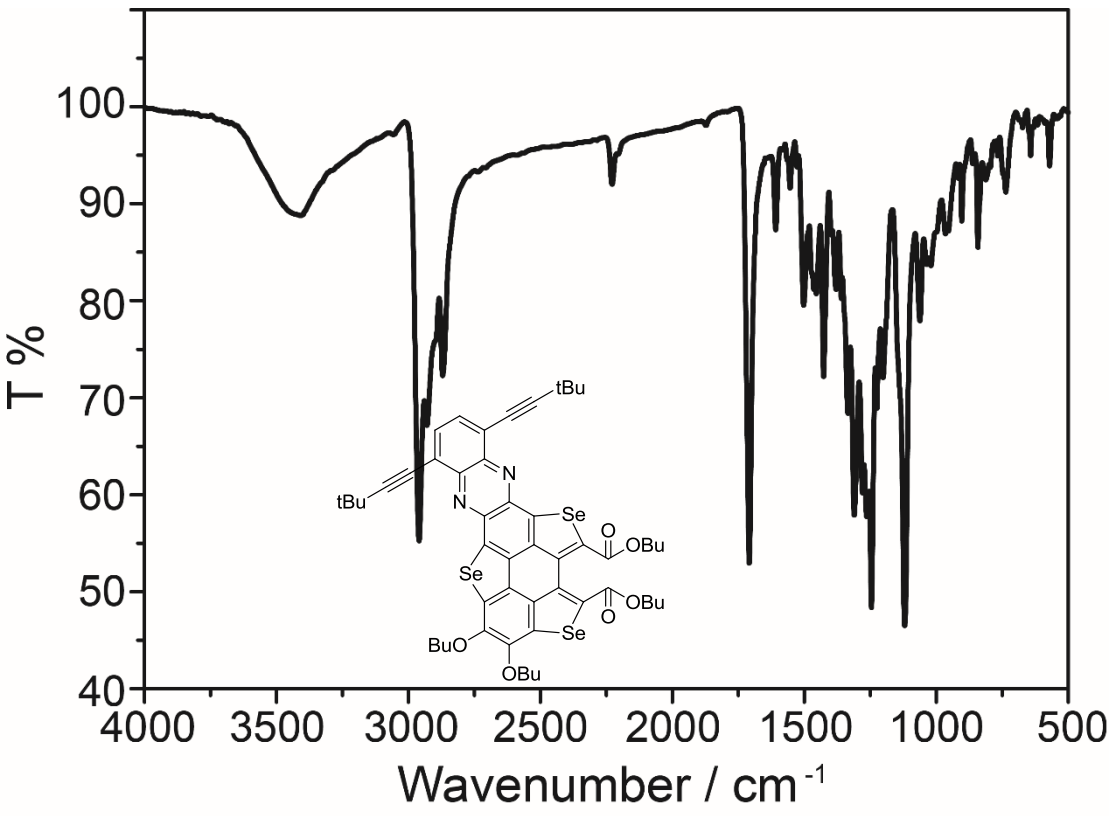
T %
100
90
80
70
60
50
40
4000
3500
3000
2500
2000
1500
1000
500
Wavenumber / cm -1
tBu
tBu
N
N
Se
Se
Se
O
OBu
O
OBu
BuO
OBu

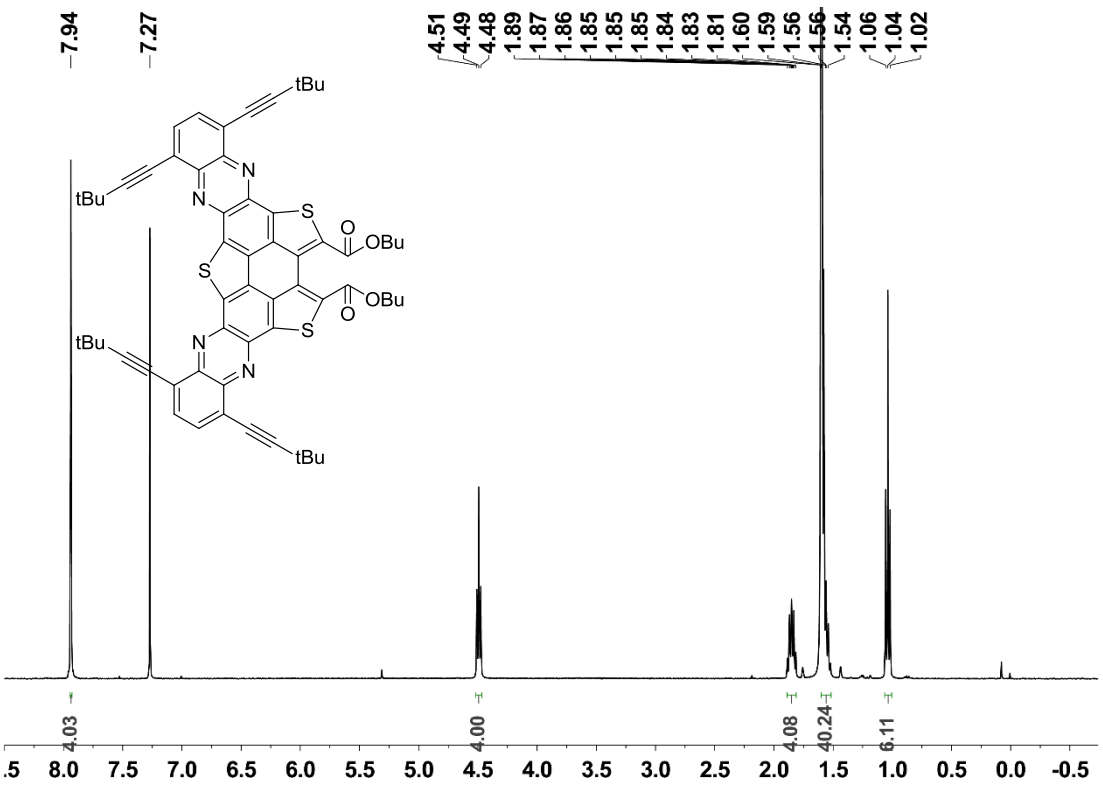
7.94
7.27
4.51
4.49
4.48
1.89
1.87
1.86
1.85
1.85
1.85
1.84
1.83
1.81
1.60
1.59
1.56
1.56
1.54
1.06
1.04
1.02
tBu
OBu
4.03
4.00
4.08
40.24
6.11

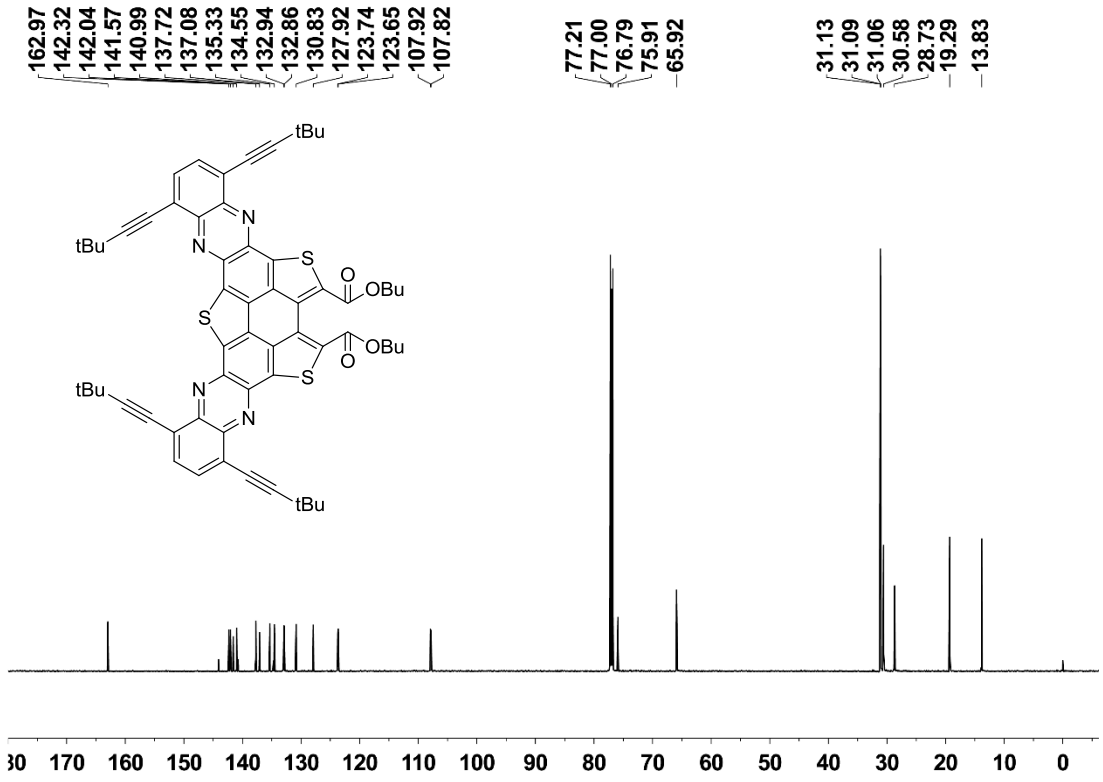
162.97
142.32
142.04
141.57
140.99
137.72
137.08
135.33
134.55
132.94
132.86
130.83
127.92
123.74
123.65
107.92
107.82
77.21
77.00
76.79
75.91
65.92
31.13
31.09
31.06
30.58
28.73
19.29
13.83
tBu
OBu

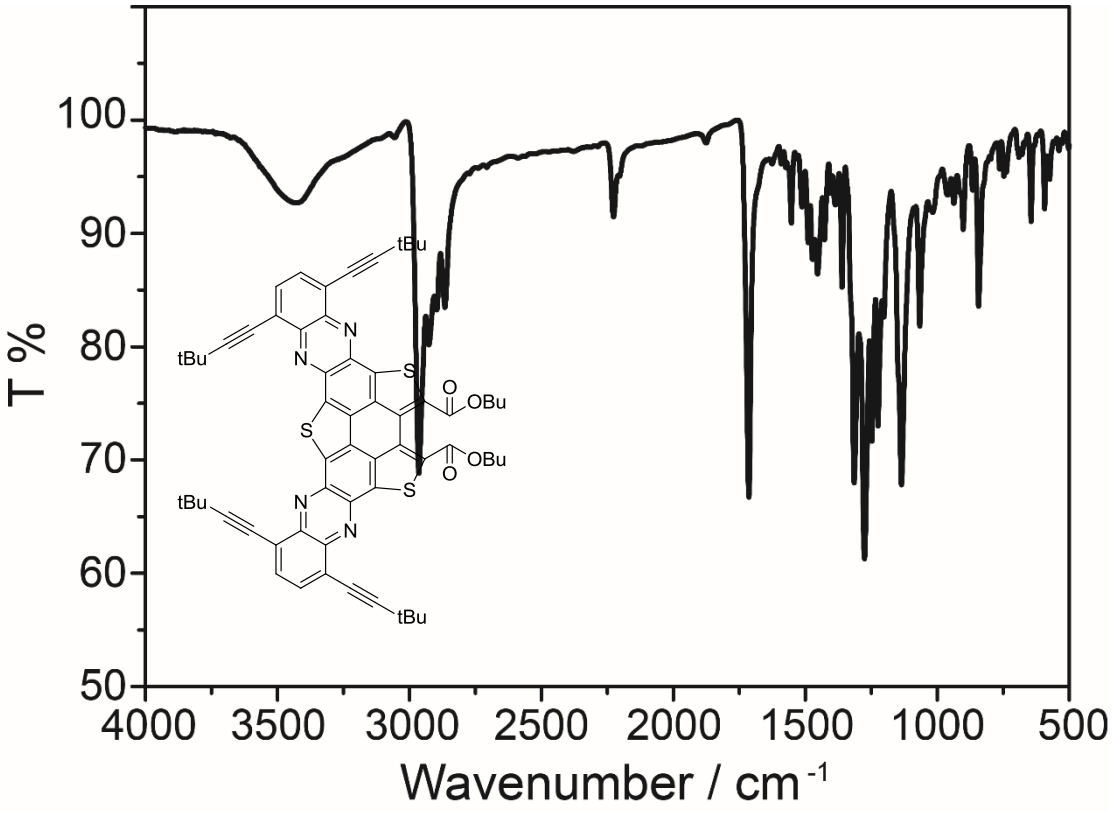
T %
100
90
80
70
60
50
4000
3500
3000
2500
2000
1500
1000
500
Wavenumber / cm -1
tBu
OBu
O
N
S

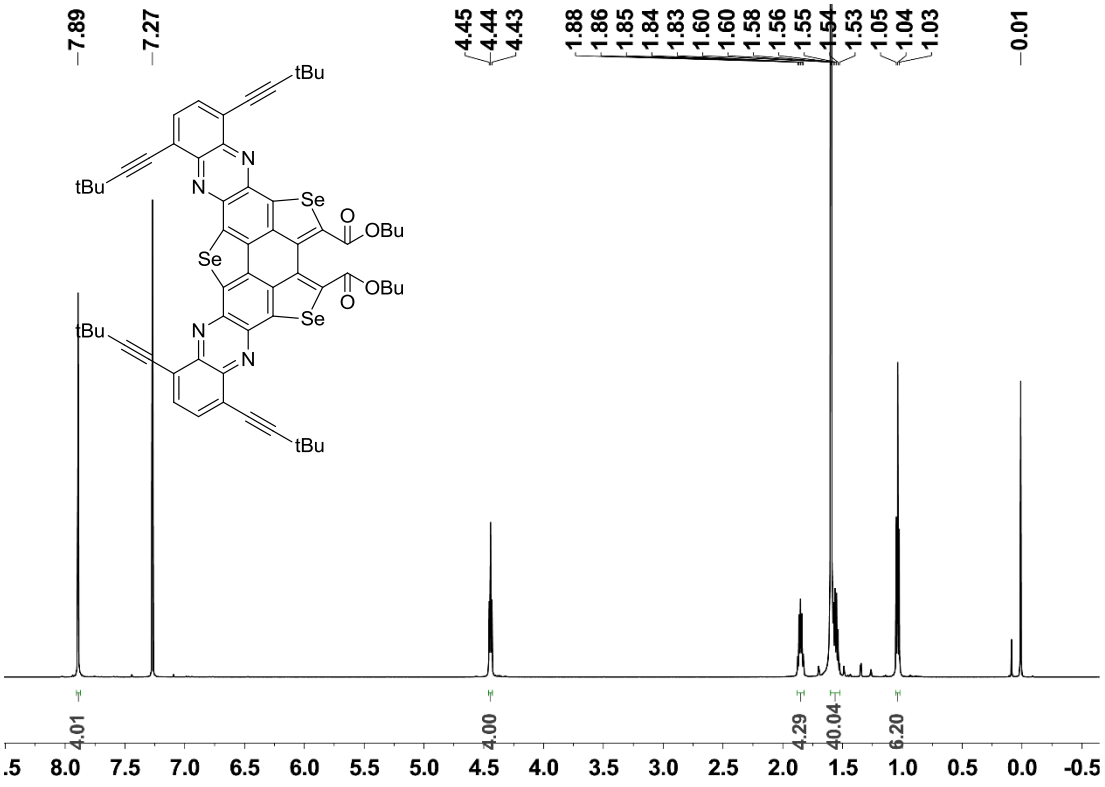
7.89
7.27
4.45
4.44
4.43
1.88
1.86
1.85
1.84
1.83
1.60
1.60
1.58
1.56
1.55
1.54
1.53
1.05
1.04
1.03
0.01
4.01
4.00
4.29
40.04
6.20
tBu
OBu
Se
N

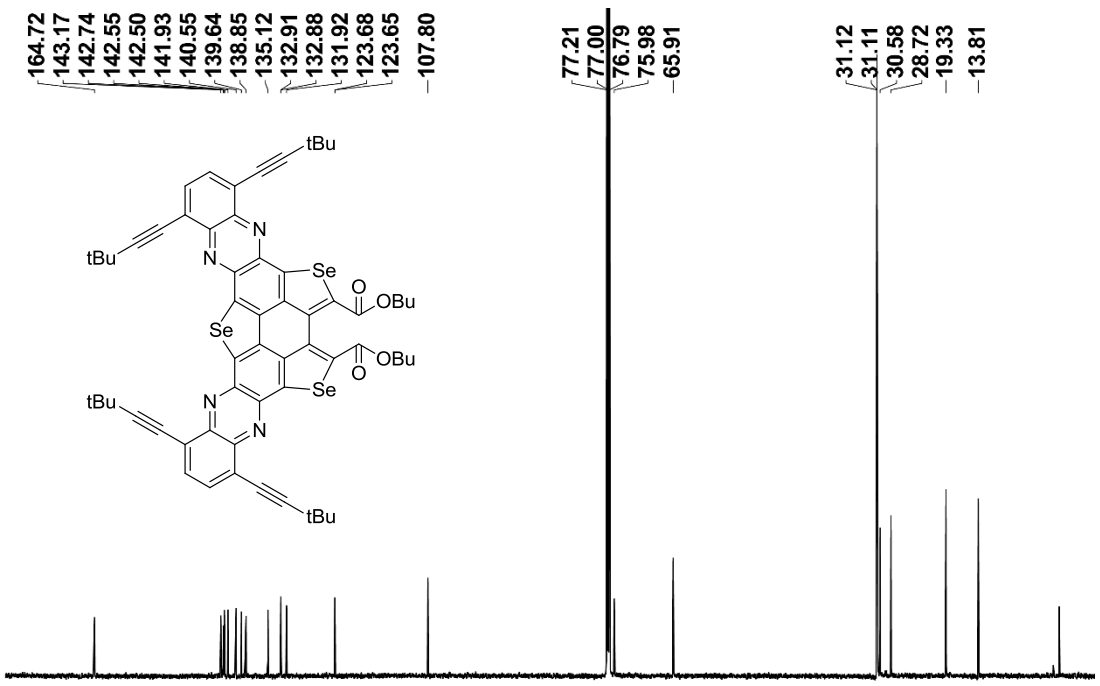
164.72
143.17
142.74
142.55
142.50
141.93
140.55
139.64
138.85
135.12
132.91
132.88
131.92
123.68
123.65
107.80
77.21
77.00
76.79
75.98
65.91
31.12
31.11
30.58
28.72
19.33
13.81
tBu
N
Se
O
OBu
170
160
150
140
130
120
110
100
90
80
70
60
50
40
30
20
10
0

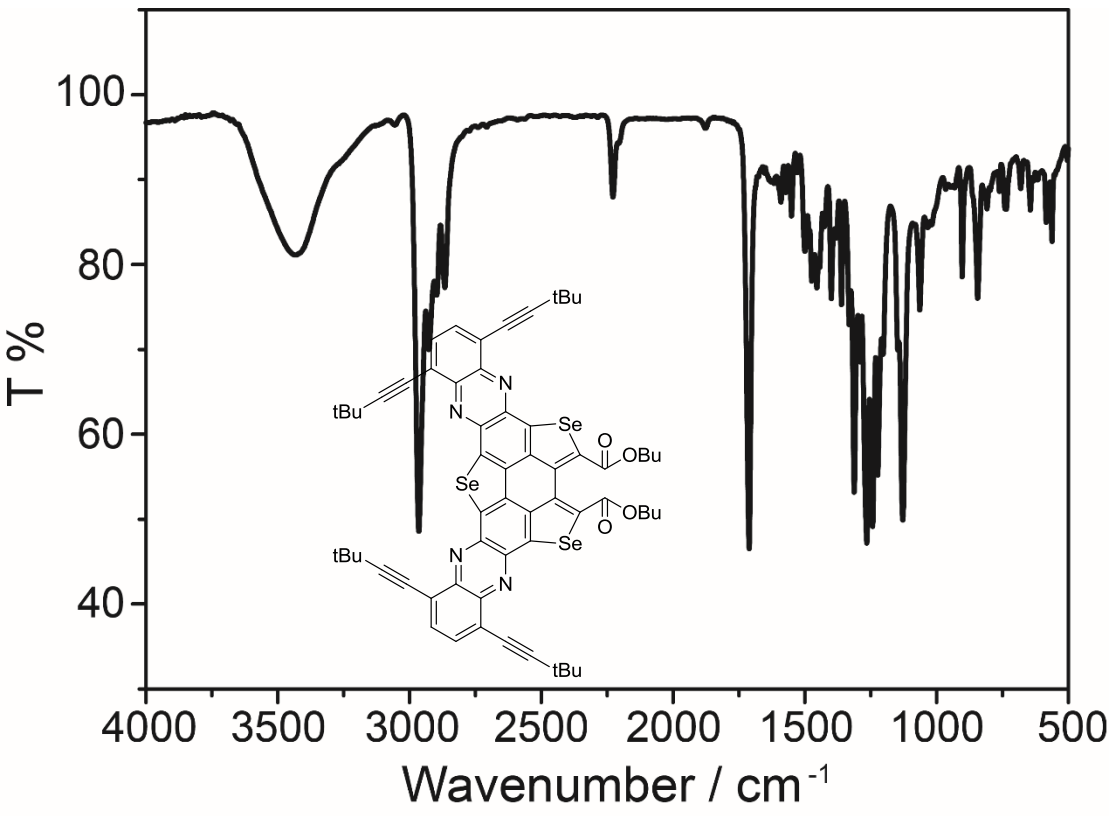
T %
100
80
60
40
4000
3500
3000
2500
2000
1500
1000
500
Wavenumber / cm -1
tBu
N
Se
O
OBu

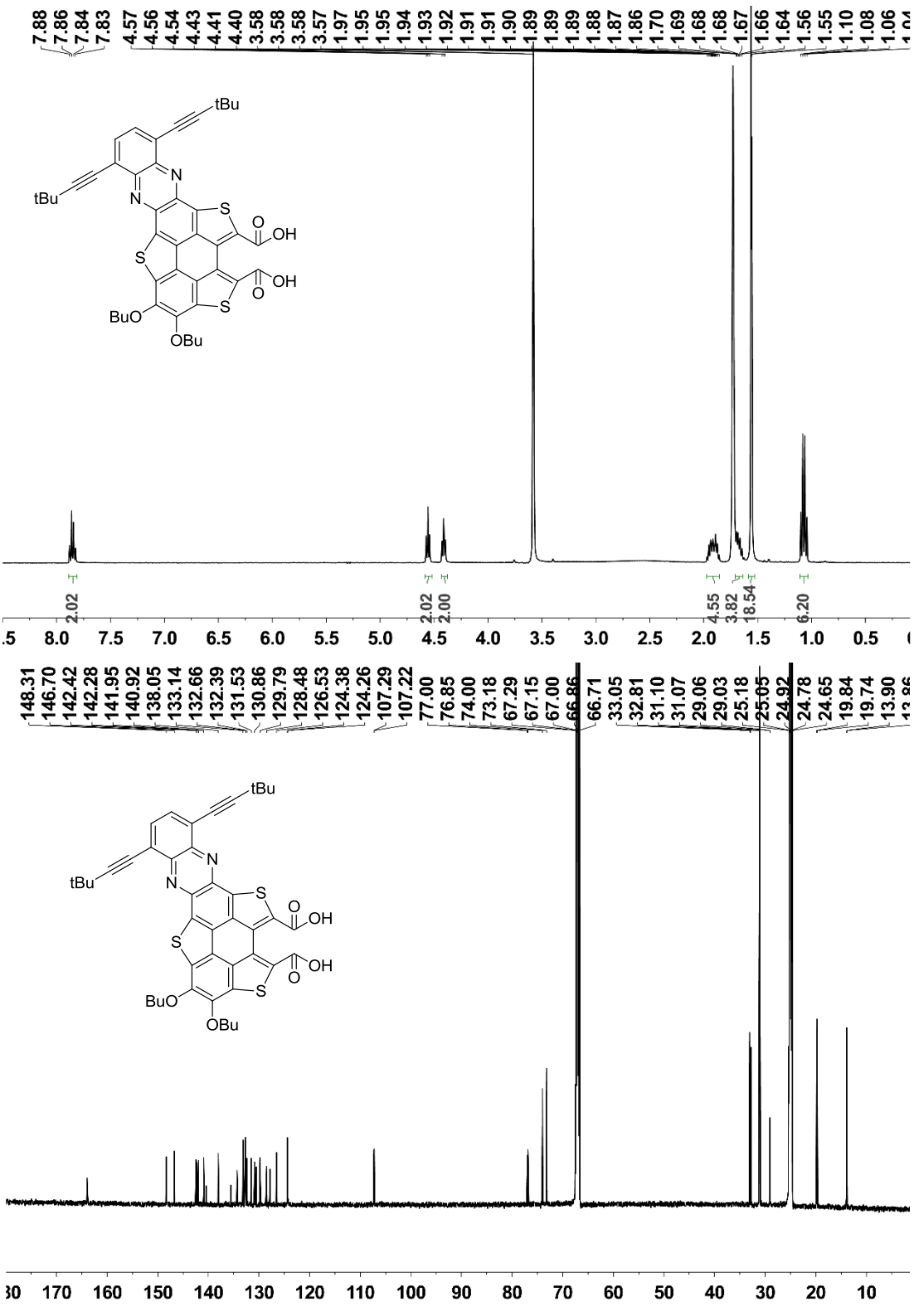
tBu
tBu
N
N
S
S
S
O
OH
O
OH
BuO
OBu
tBu
tBu
N
N
S
S
S
O
OH
O
OH
BuO
OBu

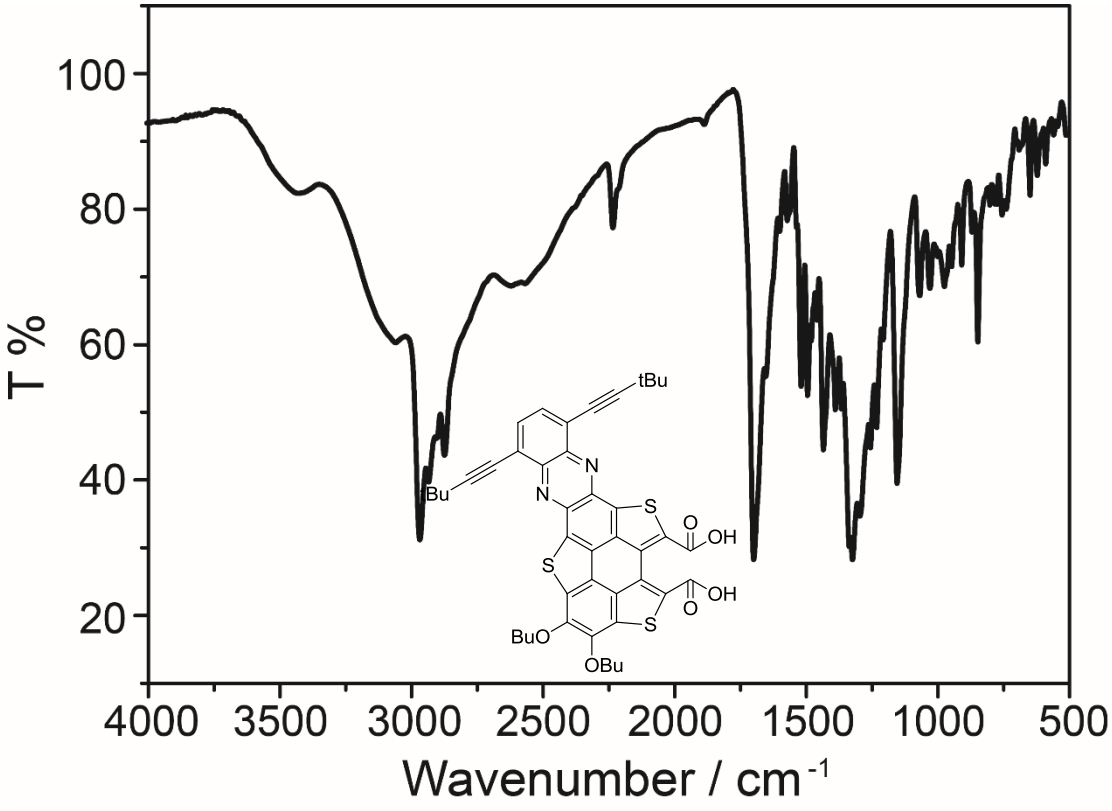
T %
100
80
60
40
20
4000
3500
3000
2500
2000
1500
1000
500
Wavenumber / cm -1
tBu
Bu
N
N
S
O
OH
S
O
OH
S
BuO
OBu

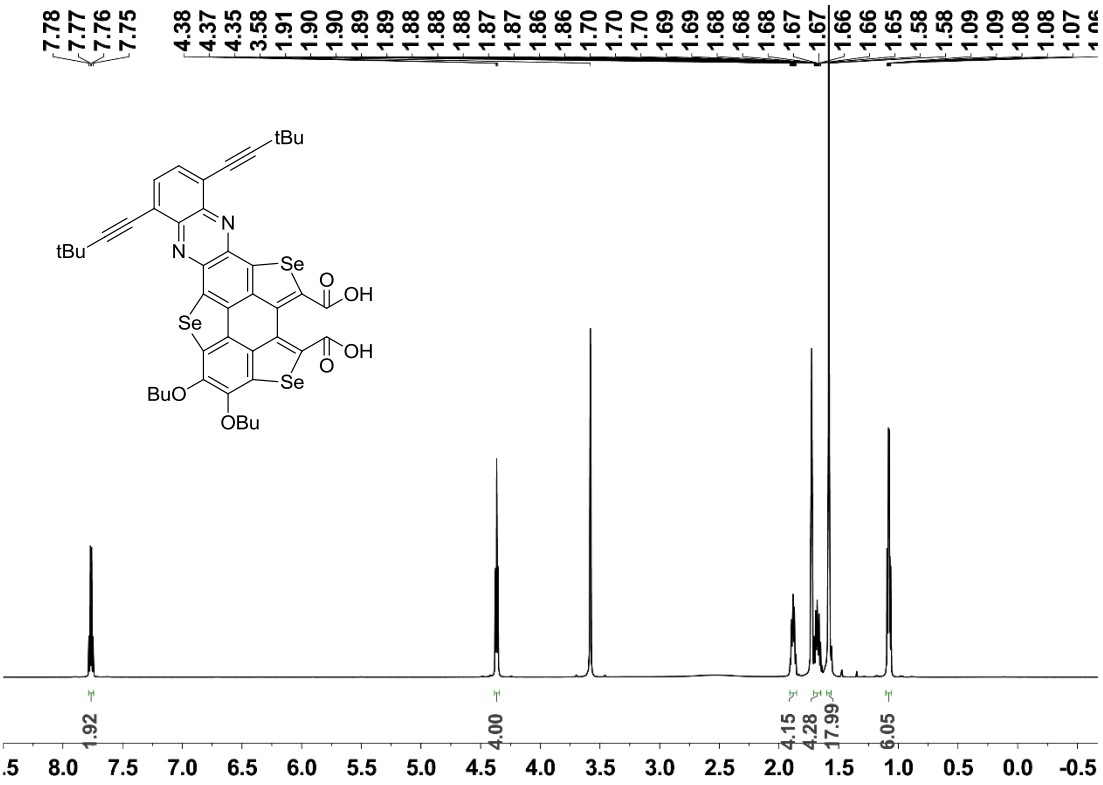
7.78
7.77
7.76
7.75
4.38
4.37
4.35
3.58
1.91
1.90
1.90
1.89
1.89
1.88
1.88
1.88
1.87
1.87
1.86
1.86
1.70
1.70
1.70
1.69
1.69
1.68
1.68
1.68
1.67
1.67
1.66
1.66
1.65
1.58
1.58
1.09
1.09
1.08
1.08
1.07
tBu
tBu
N
N
Se
O
OH
Se
O
OH
Se
BuO
OBu
1.92
4.00
4.15
4.28
17.99
6.05
.5
8.0
7.5
7.0
6.5
6.0
5.5
5.0
4.5
4.0
3.5
3.0
2.5
2.0
1.5
1.0
0.5
0.0
-0.5

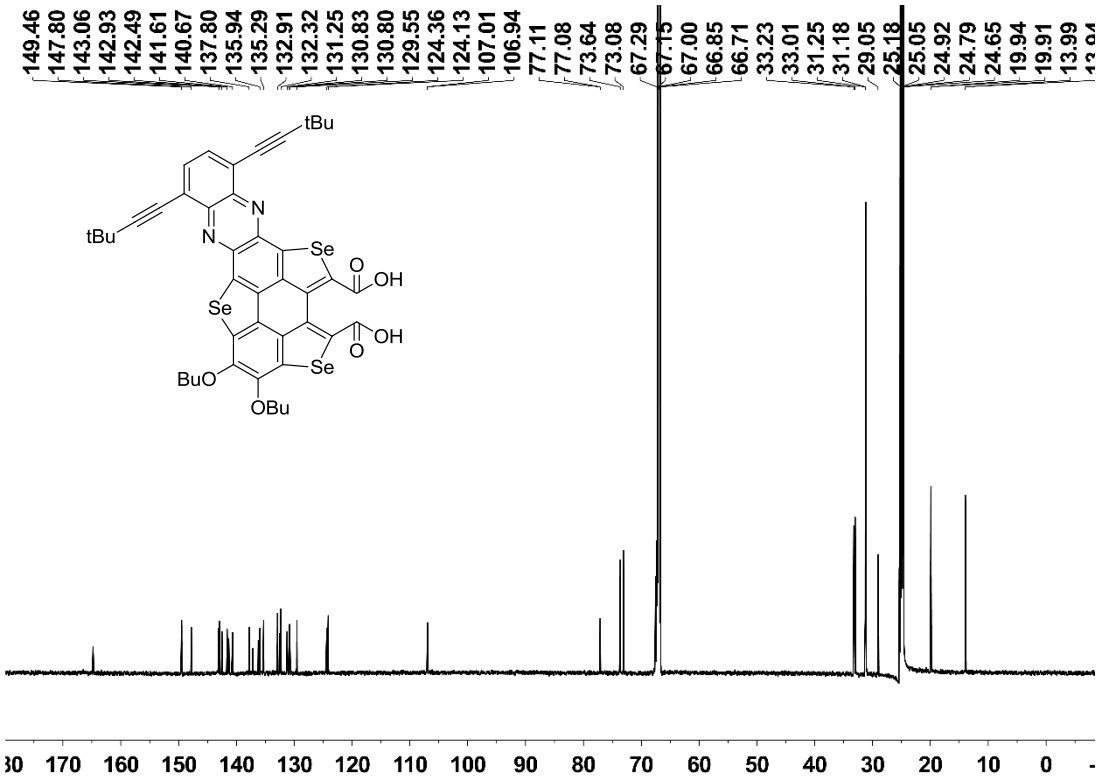
149.46
147.80
143.06
142.93
142.49
141.61
140.67
137.80
135.94
135.29
132.91
132.32
131.25
130.83
130.80
129.55
124.36
124.13
107.01
106.94
77.11
77.08
73.64
73.08
67.29
67.15
67.00
66.85
66.71
33.23
33.01
31.25
31.18
29.05
25.18
25.05
24.92
24.79
24.65
19.94
19.91
13.99
tBu
tBu
N
N
Se
O
OH
Se
O
OH
Se
BuO
OBu
170
160
150
140
130
120
110
100
90
80
70
60
50
40
30
20
10
0

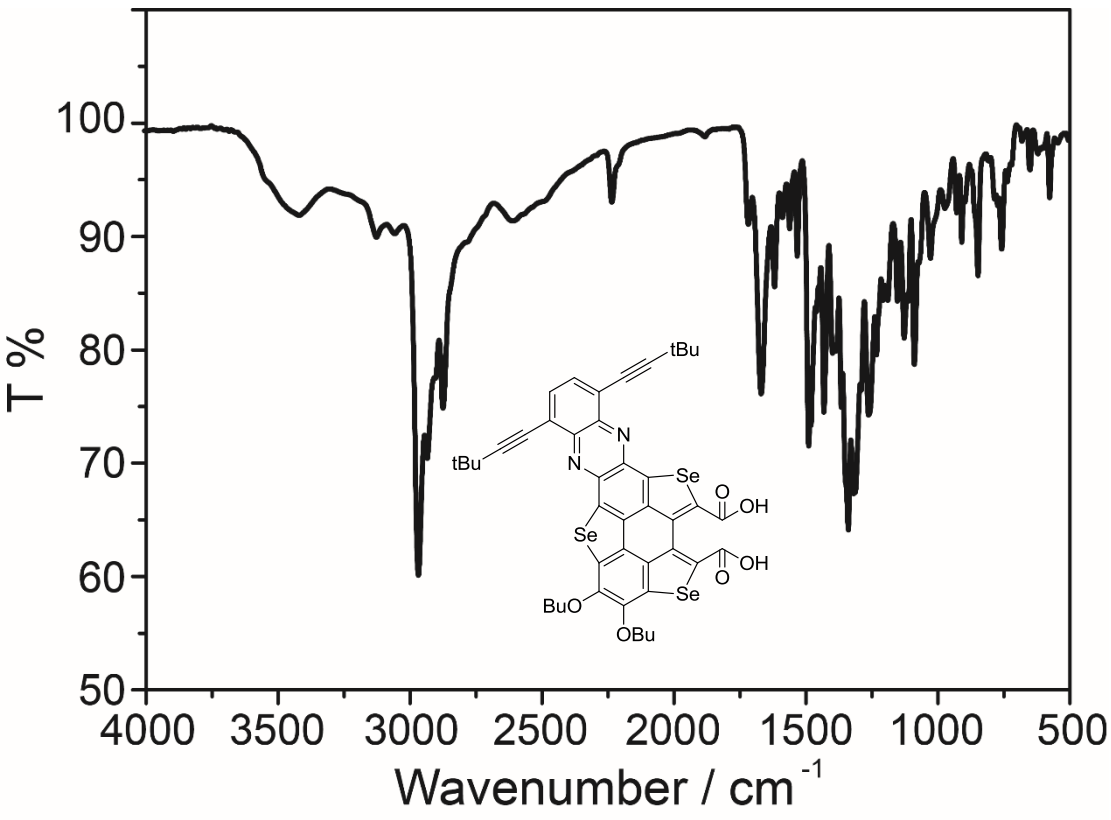
T %
100
90
80
70
60
50
4000
3500
3000
2500
2000
1500
1000
500
Wavenumber / cm -1
tBu
tBu
N
N
Se
O
OH
Se
O
OH
Se
BuO
OBu

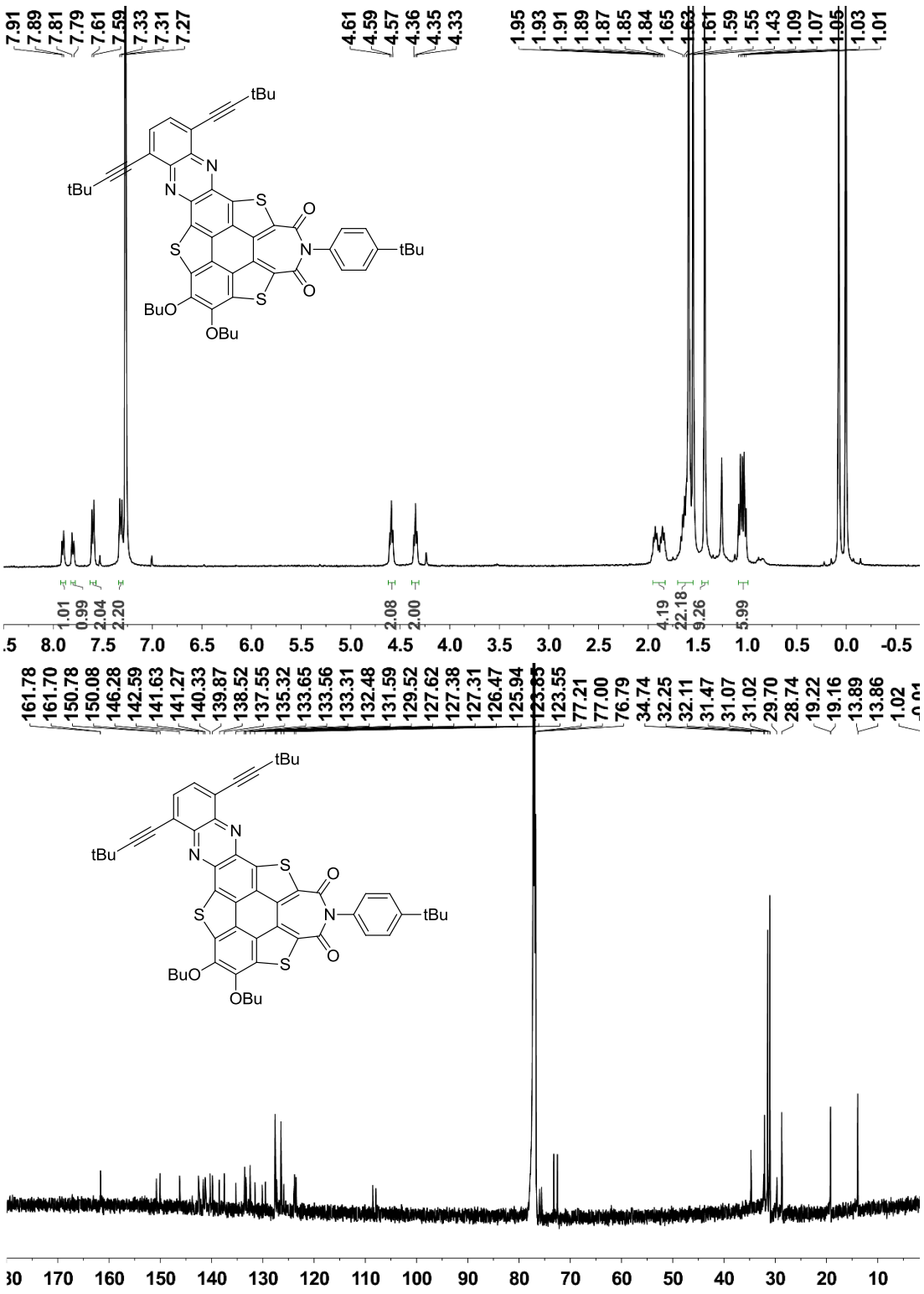
7.91
7.89
7.81
7.79
7.61
7.59
7.33
7.31
7.27
4.61
4.59
4.57
4.36
4.35
4.33
1.95
1.93
1.91
1.89
1.87
1.85
1.84
1.65
1.63
1.61
1.59
1.55
1.43
1.09
1.07
1.05
1.03
1.01
tBu
tBu
tBu
BuO
OBu
1.01
0.99
2.04
2.20
2.08
2.00
4.19
22.18
9.26
5.99
8.0
7.5
7.0
6.5
6.0
5.5
5.0
4.5
4.0
3.5
3.0
2.5
2.0
1.5
1.0
0.5
0.0
-0.5
161.78
161.70
150.78
150.08
146.28
142.59
141.63
141.27
140.33
139.87
138.52
137.55
135.32
133.65
133.56
133.31
132.48
131.59
129.52
127.62
127.38
127.31
126.47
125.94
123.83
123.55
77.21
77.00
76.79
34.74
32.25
32.11
31.47
31.07
31.02
29.70
28.74
19.22
19.16
13.89
13.86
1.02
170
160
150
140
130
120
110
100
90
80
70
60
50
40
30
20
10

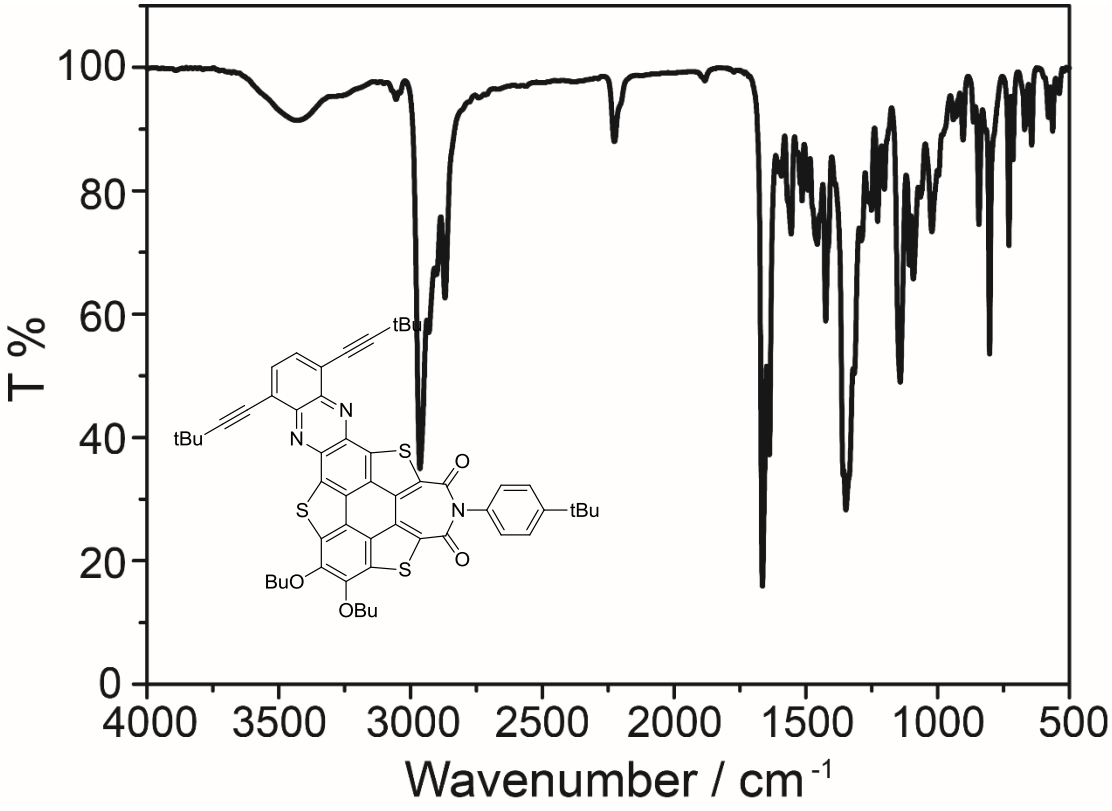
100
80
60
40
20
0
T %
4000
3500
3000
2500
2000
1500
1000
500
Wavenumber / cm -1
tBu
tBu
N
N
S
S
S
O
O
N
tBu
BuO
OBu

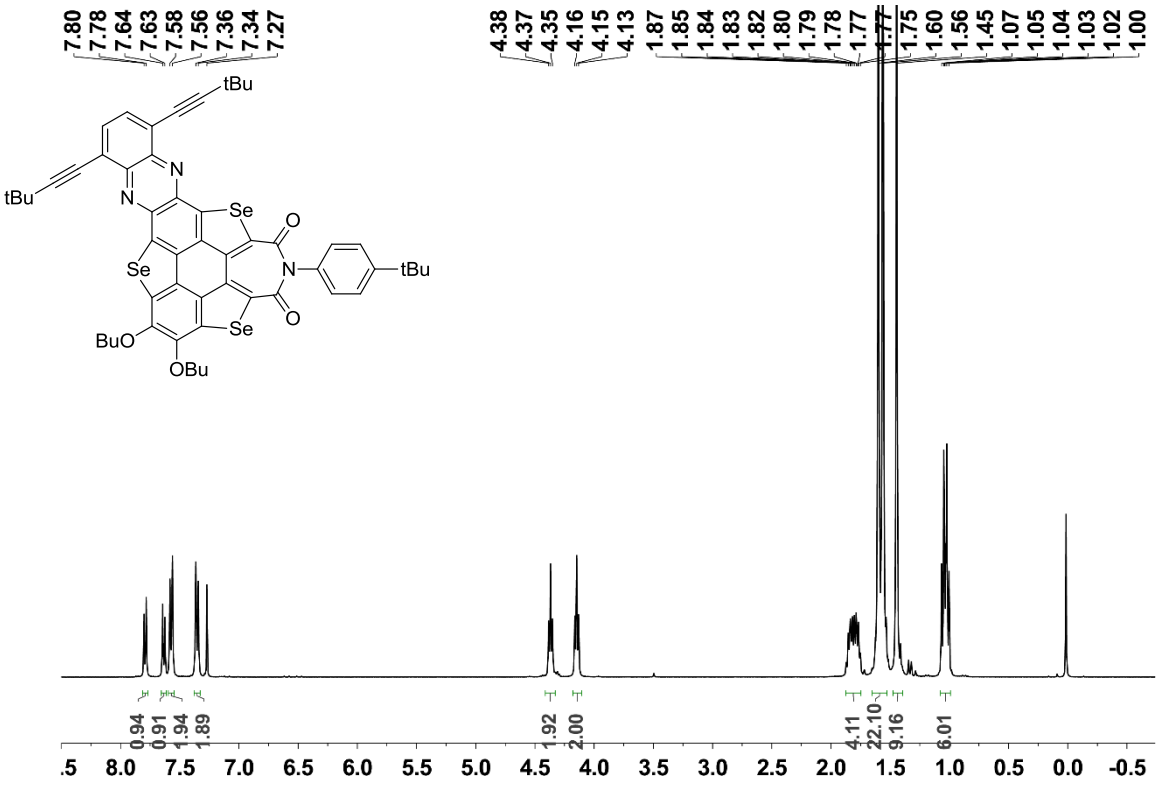
7.80
7.78
7.64
7.63
7.58
7.56
7.36
7.34
7.27
4.38
4.37
4.35
4.16
4.15
4.13
1.87
1.85
1.84
1.83
1.82
1.80
1.79
1.78
1.77
1.75
1.60
1.56
1.45
1.07
1.05
1.04
1.03
1.02
1.00
tBu
tBu
N
N
Se
Se
Se
O
O
N
tBu
BuO
OBu
0.94
0.91
1.94
1.89
1.92
2.00
4.11
22.10
9.16
6.01
8.0
7.5
7.0
6.5
6.0
5.5
5.0
4.5
4.0
3.5
3.0
2.5
2.0
1.5
1.0
0.5
0.0
-0.5

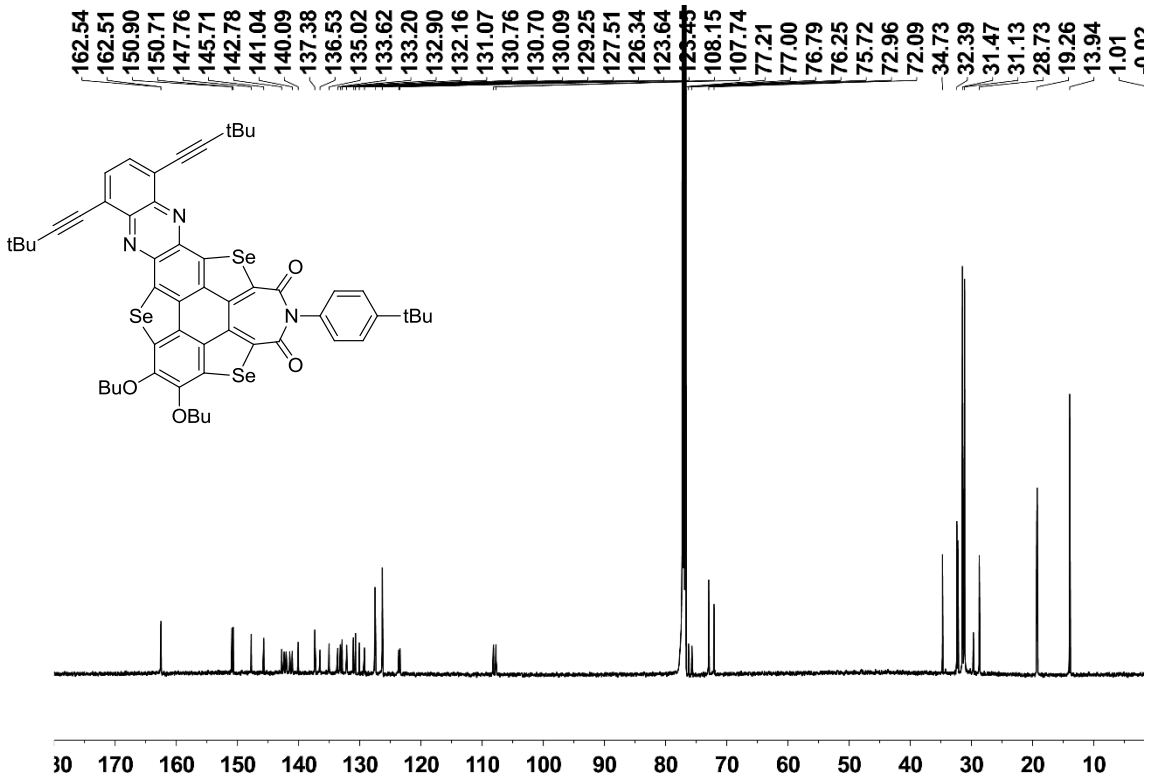
162.54
162.51
150.90
150.71
147.76
145.71
142.78
141.04
140.09
137.38
136.53
135.02
133.62
133.20
132.90
132.16
131.07
130.76
130.70
130.09
129.25
127.51
126.34
123.64
123.43
108.15
107.74
77.21
77.00
76.79
76.25
75.72
72.96
72.09
34.73
32.39
31.47
31.13
28.73
19.26
13.94
1.01
tBu
tBu
N
N
Se
O
N
tBu
Se
O
Se
BuO
OBu
30 170 160 150 140 130 120 110 100 90 80 70 60 50 40 30 20 10

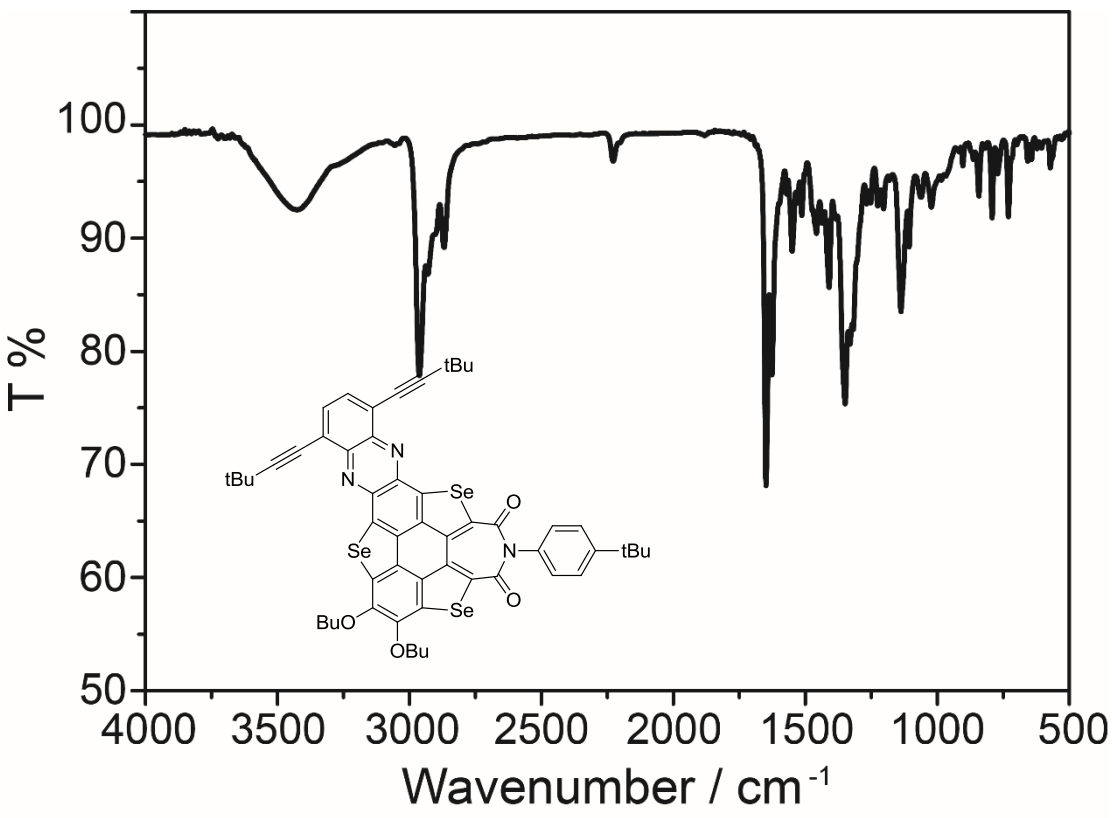
T %
100
90
80
70
60
50
4000 3500 3000 2500 2000 1500 1000 500
Wavenumber / cm -1
tBu
tBu
N
N
Se
O
N
tBu
Se
O
Se
BuO
OBu

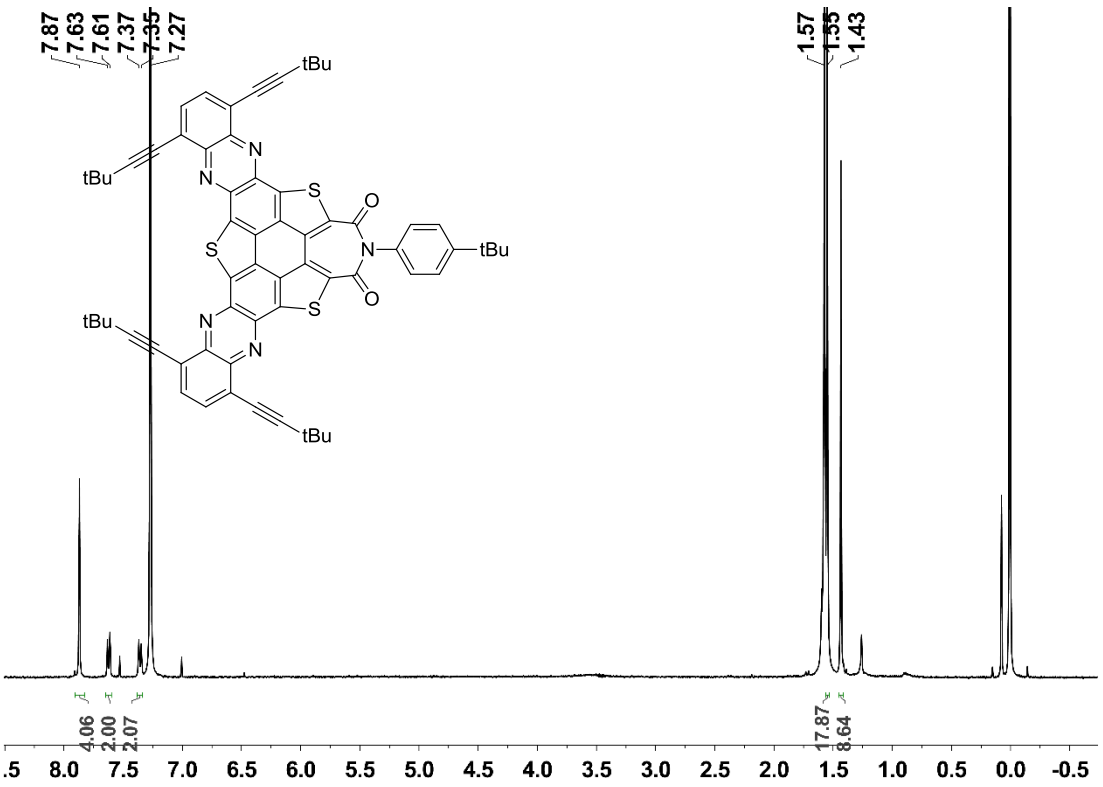
7.87
7.63
7.61
7.37
7.35
7.27
1.57
1.55
1.43
tBu
tBu
tBu
tBu
tBu
tBu
N
N
N
N
S
S
S
O
O
N
4.06
2.00
2.07
17.87
8.64
8.0
7.5
7.0
6.5
6.0
5.5
5.0
4.5
4.0
3.5
3.0
2.5
2.0
1.5
1.0
0.5
0.0
-0.5

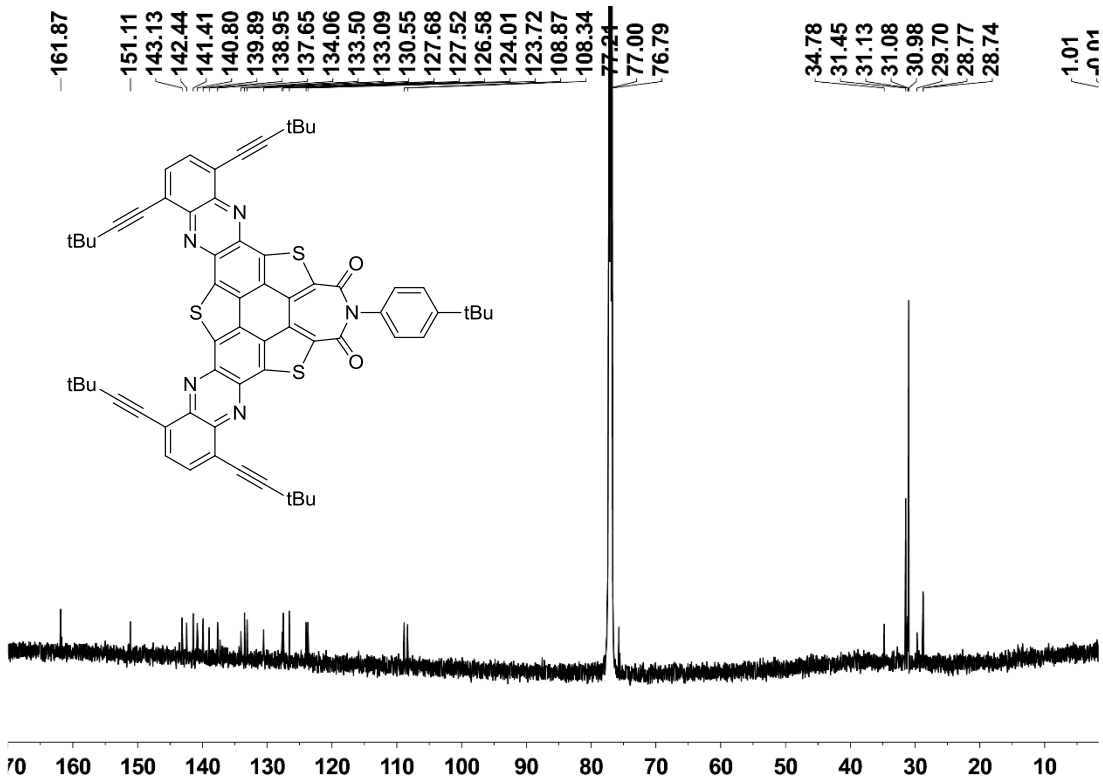
161.87
151.11
143.13
142.44
141.41
140.80
139.89
138.95
137.65
134.06
133.50
133.09
130.55
127.68
127.52
126.58
124.01
123.72
108.87
108.34
77.24
77.00
76.79
34.78
31.45
31.13
31.08
30.98
29.70
28.77
28.74
1.01
tBu
tBu
tBu
tBu
tBu
tBu
N
N
N
N
S
S
S
O
O
N
160
150
140
130
120
110
100
90
80
70
60
50
40
30
20
10

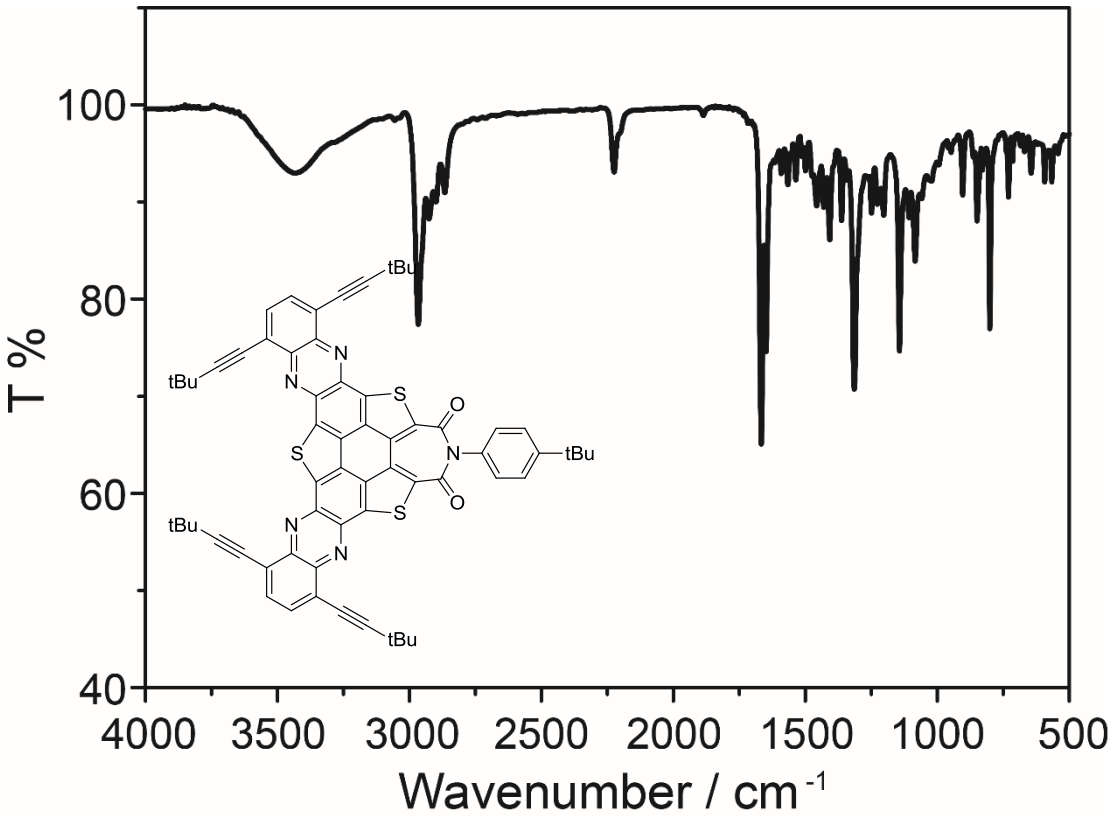
100
80
60
40
T %
4000
3500
3000
2500
2000
1500
1000
500
Wavenumber / cm -1
tBu
N
S
O

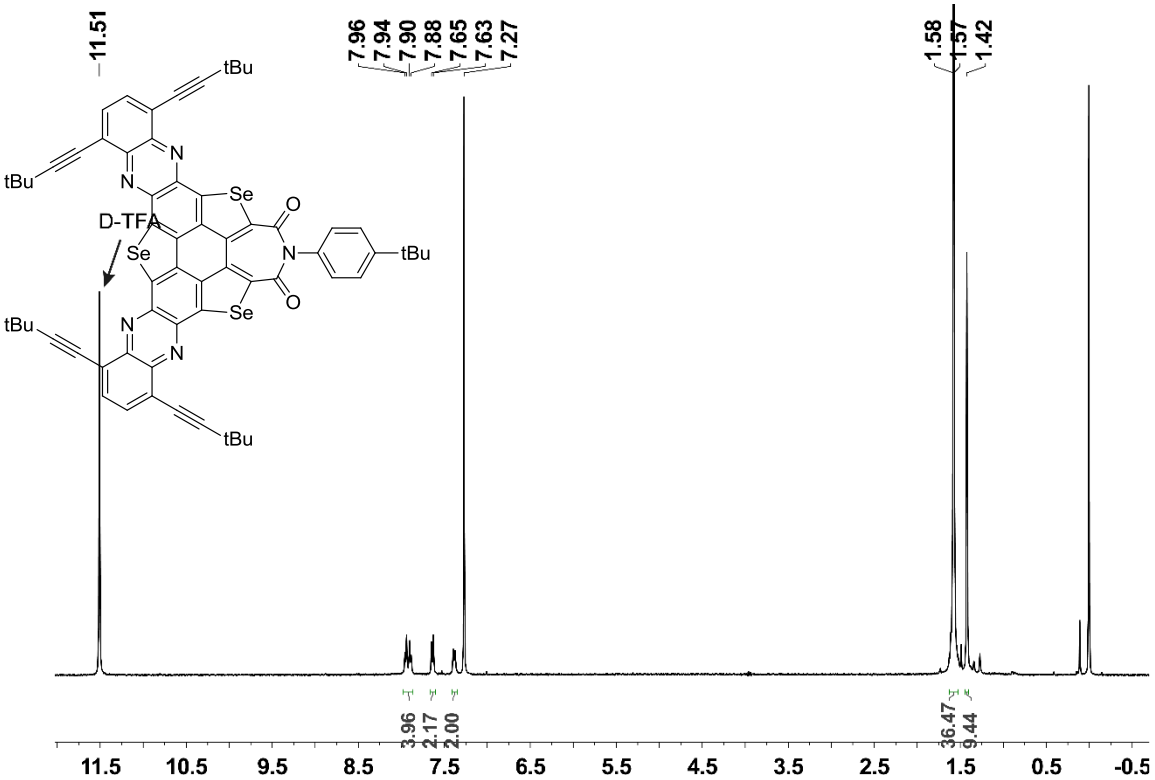
11.51
7.96
7.94
7.90
7.88
7.65
7.63
7.27
1.58
1.57
1.42
D-TFA
tBu
N
Se
O
3.96
2.17
2.00
36.47
9.44
11.5
10.5
9.5
8.5
7.5
6.5
5.5
4.5
3.5
2.5
1.5
0.5
-0.5

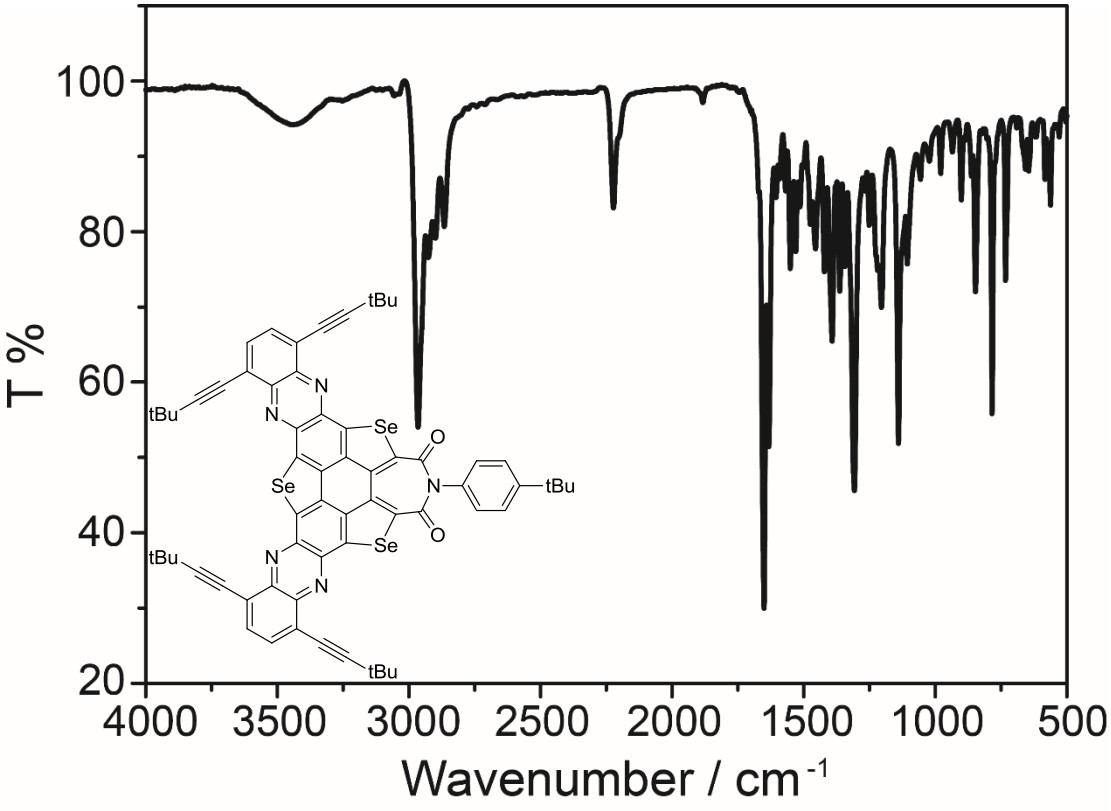
100
80
60
40
20
T %
4000
3500
3000
2500
2000
1500
1000
500
Wavenumber / cm -1
tBu
N
Se
O
tBu

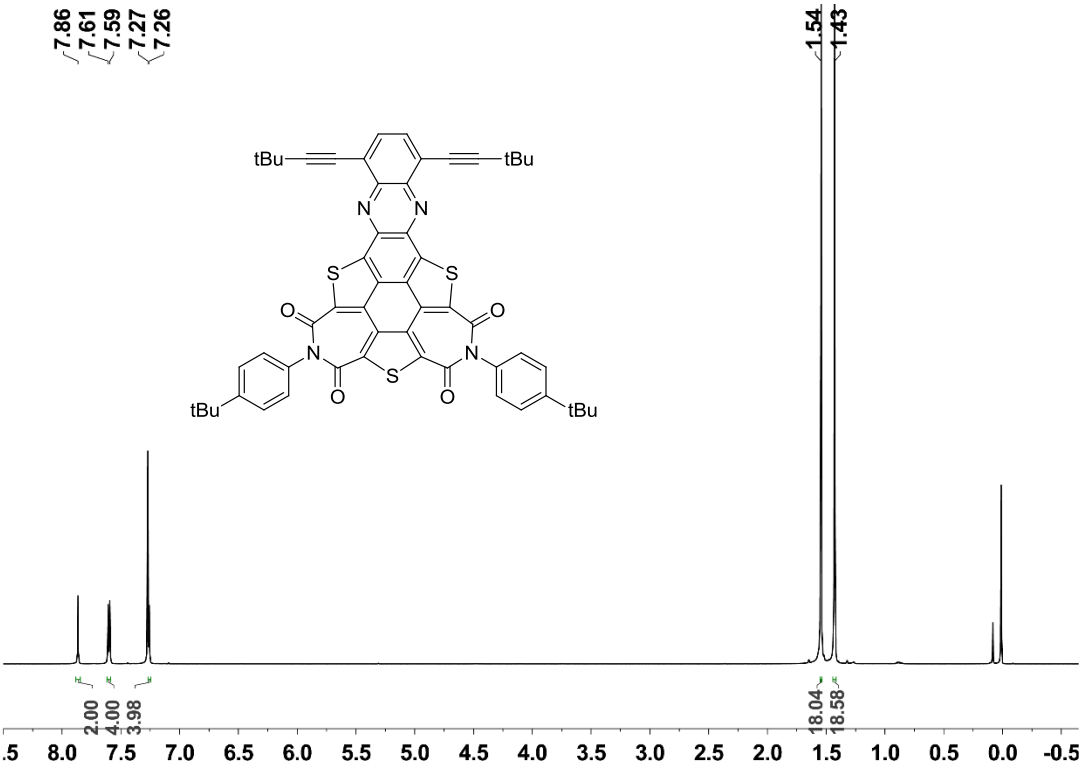
7.86
7.61
7.59
7.27
7.26
1.54
1.43
tBu
N
S
O
2.00
4.00
3.98
18.04
18.58

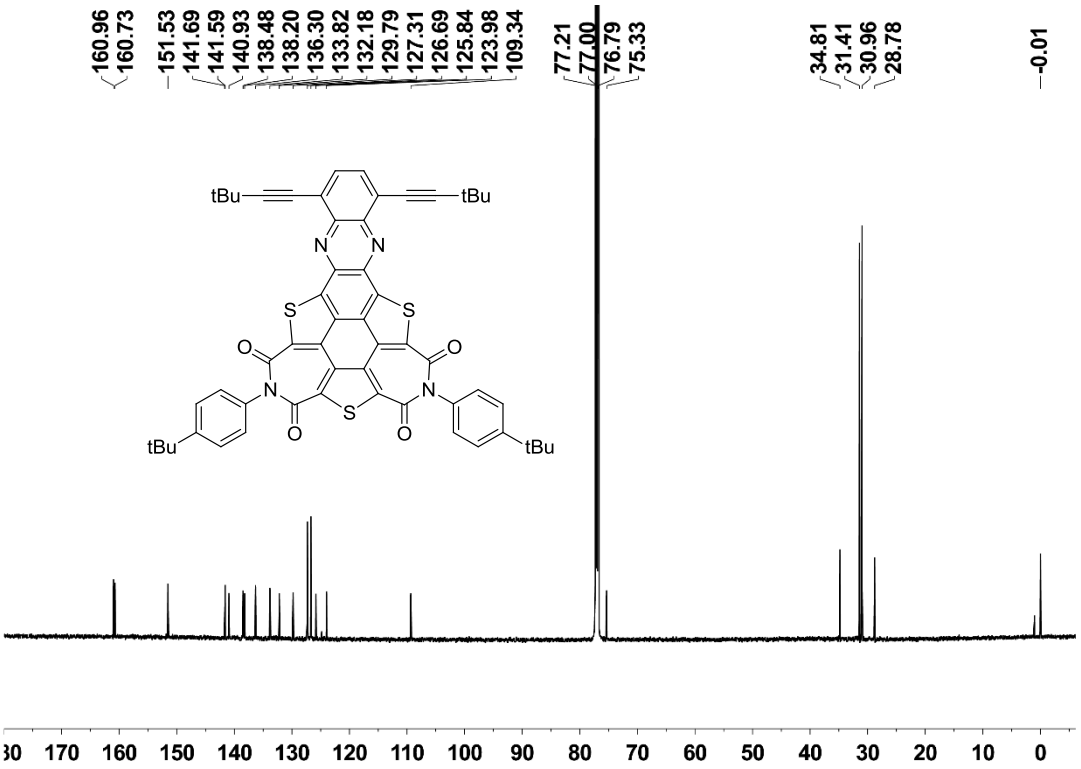
160.96
160.73
151.53
141.69
141.59
140.93
138.48
138.20
136.30
133.82
132.18
129.79
127.31
126.69
125.84
123.98
109.34
77.21
77.00
76.79
75.33
34.81
31.41
30.96
28.78
-0.01
tBu
tBu
tBu
tBu
N
N
S
S
S
O
O
O
O
N
N
170
160
150
140
130
120
110
100
90
80
70
60
50
40
30
20
10
0

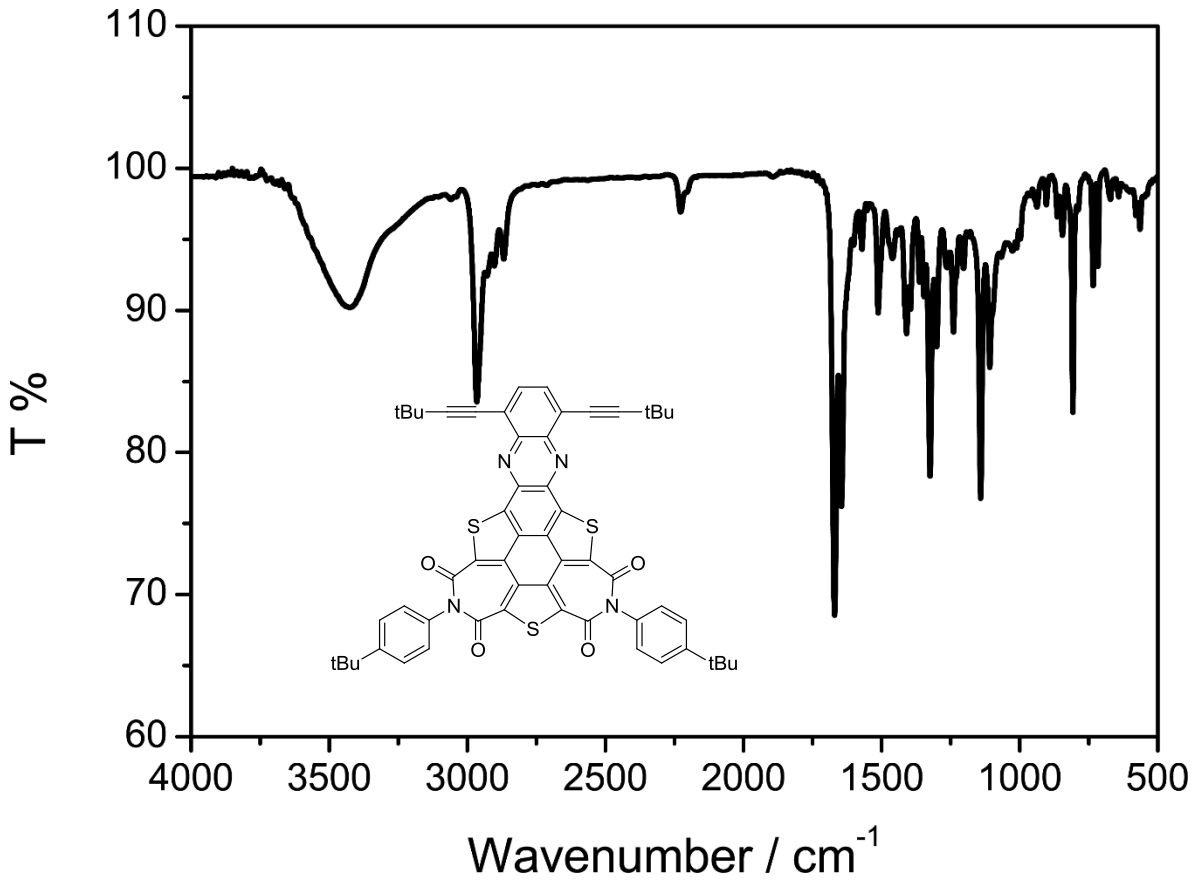
T %
110
100
90
80
70
60
4000
3500
3000
2500
2000
1500
1000
500
Wavenumber / cm-1
tBu
tBu
tBu
tBu
N
N
S
S
S
O
O
O
O
N
N

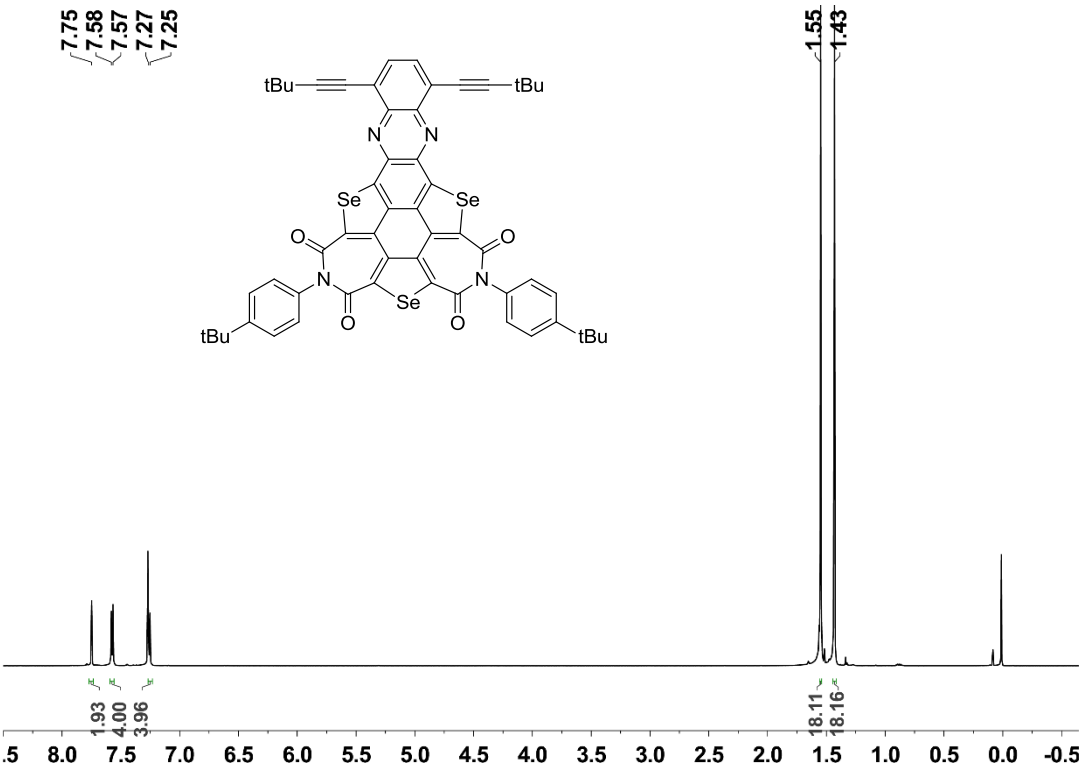
7.75
7.58
7.57
7.27
7.25
1.55
1.43
tBu
tBu
N
N
Se
Se
O
O
N
Se
N
O
O
O
tBu
tBu
1.93
4.00
3.96
18.11
18.16
.5 8.0 7.5 7.0 6.5 6.0 5.5 5.0 4.5 4.0 3.5 3.0 2.5 2.0 1.5 1.0 0.5 0.0 -0.5

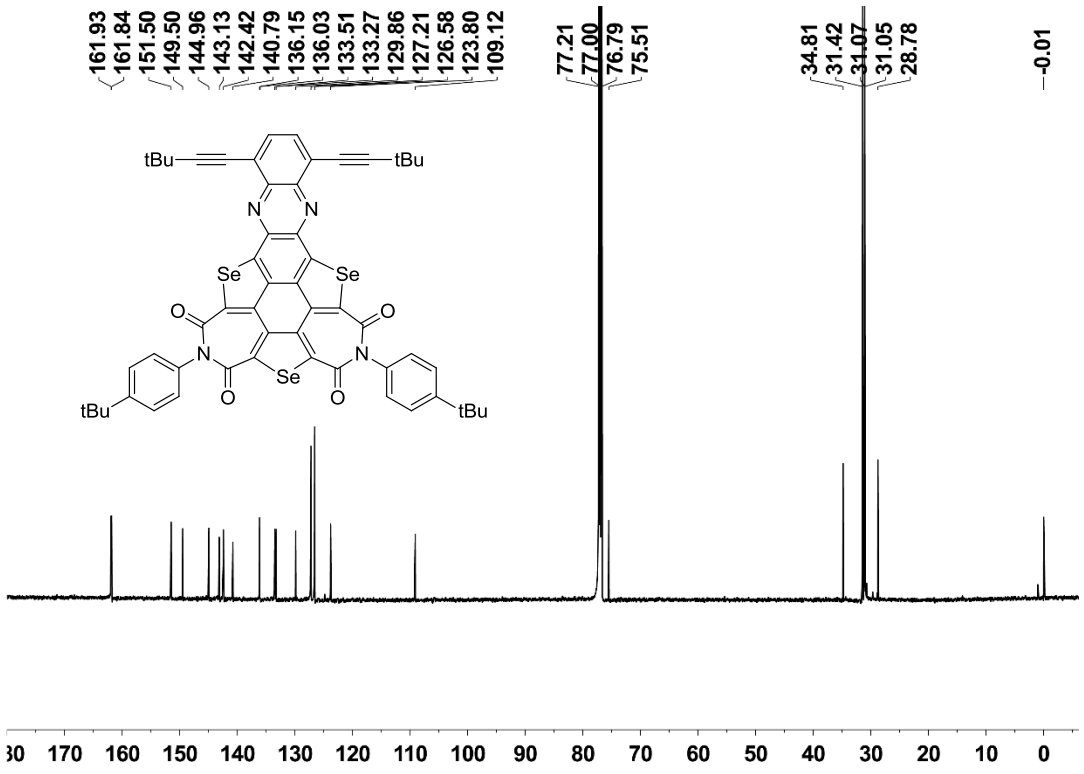
161.93
161.84
151.50
149.50
144.96
143.13
142.42
140.79
136.15
136.03
133.51
133.27
129.86
127.21
126.58
123.80
109.12
77.21
77.00
76.79
75.51
34.81
31.42
31.07
31.05
28.78
-0.01
tBu
tBu
N
N
Se
Se
O
O
N
Se
N
O
O
O
tBu
tBu
30 170 160 150 140 130 120 110 100 90 80 70 60 50 40 30 20 10 0

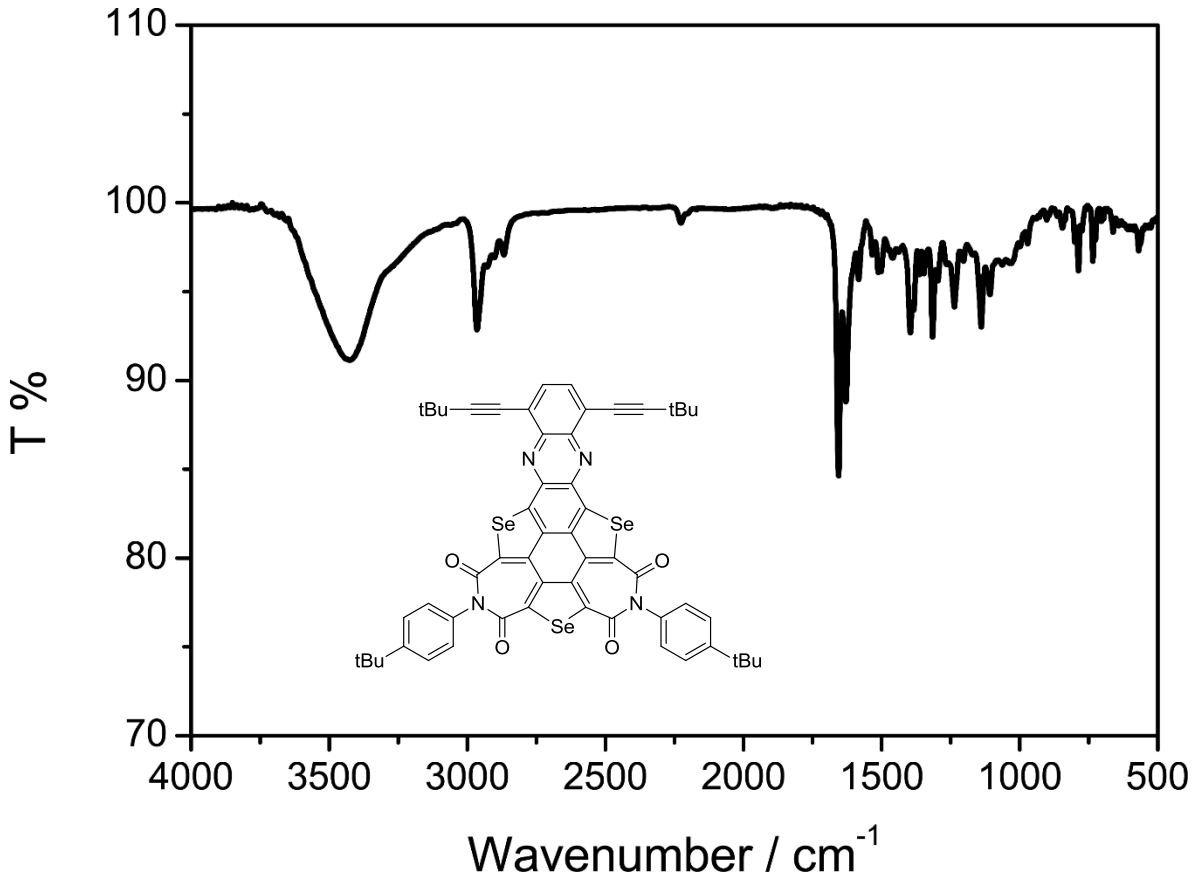
110
100
90
80
70
T %
4000
3500
3000
2500
2000
1500
1000
500
Wavenumber / cm-1
tBu
tBu
N
N
Se
Se
O
O
N
N
Se
O
O
tBu
tBu